Stony Brook University

The Exchange of Acetaldehyde between Plants and the Atmosphere: Stable Carbon Isotope and Flux Measurements

A Dissertation Presented by

Kolby Jeremiah Jardine

to

The Graduate School

in Partial Fulfillment of the

Requirements

for the Degree of

Doctor of Philosophy

in

Marine and Atmospheric Science

Stony Brook University

May 2008

Stony Brook University

The Graduate School

Kolby Jeremiah Jardine

We, the dissertation committee for the above candidate for the
Doctor of Philosophy degree, hereby recommend
acceptance of this dissertation.

John E. Mak - Dissertation Advisor
Associate Professor, Institute for Terrestrial and Planetary Atmospheres/
Marine Sciences Research Center, Stony Brook University

Manuel Lerdau – Chairperson of Defense
Professor, Department of Ecology and Evolution with courtesy appointment in
Marine Sciences, Stony Brook University

Nicole Riemer
Assistant Professor, Institute for Terrestrial and Planetary Atmospheres/
Marine Sciences Research Center, Stony Brook University

Alex Guenther
Senior Scientist, Section Head and Group Leader
Biosphere-Atmosphere Interactions Group
Atmospheric Chemistry Division
National Center for Atmospheric Research

This dissertation is accepted by the Graduate School

Lawrence Martin
Dean of the Graduate School

Abstract of the Dissertation

by

Kolby Jeremiah Jardine

Doctor of Philosophy

in

Marine and Atmospheric Science

Stony Brook University

2008

The exchange of acetaldehyde between plant canopies and the atmosphere may significantly influence regional atmospheric chemistry and plant metabolism. While plants are known to both produce and consume acetaldehyde, the exchange of this compound with forested ecosystems is complicated by physical, biological, and chemical processes that range from being poorly understood to completely unknown. This precludes a quantitative understanding of acetaldehyde exchange rates between the atmosphere and the biosphere. In this study, the processes controlling the exchange of acetaldehyde with plant canopies was investigated using concentration, flux, and natural abundance ^{13}C measurements of gas phase acetaldehyde from individual plants, soils, and entire ecosystems. Although previously only considered important in anoxic tissues, it was discovered that acetaldehyde is produced and consumed in leaves through ethanolic fermentation coupled to the pyruvate dehydrogenase bypass system under normal aerobic conditions. These coupled pathways determine the acetaldehyde compensation point, a major factor controlling its exchange with the atmosphere. Carbon isotope analysis suggests a new pathway for acetaldehyde production from plants under stress involving the peroxidation of membrane fatty acids. This pathway may be a major source of acetaldehyde to the atmosphere from plants under biotic and abiotic stresses. Plant stomata were found to be the dominant pathway for the exchange of acetaldehyde with the atmosphere with stomatal conductance influencing both emission and uptake fluxes. In addition, increasing temperature

and solar radiation was found to increase the compensation point by increasing the rates of acetaldehyde production relative to consumption. Under ambient conditions, bare soil was neutral to the exchange of acetaldehyde while senescing and decaying leaves were found to be strong source of acetaldehyde to the atmosphere due to increased decomposition processes and the loss of biological sink(s). Vertical concentration profiles and within-canopy turbulence characterization allowed for the estimation of fine scale source/sink profiles of acetaldehyde in forested ecosystems in Michigan, California, and North Carolina. The different vertical and temporal acetaldehyde exchange patterns between the sites were well described using a simple canopy exchange model based on the results from the process based branch studies. We find that net ecosystem acetaldehyde emission rates are inversely related to foliage density by influencing the extinction of sunlight in a plant canopy. While high foliage density canopies can effectively mitigate regional air pollution by behaving as a net sink of atmospheric acetaldehyde, lower density canopies may aggravate it by acting as a net source.

Dedication

I dedicate this dissertation to my best friend and wife Angie Jardine for supporting me during my pursuit of higher education over the last 10 years. Thank you for supporting me at the Colorado School of Mines, Harvard University, New York University, Arizona State University, the University of Washington, San Juan College, the South Dakota School of Mines and Technology, the National Center for Atmospheric Research, the University of Michigan Biological Station, and Stony Brook University. Thank you greatly for your excellent engineering advice related to atmospheric instrumentation which helped solve many of the analytical problems that occurred during my research. Thank you for the thousands of discussions on all sorts of science topics over the years which has helped mold me into the scientist I am today. Thank you for your unpaid help during field projects in the Black Hills of South Dakota, at the University of Michigan Biological Station, at the CHATS field study in California, and the INTEX-B field campaign in Seattle. I am extremely grateful for your tireless efforts to read and edit all of my scientific writings including this dissertation. Lastly, thank you for guiding me on incredible outdoor adventures during this graduate work from rock climbing, sea kayaking, backpacking, snowboarding, back country skiing, power kiting, mountain biking, and mountaineering.

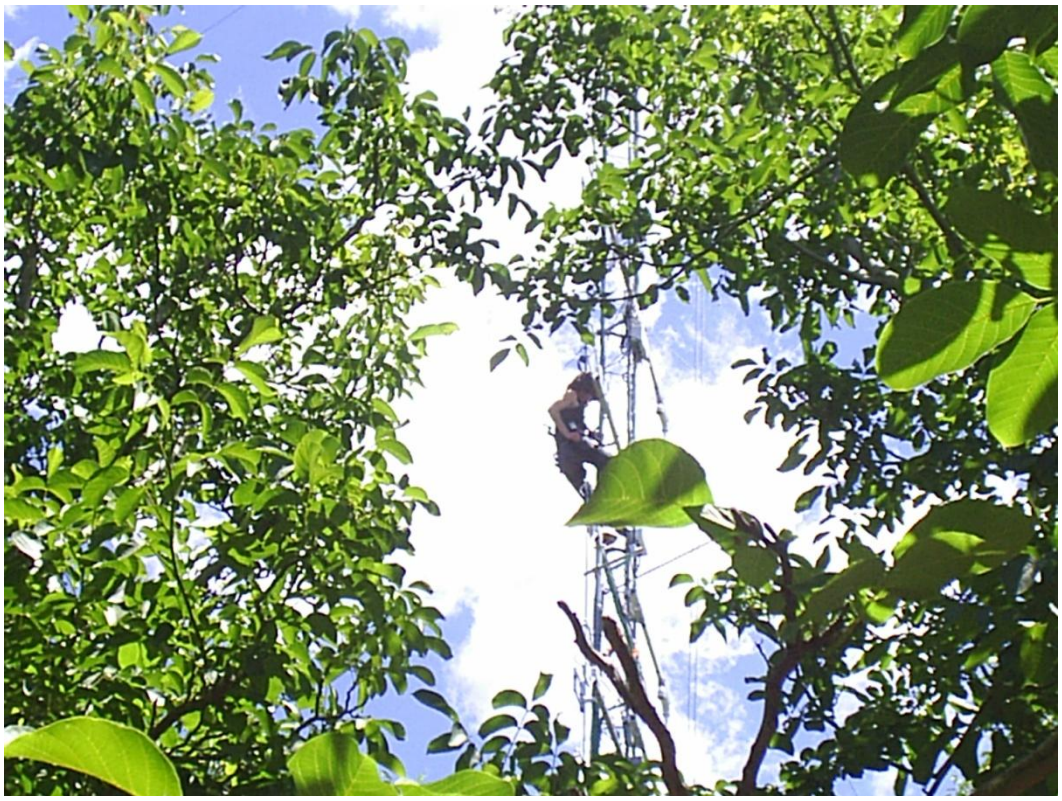

Table of Contents

List of Figures

Acknowledgements

I would like to kindly thank my advisor John Mak for providing me with the opportunity to explore the fascinating field of stable isotopes in trace gas chemistry. My path of searching and eventually finding an exciting research project came only through his guidance. I would like to thank him for the large financial support of my projects as well as the encouragement necessary to succeed. Most of all, I would like to kindly thank him for teaching me the secret of success in interdisciplinary science: To be both intimately focused on one field while at the same time acquiring a large breadth of knowledge of others. I would also like to thank Alex Guenther for providing me with excellent learning and research opportunities all over the world, for financial support, and for teaching me the high value of simplicity in science and engineering. I would also like to extend a big thank you to Jim Greenberg and William Bradley at NCAR who mentored me while I designed and constructed a VOC preconcentration inlet. Since then, I have built a second inlet system as well as countless other devices. These experiences have demystified scientific equipment in my mind and for this I am extremely grateful. For our many discussions on oxygenated VOCs and for his tireless work in editing my proposals, papers, and dissertation, I would like to greatly thank Manuel Lerdau. I am happy to thank Eric Apel for his time preparing highly accurate gas standards for my research and Nicole Riemer for her atmospheric chemistry and boundary layer meteorology courses. A big shout out goes to my good friend Thomas Karl for his continuous support of my research in both the lab and the field and for inviting me on the NASA INTEX-B aircraft campaign which has permanently excited me about global atmospheric chemistry. I would also like to thank him for the many adventures that we have been on together and will surely go on in the future (sailing, mountain biking, power kiting, camping, rock climbing, etc.). Lastly, I would like to thank Mary Anne Carroll and everyone at the University of Michigan Biological Station for allowing me the opportunity to enter the BART program. The intimate connection with the natural environment, the extensive mentoring, the available instrumentation and facilities, the future collaborations and opportunities made available, as well as the interactions with the UMBS community has caused the BART experience to have a profound impact on my life as a scientist.

Curriculum Vita

EDUCATION

- PhD candidate in Atmospheric and Marine Sciences: Stony Brook University, Advisor: Dr. John Mak. Fall 2004-present. Dissertation: Stable carbon isotope ratio measurements of abundant oxygenated volatile organic compounds

- MS Atmospheric Chemistry: South Dakota School of Mines and Technology Advisor: Dr. Brad Baker. Spring 2003-Spring 2004. Thesis: Leaf, plant and ecosystem scale flux measurements of volatile organic compounds

- Graduate: Arizona State University, Tempe, AZ. Fall 1999-Fall 2000. ASU Center for the Study of Early Events in Photosynthesis.

- BS in Biochemistry: New York University, New York, NY. Fall 1997–spring 1999.

- Undergraduate: Colorado School of Mines, Golden, CO Fall 1995 – spring 1997.

RESEARCH EXPERIENCES

National Center for Atmospheric Research (NCAR), Boulder, CO, June 2007-present

Identify the biochemical pathways that lead to the production and consumption of acetaldehyde in plants and its relationship between photosynthesis and respiration. Determine the plant physiological and environmental controls over the exchange of acetaldehyde between plants and the atmosphere. Development of a canopy scale compensation point model for acetaldehyde.

Canopy Horizontal Array Turbulence Study (CHATS) field experiment, Dixon, CA, summer 2007

The objective of CHATS was to make spatial measurements of the velocity and scalar turbulence fields in a uniformly vegetated canopy, using arrays of sonic anemometer/thermometers augmented with fast response water vapor and carbon dioxide sensors. With this spatial information, the three-dimensional fields of velocity and scalar fluctuations were studied to quantify turbulence transport processes and coherent

structures throughout the canopy layer. My role was to help characterize the turbulent structure of the fields of aerosols and trace chemical species within and above the orchard canopy. Measurements included aerosol vertical concentration and flux measurements including species such as volatile organic compounds, ozone, NOx, NOy, H_2O, CO_2, etc.

Intercontinental Chemical Transport Experiment (INTEX-B), Seattle, WA, spring 2006

Participated in NASA/NCAR aircraft study designed to better understand the transport and transformation of gases and aerosols on transcontinental/intercontinental scales. Primary responsibilities were the operation of a PTR-MS instrument for fast VOC concentration measurements aboard the NCAR C-130 research airplane.

Stony Brook University, Stony Brook, NY, Fall 2004 – Spring 2008

Design, fabrication, and control of instrumentation for gas chromatography-combustion-isotope ratio mass spectrometry. Branch enclosure measurements of carbon isotope ratio signatures of oxygenated volatile organic compounds from various biological sources. Investigation into biochemical pathways and plant physiological controls over OVOC exchange.

University of Michigan Biological Station, Pellston, MI, summer 2005 and 2006

Part of NSF Biosphere Atmosphere Research and Training Fellowship. Participated in climate change, plant ecology, atmospheric chemistry, and science and society workshops. Conducted flux measurements of oxygenated volatile organic compounds from soils and litter by GC-FID. Testing of an experimental dehydration membrane for removing water vapor from VOCs in air samples.

National Center for Atmospheric Research (NCAR), Boulder, CO, summer 2004

Visiting scientist. Design and fabrication of a cryogenic preconcentration inlet for the analysis of volatile organic compounds by GC-MS.

Black Hills Ameriflux tower, South Dakota and Duke University Experimental Forrest (CELTIC study), summer 2003

Above canopy disjunct eddie covariance flux measurements of biogenic VOCs and vertically resolved flux estimates from inverse Lagrangian modeling. Comparison of VOC flux measurements between two Ionicon PTR-MS

instruments and a Fast Isoprene Sensor. Gas Chromatography/Proton Transfer Reaction Mass Spectrometry to verify identity of molecules.

Arizona State University, Tempe, AZ, Fall 1999 – Fall 2000

Participated in a group project to design a nanocrystaline solar cell using Gratzel Cell technology. We utilized both synthetic dye molecules and a purified recombinant Light Harvesting II protein from photosynthetic bacteria as photosensitizers to produce a light driven current.

MS research: Utilization of artificial photosynthetic reaction centers inserted in liposome membranes to pump protons in a light dependent manner into the interior of the vesicles creating a proton motive force. This was then used by the enzyme CFoF1 ATPsynthase to synthesize ATP from ADP and Pi. The ATP was then used be to power a large number of energy requiring biochemical processes such as the fixation of carbon dioxide.

University of Washington, Center for Nanotechnology, Seattle Washington, summer 2001

Project to develop light powered nanotrains for nanoscale transport of material by integrating biological and biomimetic components. Techniques included protein purification, surface nanopaterning with Teflon, liposome reconstitution of biological and biomimetic components, assembly of microscope flow cells, flowing in individual components and generating fluorescence microscopy movies.

New York University, NY, NY, Spring 1998 – Spring 1999

Worked for two semesters on a DNA nanotechnology experiments with Ned Seeman in the Chemistry Department at NYU. Techniques included DNA sequence design and self-assembly engineering, molecular modeling, operation of automated DNA synthesizers, gel electrophoresis, DNA sequencing, and atomic force microscopy to visualize the products of self-assembly .

Harvard University, Cambridge MA, summer 1997

Summer research internship in the Department of Organismic and Evolutionary Biology. Worked in Dan Hartl's lab on a fly genetics project. Using forward genetics techniques we investigated the ability of the transposase gene product to excise the transposable element mariner from a target sequence. Techniques involved fly mutagenesis, mutant collection, element amplification by PCR, bacterial transformation, gel electrophoresis, and DNA sequencing.

Colorado School of Mines, Golden CO, Spring 1997

Worked with Dr. Kevin Mandernack on microbial influences of biogeochemical cycles.

TEACHING EXPERIENCE

San Juan College, Farmington, New Mexico, Fall 2001-Fall 2002. Instructor in Introductory Chemistry, Math for Electronics, and Microbiology. Developed web based testing for all classes and was responsible for maintaining and demonstrating a Scanning Electron Microscope to students and faculty.

PUBLICATIONS AND PRESENTATIONS

Spring 2004-Spring 2006: President of the Stony Brook Outdoor Club. Lead extensive outdoor trips and gave lectures/demos on snow camping, snowboarding, power kiting, rock climbing, ultralight weight backpacking, mountain biking, and sea kayaking.

Papers

Karl T, Harley P, Guenther A, Jardine K et al. The bi-directional exchange of oxygenated VOCs between a loblolly pine (Pinus taeda) plantation and the atmosphere. Atmospheric Chemistry and Physics 5: 3015-3031 NOV 10 2005

Jardine K, Karl T, Guenther A., Lerdau M, Harley P, Mak J. Plant physiological and environmental controls over the exchange of acetaldehyde between plant canopies and the atmosphere. Biogeosciences, submitted.

Jardine K, Karl T, Guenther A., Lerdau M, Harley P, Mak J. Stable Acetaldehyde production in plants: Stress induced production from the peroxidation of fatty acids? Plant Cell and Environment, submitted.

Jardine K, Karl T, Guenther A., Lerdau M, Harley P, Mak J. Ethanolic fermentation and the pyruvate dehydrogenase bypass system in plants under aerobic conditions. Plant Cell and Environment, submitted.

Jardine K. The exchange of acetaldehyde, acetone, and isoprene with soils and litter in a northern Michigan forest. Manuscript in preparation.

Karl T, Jardine K, Guenther A. Temperature Stress Triggers Ecosystem-scale Emission of the Plant Hormone Methyl-Salicylate. Nature, submitted.

Poster Presentations/Talks

Jardine K, Sands D, Morris C, Christner B, Guenther A (2008) Microbial and biopolymer primary organic aerosols. **To be presented at the 2008 Workshop on Aerosols in the Amazon - Changes and their Consequences from Past and Future Human Activities. Manaus, Amazônia, Brazil.**

Jardine K, Guenther A, Karl T, Mak J (2007) [1] The exchange of acetaldehyde between the atmosphere and plant canopies [2] Stable carbon isotope composition of volatile organic compounds**. Presented at the 2007 Global Emission Inventory Activities (GEIA) Summer School, ile d'Oleron, France.**

Jardine K, Guenther A, Lerdau M, Mak J (2007) Biogenic hydrocarbons and the atmosphere: The bidirectional exchange of acetaldehyde. **Presented at the 2007 GRC meeting on biogenic hydrocarbons and the atmosphere, Ventura, California.**

Jardine K, Guenther A, Lerdau M, Mak J (2006) Stable Carbon Isotope Ratio Analysis of Methanol and Acetaldehyde from Live and Decaying Vegetation. **Presented at the 2006 IGAC meeting on Atmospheric Chemistry at the Interfaces, Cape Town, South Africa.**

Jardine K, Karl T, Baker B, Guenther A, (2004) Virtual Disjunct Eddy Covariance Flux Measurements of Biogenic Volatile Organic Compounds from the Duke Forest using proton transfer reaction mass spectrometry**. Presented at the 2004 American Geophysical Union meeting, San Francisco, CA.**

Jardine K, Belote A, Engelberth J, Baker B, (2004) Kinetics of Green Leaf Volatile Emissions and Endogenous Jasmonic Acid Accumulation in Wounded Alfalfa Field Plants. **Presented at the 2003 Gordon Research Conference on Hydrocarbons in the Atmosphere, Barga, Italy.**

Hess H, Jardine K, et al. (2000) Light powered molecular shuttles fueled by an artificial photosynthetic system. **Presented at the 2000 Forsight Conference on Molecular Nanotechnology in Palo Alto, CA.**

Jardine K et al. (2000) Light-driven carbon dioxide fixation catalyzed by pyruvate carboxylase and FoF1 ATPsynthase in an artificial photosynthetic membrane. **Presented at IPS 2000 conference on photochemical conversion and the storage of solar energy hosted by NREL in Aspen, CO.**

Gust D, Jardine K, et al. (2000) Mimicry of biological energy transduction using artificial photosynthetic membranes. **Presented at the 2000 American Chemical Society meeting.**

Jardine K et al. (1999) Developing high output photovoltaic devices based on biomimetic systems. **Presented at ninth western regional photosynthesis conference in Monterey, CA.**

Jardine K, Seeman N (1999) Design and self-assembly of two-dimensional crystals from tetra-crossover DNA molecules. **Presented at the 1999 New York State Undergraduate Research Conference, New York, NY.**

Jardine K, Seeman N (1998) Design and self-assembly of triple, tetra, and penta-crossover DNA molecules. **Presented at the 1998 New York State Undergraduate Research Conference, New York, NY.**

FELLOWSHIPS, GRANTS, and SCHOLARSHIPS

- University of Michigan 2 year NSF Fellowship in the Biosphere Atmosphere Research and Training program ($60,000 + tuition + travel + equipment).
- Young scientist award to attend workshop on Aerosols in the Amazon, Manaus, Brazil ($2000)
- Stony Brook University Presidential Scholarship ($2,000).
- Invited to attend 2 day workshop on Biogenic VOCs, Boulder, CO ($1000).
- National Center for Atmospheric Research Visiting Scientist Grant ($5,000).
- Gordon Research Conference early scientist award, Italy ($2,000).
- IGAC young scientist support, South Africa ($5000).
- GEIA summer school award, France ($1000).
- Marie Curie ILEAPS atmosphere biosphere instrumentation training course, Finland ($3000).
- Arizona State University 2 year NSF Research Training Grant in Optical Biomolecular Devices ($40,000).
- New York State Pell Grant ($10,000).
- NYU Undergraduate Research Scholarship ($3,000).
- Harvard University summer internship for undergraduates funding.
- John Nelson Stoddard Memorial National Scholarship (Full ride scholarship to the Colorado School of Mines ($44,000)).

Chapter 1: Introduction

1.1 Biogenic VOCs

Powered by ATP and NADPH produced during the light reactions of photosynthesis, plants fix atmospheric carbon dioxide into organic matter via the dark reactions of the Calvin cycle. This organic carbon can then be used as an energy source or converted into biomass such as carbohydrates, fatty acids, proteins, lipids, and nucleic acids. A small percentage of this carbon is released back into the atmosphere by plants in the form of volatile organic compounds (VOCs) and thus represents a reduction in net primary production for an ecosystem (Lerdau et al., 1997). Plants release thousands of VOCs into the atmosphere, which in total have been estimated to be several times higher than anthropogenic emissions (Guenther et al., 1995). These emissions have a strong influence on atmospheric chemistry including the oxidative capacity of the atmosphere and the formation of particulate matter. The vast collection of biogenic VOCs includes alkenes, aldehydes, ketones, ethers, esters, alcohols and acids (Arey et al., 1991; Arey et al., 1995; Fall et al., 1999; Kesselmeier and Staudt, 1999; Fall, 2003). Despite the dizzying array of known compounds, field research has shown that the dominant non methane VOCs emitted from plant canopies are restricted to terpenoid compounds (isoprene, monoterpenes, sesquiterpenes) and select oxygenated VOCs (acetaldehyde, acetone, methanol, 2-methyl-3-butenol) (Karl et al., 2002; Karl et al., 2004; Karl et al., 2004; Karl et al., 2005). While the biochemistry and emission controls of terpenoid production and emission are in general well understood, those of the oxygenated compounds are not.

1.2 Brief History of Biogenic VOCs

American research on biogenic VOCs began in the 1950's when Went, (1960) suggested that the "blue hazes" often seen in the Smokey Mountains were a result of the photochemical oxidation of biogenic VOCs. This stimulated studies motivated by the idea that biogenic VOCs play an important role in urban ozone formation and primarily focused on monoterpenes. Using branch enclosures, Rasmussen and Went, (1965) and Sanadze, (1957) discovered that many plant species also emit isoprene in large amounts. This spurred the systematic enclosure surveys of North American vegetation as thousands of leaves, branches, and plants were enclosed in jars, bags, and cuvettes of all sorts while above-canopy flux measurements of emissions from whole ecosystems were carried out (Rasmussen, 1972; Arnts et al., 1982; Greenberg et al., 1994; Guenther et al., 1996; Kinnee et al., 1997; Isebrands et al., 1999; Karlik et al., 2002). Following the first IGAC-GEIA natural VOC meeting in Boulder, Colorado in 1992, a global biogenic VOC emission inventory was developed (Guenther et al., 1995). From these modeling studies, it was estimated that 1150 Tg of carbon are released

into the atmosphere every year in the form of biogenic VOCs from vegetation. However, the largest uncertainties in global estimates of biogenic VOC emissions are associated with the biogenic oxygenated VOCs like acetaldehyde, methanol, and acetone. In the mass balance of biogenic VOCs from woodland landscapes in the US (Guenther et al., 1996), emissions were composed of approximately 58% isoprene, 18% terpenes, and 24% other VOCs (Other VOCs consist mainly of oxygenated VOCs). Models describing seasonal and spatial variations in biogenic VOC emissions were then developed based on leaf level emission studies of isoprene (Guenther, 1997). Constrained by top down estimates from satellite measurements of formaldehyde (a major oxidation product of isoprene), new enclosure measurements, and new in situ canopy scale field measurements, improvements in the bottom up emission estimates of isoprene were made which have now replaced older algorithms (Guenther et al., 2006). Unfortunately, the oxygenated VOCs have not been given as much attention as isoprene. While leaf level emission studies of isoprene can relatively easily be scaled up to the ecosystem scale with high accuracy, similar exercises with oxygenated VOCs are not as successful. This is partially due to the complex array of both primary and secondary sources within canopies, the presence of significant sinks within canopies, and a lack of knowledge of what processes contribute to their metabolism and how environmental and plant physiological variables influence their exchange with the atmosphere. While isoprene dominates global emissions of biogenic VOCs, it is emitted in scant quantities by many ecosystems lacking the proper plant genetics (the isoprene synthase gene). In contrast, all plants studied to date emit methanol, acetone, and acetaldehyde.

1.3 Acetaldehyde

Acetaldehyde is known to be both emitted and consumed by live plants and is thought to represent a "leaky intermediate" in biochemical pathways that both produce and use it (Fall, 2003). Because it is highly volatile and only moderately water soluble (boiling point of 21^{o} C and Henry's Law constant of 7.0 Pa m^{-3} mol^{-1}), it can partition to the gas phase where it can then escape the plant. On the other hand, if the biological sink(s) draw the internal gas phase acetaldehyde concentrations below the ambient concentration, then net uptake from the atmosphere will occur. The atmospheric concentration at which there is no net exchange is called the compensation point.

From an evolutionary viewpoint, plants have evolved the ability to use VOCs for many important physiological and ecological functions (Lerdau, 2002; Lerdau and Gray, 2003). For example, acetaldehyde can have potent antimicrobial properties that may help prevent infections (Utama, 2002) and may be involved in a more sophisticated role of altering gene expression patterns during the

hypersensitive response (HR). Acetaldehyde is a particularly important compound with respect to biosphere-atmosphere interactions because it lies at the heart of both atmospheric chemistry and plant biochemistry. Virtually all alkane and alkene compounds of both biogenic and anthropogenic origin in the atmosphere form acetaldehyde in high yields as an intermediate during their oxidation. In plants, acetaldehyde also appears to have a central role in integrating the carbon metabolisms of photosynthesis, fermentation, and respiration and supporting the biosynthesis of fatty acids, amino acids, and terpenoid compounds.

Acetaldehyde is a ubiquitous hydrocarbon in the atmosphere. It is present everywhere from polluted to pristine atmospheres ranging from megacities to remote forested, polar, and marine air masses. Although its concentrations and lifetimes tend to be low (concentrations < 1 ppbv and lifetimes < 1 day), it is highly reactive and participates in gas phase chemistry, photochemistry, and heterogeneous reactions. These reactions can lead to the production of a wide variety of important atmospheric species including formaldehyde, free radicals, ozone, peroxyacetyl nitrate (PAN), and particulate matter that may significantly influence air quality and climate. Partially due to the development of the ultra fast and sensitive proton transfer reaction mass spectrometer (PTR-MS), global budgets have recently been estimated for the oxygenated VOCs methanol (Jacob et al., 2005) and acetone (Marandino et al., 2005). However, a quantitative global budget of acetaldehyde has not been produced due to a complex array of primary and secondary sources of both biogenic and anthropogenic origin as well as a variety of atmospheric sinks including photolysis, oxidation, and deposition. In addition, the magnitude of many of the sources and sinks remains highly uncertain. The role of the biosphere is particularly uncertain due to the presence of both sources and sinks within plant canopies whose identities and controls are poorly understood. At the leaf level, it is known that plants can both emit and take up acetaldehyde, but the underlying biochemical pathways that give rise to acetaldehyde metabolism and how environmental variables influence them are not known. The role of plant litter and soils in the exchange of acetaldehyde with the atmosphere also remains unclear. Our lack of understanding is quickly revealed by the fact that we cannot currently answer the fundamental question of why some ecosystems behave as net sources while others act as net sinks. Therefore, the role of the biosphere in the exchange of acetaldehyde with the atmosphere is not accurately represented in current emission models such as the Model of Emissions of Gases and Aerosols from Nature (MEGAN) developed at NCAR (Guenther et al., 2006) or in regional air quality models such as the community multi-scale air quality (CMAQ) modeling system developed at the EPA (Mathur et al., 2005). However, because the majority of Earth's terrestrial surface is covered by plant canopies, the possible impact of acetaldehyde exchange on atmospheric chemistry, the carbon cycle, and climate is potentially significant but

highly uncertain. The goal of this dissertation is to alleviate this knowledge gap by providing an understanding of the biological, chemical, and physical processes that control the exchange of acetaldehyde with the atmosphere, and by making flux measurements of acetaldehyde between the atmosphere and plants, litter, soils and entire ecosystems. Finally, suggestions are made for modeling the exchange of acetaldehyde with plant canopies based on environmental variables such as light and temperature and their effect on the acetaldehyde compensation point and stomatal conductance.

1.4 Sources and Sinks of Acetaldehyde

Oxygenated VOCs have recently been shown to be of surprisingly high abundance in the global troposphere. In one study over the Atlantic, methanol, acetaldehyde, and acetone contributed up to 85% of the total mass of non-methane hydrocarbons and 80% of the OH organic sink (Lewis, 2005). Unfortunately, little is known about the global sources of acetaldehyde and no global inventory is available. Singh et al., (2004) estimated that the total global annual source of oxygenated VOCs to the atmosphere is extremely high but poorly constrained at approximately 150-500 Tg C yr^{-1}. Acetaldehyde in the troposphere is derived from a highly complex array of sources including primary and secondary biogenic and anthropogenic sources, but quantitative knowledge is sparse (Guenther et al., 1995). The known sources include direct emissions from live and decaying terrestrial vegetation, secondary photochemical production from both biogenic and anthropogenic precursors, biomass burning, as well as anthropogenic sources such as evaporation of solvents and the incomplete combustion of fossil fuels. Unfortunately, while biodiesel has a reduced emission of particulate matter and total hydrocarbons, the emissions of acetaldehyde is enhanced (Pang et al., 2006; Shi et al., 2006). However, the total primary anthropogenic emissions are considered to be minor (<1 Tg/yr) (Singh et al., 2004). On the other hand, biogenic emissions from plants appear to be substantial with acetaldehyde emissions of up to 0.05 % of assimilated carbon (Kesselmeier et al., 1997). Scaling this up to global net primary production results in an emission source from the biosphere of 25-45 Tg/yr. Taking average emission measurements from various plant enclosures reported in the literature, Singh et al., (2004) estimated a biogenic source of 13-77 Tg C yr^{-1}. These estimates remain highly speculative given that plants also contain a sink for acetaldehyde and are known to emit acetaldehyde in much higher rates under conditions such as root flooding (Holzinger et al., 2000), light dark transitions (Karl et al., 2002), and stresses such as mechanical wounding, desiccation, and ozone fumigation (de Gouw et al., 1999). In addition, the role of decaying litter remains unclear, but also appears to be a significant source (Warneke et al., 1999; Schade and

Goldstein, 2001). Emissions from biomass burning have been estimated to be as low as 4 Tg/yr (Andreae and Merlet, 2001) to as high as 11 Tg/yr (Holzinger et al., 1999).

Acetaldehyde can also be produced as a secondary oxidation product in the atmosphere from a large number of biogenic and anthropogenic VOCs such as from the reaction of ozone with isoprene (yield 3%), Z-3-hexenol (yield 13%), and Z-3-hexenyl acetate (yield 5%) (Atkinson and Arey, 2003). Because a large number of anthropogenic compounds can also contribute to the secondary production of acetaldehyde, studying this important compound can provide important information on fundamental atmospheric oxidation processes. Virtually all >C1 alkanes and >C2 alkenes produce acetaldehyde as an intermediate during their oxidation in the atmosphere, with some having yields of greater than 50% (Warneke et al., 1999)! According to a recent air quality modeling study of toxic VOCs in the US, the majority of atmospheric acetaldehyde is derived from secondary photochemical sources (Luecken et al., 2006) and this may explain the surprisingly high concentrations of acetaldehyde in remote locations such as over the Pacific and Atlantic Oceans. Using a simple chemistry scheme for atmospheric chemistry, Singh et al., (2004) estimated that the secondary production from alkane/alkene oxidation is 20-50 Tg/yr. Another paper suggested that the ocean is a major source of acetaldehyde with emissions of 125 Tg/yr (Singh et al., 2003), clearly dominating all other sources. However, more recent aircraft based studies instead have shown the ocean is instead a sink for acetaldehyde and not a source.

Currently, it is thought that the major sink for acetaldehyde in the atmosphere is by reaction with OH radicals (Li et al., 2004; Taylor et al., 2006) and photolysis (Kurosaki, 2006). In addition, gas phase reactions (Becerra et al., 2001), heterogeneous reactions (Li et al., 2001), and dry deposition (Warneke et al., 2002) may also play a role. The ability of plant canopies to act as a sink for tropospheric acetaldehyde is becoming clear with several canopy scale exchange measurements showing net uptake (Karl, 2005). However, the global significance of this sink is unknown but is potentially significant. Although various field studies have demonstrated dry deposition to plant canopies, the relative roles of uptake via plant stomata versus dry deposition onto leaf surfaces has not been critically examined. This difference is significant because if uptake followed by metabolic consumption within the plant dominates, this may significantly contribute to the fixed carbon and energy supplies of the plant.

1.5 Atmospheric Chemistry of Acetaldehyde

The atmospheric chemistry of carbonyl compounds like acetaldehyde is very interesting because they are strongly affected by chemical and physical processes (Ceron et al., 2006). Other than NO_2, they are the most abundant photolized compounds in the atmosphere and therefore they greatly contribute to the production of free radicals in polluted regions. Acetaldehyde processing in the atmosphere has a major effect on the oxidative capacity of the atmosphere by influencing the HOx radical budget. In the remote and free troposphere, if the reaction with OH dominates as the major sink, then acetaldehyde acts as a net sink for OH. However, if photolysis dominates it acts as a source for HO_2 (Sommariva et al., 2006). If the first scenario manifests itself leading to a net destruction of OH, this may result in a longer lifetime of greenhouse gases like methane leading to enhanced global warming (Brasseur, 1991). A recent box model aimed at modeling the HOx budget demonstrated that the accuracy of the model for a coastal location was greatly improved when it was constrained to oxygenated VOCs (Sommariva et al., 2006). These results demonstrate the importance of acetaldehyde for radical budgets in the atmosphere.

VOCs in general can have a large impact on the tropospheric production of ozone (Trainer et al., 1987; Chameides et al., 1988) which is formed by the photoxidation of VOCs in the presence of nitrogen oxides (NO_x) (Haagensmit and Fox, 1956). Because acetaldehyde is relatively reactive and is a major carbonyl in both suburban and urban air, it contributes considerably to ground level ozone. Ground level ozone is toxic to animals and plants at elevated levels and there is strong evidence that acetaldehyde itself is a carcinogen in humans which is a serious concern for public health in cities with polluted atmospheres. Therefore the EPA has classified acetaldehyde as a hazardous air pollutant (HAP) and has included it in toxic air monitoring stations across the country. When measured fluxes of oxygenated VOCs above a subalpine forest site in Colorado were included in a photochemical box model, a 10-40% increase in local tropospheric ozone concentrations resulted (Karl et al., 2002).

The oxidation of acetaldehyde in the atmosphere can also lead to the production of acetic acid, which can acidify the atmosphere and may be involved in secondary organic aerosol formation (Andreae and Crutzen, 1997; Bode, 1997). Aerosols have both direct and indirect effects on Earth's climate and participate in heterogeneous reactions (Hamilton *et al.*, 2004). A modeling study recently concluded that acetaldehyde can add to the mass of acidic aerosol particles containing sulfuric acid by Aldol type condensation reactions and experimental evidence has emerged for this (Noziere and Riemer, 2003). A new exciting experiment has revealed that the photolysis products of acetaldehyde alone can produce secondary organic aerosols (Dubtsov et al., 2000; Skubnevskaya et al.,

2004). The absorption cross-section and the quantum yield of photodissociation are available for acetaldehyde although no reaction with ozone has been observed (Atkinson and Arey, 2003). Interestingly, detailed analysis of the rate constant for the reaction of acetaldehyde with OH shows a negative temperature dependence at temperatures below room temperature but increase with temperature at temperatures above room temperature. Although this phenomenon is not fully understood, what is known is that the hydrogen abstraction by OH and NO_3 occurs almost exclusively with the CHO group and not the CH_3 group of acetaldehyde (CH_3CHO). The resulting Acyl Radical CH_3CO reacts with O_2 to form an acyl peroxy radical $CH_3C(O)OO$. Reaction of the acyl peroxy radical with NO produces NO_2, CO_2, and the methyl radical. NO_2 can go on to produce tropospheric ozone. Reaction of acyl peroxy radical with NO_2 can result in the formation of the peroxyacetyl nitrate (PAN) $CH_3C(O)OONO_2$ which can have a negative effect on human and plant health. PAN can be transported long distances where it can thermally break down to release ozone precursors and therefore affect air quality in regions distant from the source (Atkinson and Arey, 2003).

Chapter 2: Experimental Methods

2.1 Abstract

Measurements of trace gas concentrations in the atmosphere are critical towards the goal of better understanding the interactions between atmospheric chemistry, air quality, and climate. For example, measurements of trace gas concentrations can provide information on emission, transport, chemistry, and deposition processes. However, this poses a technical challenge because the species of interest is usually present in very trace quantities and an extremely sensitive instrument is required to directly measure it. In addition, the compound of interest is usually in the presence of a large number of other substances, many of which have similar chemical and physical properties and may be present in much higher concentrations. Because of its low abundance, high reactivity, and slight water solubility, acetaldehyde is an extremely difficult compound to quantify in the atmosphere. Many studies referenced in this dissertation measured gas phase acetaldehyde concentrations by derivitization with 2,4-dinitrophenylhydrazine (DNPH)-coated solid sorbents. These measurements typically require very large volumes of air to be passed over the solid sorbents and therefore lead to long sampling times and poor time resolution. Recent evidence shows that while collection efficiencies on DNPH-coated sorbents for formaldehyde can be high, those for acetaldehyde can be as low as 1% (Herrington et al., 2007). Unfortunately, it has been widely assumed in the literature that collection efficiencies are 100% with this technique.

The direct measurement of acetaldehyde by gas chromatography and mass spectrometry techniques has greatly improved our ability to accurately measure trace concentrations of this important VOC in complex air samples. In this dissertation, concentration measurements of acetaldehyde, acetic acid, ethanol, acetone, methanol, and isoprene were made by a gas chromatograph with a flame ionization detector (GC-FID) and the extremely fast and sensitive Proton Transfer Reaction-Mass Spectrometer (PTR-MS). Stable carbon isotope ratio measurements of methanol and acetaldehyde were made with a gas chromatograph-combustion-isotope ratio mass spectrometer (GC-C-IRMS). The GC systems were interfaced with custom designed cryogenic VOC preconcentration units. These units were designed, built, interfaced and automated with help from Jim Greenberg and William Bradley at NCAR.

2.2 Plants

Potted poplar (*Populus deltoids*) individuals were obtained from the Stony Brook University greenhouse (Stony Brook, NY), the University of Colorado greenhouse (Boulder, CO), and the National Center for Atmospheric Research (NCAR) greenhouse (Boulder, CO). Potted holly oak (*Quercus ilex*) was also obtained from the NCAR greenhouse. White oak (*Quercus rubra*), red maple (*Acer rubrum*), and sassafras (*Sassafras albidum*) branches were obtained from

field plants in the forest surrounding the Marine Science Research Center at Stony Brook University. Post senescent red maple leaves were obtained from the forest floor immediately following the dropping of leaves by trees during the fall and continued until early winter.

2.3 Zero Air Generator and VOC standards

The production of zero air (air lacking hydrocarbons) is necessary in order to obtain a background signal for the GC-FID, GC-C-IRMS, and PTR-MS instruments. In addition, zero air is often needed as the air which enters plant branch enclosures and is used to dilute VOC standards for instrument calibration purposes. Many zero air sources are unsuitable for use with plant enclosures due to the lack of carbon dioxide and water vapor. Also, because purchasing ultra high purity zero air in cylinders is very expensive, I decided to build my own. In order to generate zero air both in the laboratory and in the field I decided to make it relatively portable and include components necessary for the dilution of VOC standards. The basics of this design are platinum coated silicagel beads packed in a ½"x 12" stainless steel tube caped with 1 micron stainless steel filters. This catalytic converter is heated to 400^{o} C with a heat rope and temperature controller while room air or compressed air is allowed to pass through it with a maximum flow rate of 1.0 L min^{-1}. Flows higher than this were shown to lead to incomplete VOC oxidation. This air can then be directly used in plant enclosure studies due to the presence of room water and carbon dioxide levels or used to dilute a concentrated VOC standard as shown below. With the use of a 1-10 ml min^{-1} mass flow controller (MKS), the system produced dilution factors between 0.001 and 0.01. Therefore, this system allowed for the generation of between 2.0 and 19.8 ppbv (acetaldehyde) and 3.0 and 29.7 ppbv (methanol and acetone) from 2.0 ppmv (acetaldehyde) and 3.0 ppmv (methanol and acetone) gravimetrically prepared standards (Apel-Riemer, Denver). Higher and lower concentrations were made by injecting known volumes of the concentrated standard into 2 L static Tedlar sample bags. During instrument calibration, the dynamic dilution system was allowed to run for 1-2 hours prior to measurements to allow for VOC equilibration with tubing and to allow the catalytic converter to "warm up" to complete combustion efficiencies. 3-5 calibration concentrations were generated by the dynamic dilution system with multiple measurements at each concentration to assess instrument variability. For all experiments presented in this dissertation, instrument blanks were run by closing the solenoid valve on the MFC supplying the VOC standard. The tubing and/or enclosure is flushed continuously with zero air and "blanks" are then run. All flow rates are either calibrated with a Drycal automatic flow rate measuring device or manually using a bubble meter (average of three runs).

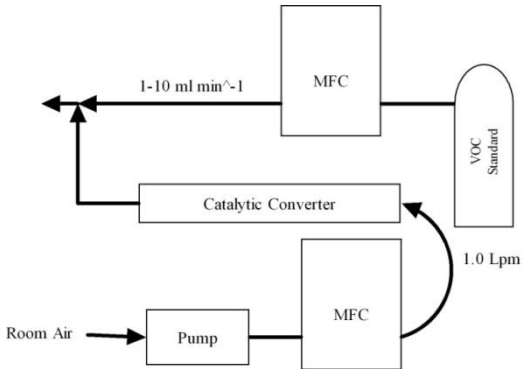

Figure 1: Plumbing diagram of the zero air generator and dynamic VOC standard dilution system.

2.4 Development of a GC-C-IRMS system for Compound Specific Stable Carbon Isotope Ratio Measurements of Volatile Organic Compounds

The direct coupling of a gas chromatograph (GC) and a combustion chamber with a continuous-flow isotope ratio mass spectrometer (IRMS) allows for compound specific $\delta^{13}C$ measurements of VOCs (Rudolph et al., 1997). This technique was recently used in the trace gas analysis laboratory at Stony Brook University (where $\delta^{13}C$ measurements of VOCs where made in this dissertation) to demonstrate a shift in carbon sources for isoprene production during plant stress events (Funk et al., 2004). Another example from this laboratory, is the development of a technique for the determination of $\delta^{13}C$ and $\delta^{18}O$ in atmospheric carbon monoxide (Mak et al., 1987; Mak and Brenninkmeijer, 1994; Mak and Yang, 1998) and the deuterium/hydrogen ratio in atmospheric hydrogen (Rhee et al., 2004).

While concentration measurements of oxygenated VOCs like methanol and acetaldehyde are difficult, stable carbon isotope ratios measurements are extremely difficult. Some reasons for this include the loss of sample at the open split (interface between combustion oven and IRMS) and strict requirements of well separated, sharp, symmetric chromatography peaks with stable baselines. In addition, because we are interested in the carbon isotopic composition of the original sample, it is imperative that fractionation does not occur during sample processing. In light of the low collection efficiencies of DNPH cartridges for acetaldehyde, this technique would not be a good choice because of possible fractionation during collection. During $\delta\ ^{13}C$ measurements of acetaldehyde Wen et al., (2005) did not take this into account although they did correct for fractionation that occurred due to derivitization because of the introduction of additional carbon atoms not from acetaldehyde. However, using the derivitization technique, the volume required for an isotopic ratio measurement of ambient air required a flow rate of 2 L min^{-1} for 24 hours through a DNPH cartridge resulting in a total volume of 2280 Liters! However, no correction was made for an actual

collection efficiency of less than 100%. In this dissertation, I greatly improve the time resolution of $\delta^{13}C$ measurements without the need for derivitization by coupling traditional cryogenic preconcentration of VOCs from ambient air (Greenberg and Zimmerman, 1984) to a GC-C-IRMS system. The time resolution was reduced to approximately 30 minutes by relaxing the required volume needed for each sample to 2.5 L.

A custom VOC pre-concentration system was built in order to preconcentrate gas phase methanol and acetaldehyde as well as separate them from the common components of air (N_2, O_2, Ar) and trace species including water and carbon dioxide. All tubing and traps are composed of fused silica-lined stainless steel tubing (Restek, Bellefonte, PA) or Teflon. Stainless steel switching valves (VICI, Houston, TX) are heated to 100 ^oC and the tubing where the sample passes through is continuously heated to 200 ^oC using a heating rope (Omega) and a Variac set to 60 VAC. The preconcentration system was fully automated with Labview 6.0 and Chemstation 10.01. The sample is drawn into the preconcentration system by a diaphragm pump (Pfeiffer Vacuum, Nashua, NH) connected to a mass flow controller (Omega, Stamford, CT) at 250 mL min^{-1} for 10 minutes resulting in a sampled volume of 2.5 L. The air sample first passes through a drying trap (a 3 foot coil of 1/8" O.D. Teflon tubing) held at 0 ^oC in order to condense a large percentage of the water vapor. This step was shown to not affect the concentration of acetaldehyde although alternate methods using solid adsorbents had deleterious effects on acetaldehyde. Johnson and Dawson, (1993) found that the equilibrium carbon fractionation associated with the partitioning of gaseous formic acid into an aqueous phase is negligible. The authors concluded that the carbon isotope signatures of oxygenated organics are not affected by wet deposition. Because formic acid is much more soluble than acetaldehyde (Henry's law constant value of 0.0176 for formic acid and 7.00 for acetaldehyde (Niinemets and Reichstein, 2003), carbon isotope fractionation during the partitioning of acetaldehyde into the condensed water during this step is most likely negligible. The sample is then passed through a hydrocarbon trap (1/4" O.D. x 9" Silcosteel tube packed with TENAX-TA (Sigma-Aldrich)) held at -50 ^oC with liquid nitrogen through the use of an automated on/off valve. Hydrocarbon trap temperatures above 0 ^oC were shown to strongly fractionate acetaldehyde due to an incomplete trapping efficiency (acetaldehyde breakthrough). During this step, VOCs are quantitatively trapped while the common components of air are not (N_2, O_2, Ar). At these low temperatures, some carbon dioxide is trapped although it is separated from acetaldehyde during the subsequent chromatographic step. The concentrated sample is then injected directly onto the GC column (0.53mm x 30m: RTX-624) by rapidly heating the hydrocarbon trap to 200 ^oC for five minutes and back flushing the trap with UHP helium at a flow rate of 1.0 ml min^{-1}. After the injection, the preconcentration

system is continuously back-flushed with UHP helium at a flow rate of 25 ml min^{-1} until the next sample is ready for collection.

In order to improve peak separation and shape, a cryofocusing trap was used which involved the emersion of two small loops of the GC column at the beginning immersed in a liquid nitrogen bath during the time that the sample is transferred from the Tenax-TA trap to the column. The cryofocusing trap is then rapidly heated by removing the liquid nitrogen bath and the VOCs are subsequently separated by the GC column. During the chromatographic step, the GC oven (6890 GC, Agilent Technologies, Santa Clara , CA) under the control of the Chemstation 10.01 software was maintained at 25 ^{o}C for 10 min and then rapidly heated to 200 ^{o}C for two minutes at the end of the run to "bake out" the GC column. Eluents of the GC column then undergo oxidation to water and carbon dioxide in an alumina tube packed with CuO, NiO, and Pt wires held at 950 ^{o}C. The oxidation oven was reoxidized weekly with molecular oxygen at 950 ^{o}C. The oxidation products then pass through a Nafion drying membrane (Permapure Inc., Toms River, NJ) in order to remove the water from the VOC derived CO_2.

Chromatographic peaks are introduced into an isotope ratio mass spectrometer (IRMS) (Finnigan Delta Plus; Finnigan MAT, Bremen, Germany) through an open split system providing ~0.5 mL min^{-1} to the ion source. Prior to the arrival of the acetaldehyde peak at the IRMS, three injections of a carbon dioxide standard of known isotopic composition (-42.7 ‰) was preformed automatically into the IRMS using the ISODAT NT 2.0 software in order to calibrate the $\delta^{13}C$ measurement. The pressure of the reference carbon dioxide was adjusted prior to the run to approximately match the expected peak height of the sample. Peaks were identified based on retention time relative to calibration standards (acetaldehyde, methanol, acetone, isoprene). Isotope data is expressed in the conventional δ notation in units of per mil (‰),

$$\delta^{13}C = \frac{R_{sample} - R_{standard}}{R_{standard}} \cdot 1000$$

where R is the ratio of the peak area for m/z 45 ($^{13}CO_2$) to m/z 44 ($^{12}CO_2$) for sample and standard (V-PDB-CO_2). The $\delta^{13}C$ values were calculated by the ISODAT NT 2.0 software and a manual correction based on a linear dependence of $\delta^{13}C$ on the difference in peak heights between the reference carbon dioxide peak and the VOC derived carbon dioxide peak was applied. The precision of the instrument was measured to be between 0.2 and 1.0 ‰ (V-PDB) determined by calculating the standard deviation of $\delta^{13}C$ values from multiple measurements of a 30 ppbv acetaldehyde standard diluted in zero air with a dynamic dilution system. Due to losses at the split (50 %) and IRMS sensitivity problems, the minimum acetaldehyde concentration needed to produce a 1.0 volt peak for an accurate $\delta^{13}C$

measurement was determined to be ~10 ppbv. Peaks smaller than 0.5 V were not included in the analysis.

Brief GC-C-IRMS Development History: Towards High Peak Resolution, Sensitivity, and Precision

1) Reduced column flow from 3 mL/min to 1 mL/min. Result: increased amount of sample entering IRMS by ~300%. However, peaks became broad and many were overlapping.
2) Designed, built, and installed an automated cryogenic cooler for the Tenax-TA hydrocarbon trap. Result: Collections at -50^{o}C eliminated VOC breakthrough and fractionation during sample collection. Peak resolution as well as peak shape was greatly improved. Width (30 seconds compared with 60 seconds) and height (1.0 V with 10 ppbv Acetaldehyde compared with 1.0 V with 120 ppbv Acetaldehyde).
3) Used first part of column (two small loops) in liquid nitrogen as a cryofocus trap. Increased peak separation, sharpened peaks, and increased peak height significantly.
4) The above changes lead to increased precision measurements from 1-3 ‰ before changes to 0.2-0.9 ‰ after changes and decreased the minimum required concentration for a 1.0 V peak from 120 ppbv to 10 ppbv.

It should be noted here that the absolute values of the stable carbon isotope ratios reported in this dissertation may not be highly accurate since they were obtained by comparison with an internal CO_2 standard of known isotopic composition with respect to PDB. Among other reasons, an offset is expected between the measured isotope ratios and the actual ratios because this CO_2 standard did not pass through the preconcentration system, the GC column, and is not derived from the oxidation of acetaldehyde. On the other head, relative changes in the measured isotopic ratio from sample to sample are expected to be accurate.

Figure 2: GC-C-IRMS instrument at Stony Brook University

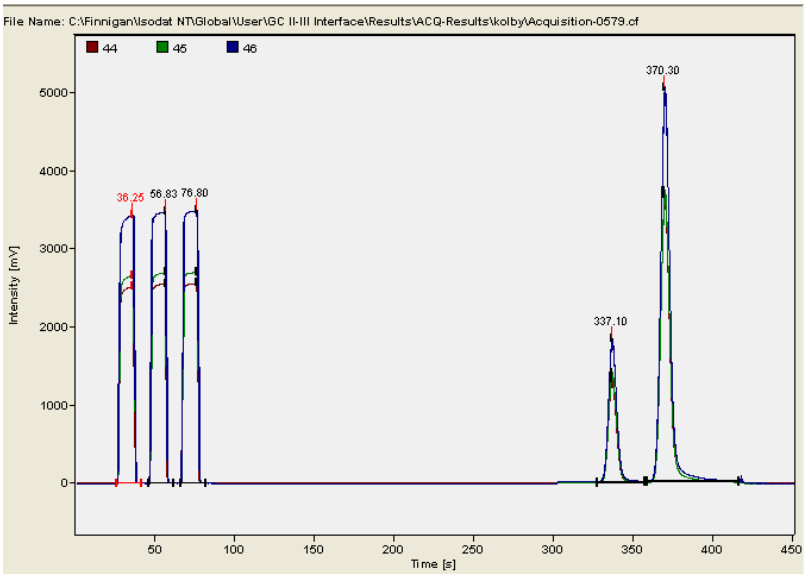

Figure 3: Example of GC-C-IRMS chromatograph of acetaldehyde (first peak) and methanol (second peak) from a plant enclosure sample.

Note that following the addition of the three carbon dioxide reference peaks, the split is off in order to prevent the overwhelming amount of carbon dioxide collected on the Tenax-TA trap from entering the IRMS. 40 seconds prior to the arrival of the first peak (acetaldehyde), the split is turned on.

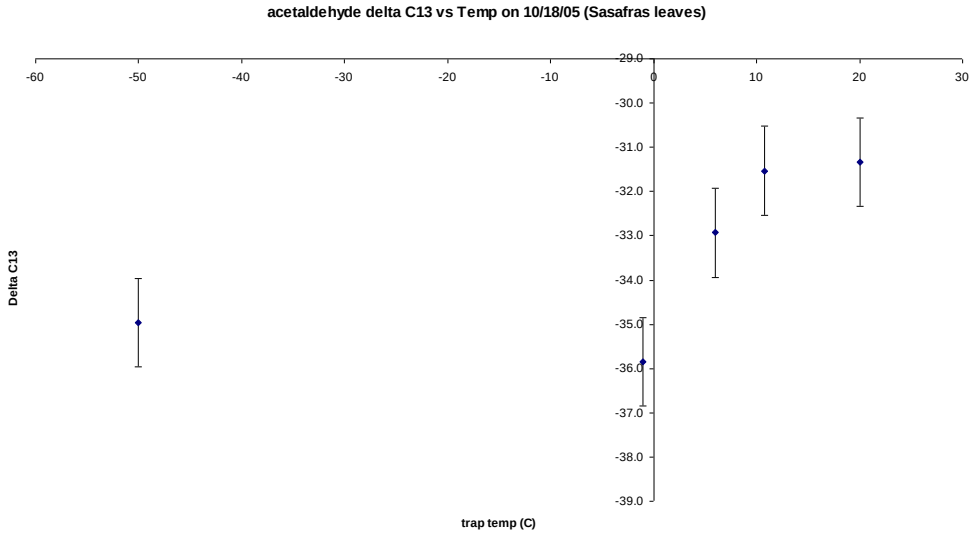

Figure 4: $\delta^{13}C$ measurements of acetaldehyde emitted from wounded Sassafras leaves as a function of trap temperature.

Tenax-TA trap temperatures above 0 ^{o}C strongly fractionate the sample due to breakthrough. However, below 0 ^{o}C no fractionation is apparent. This is caused by the preferential adsorption of the heavier isotopologues of acetaldehyde due to incomplete trapping (breakthrough). Lower temperatures increases the breakthrough volume allowing for nearly complete trapping efficiencies at temperatures below 0^{o} C. Therefore, during sample collection by GC-C-IRMS, trap temperatures were set to -50^{o}C.

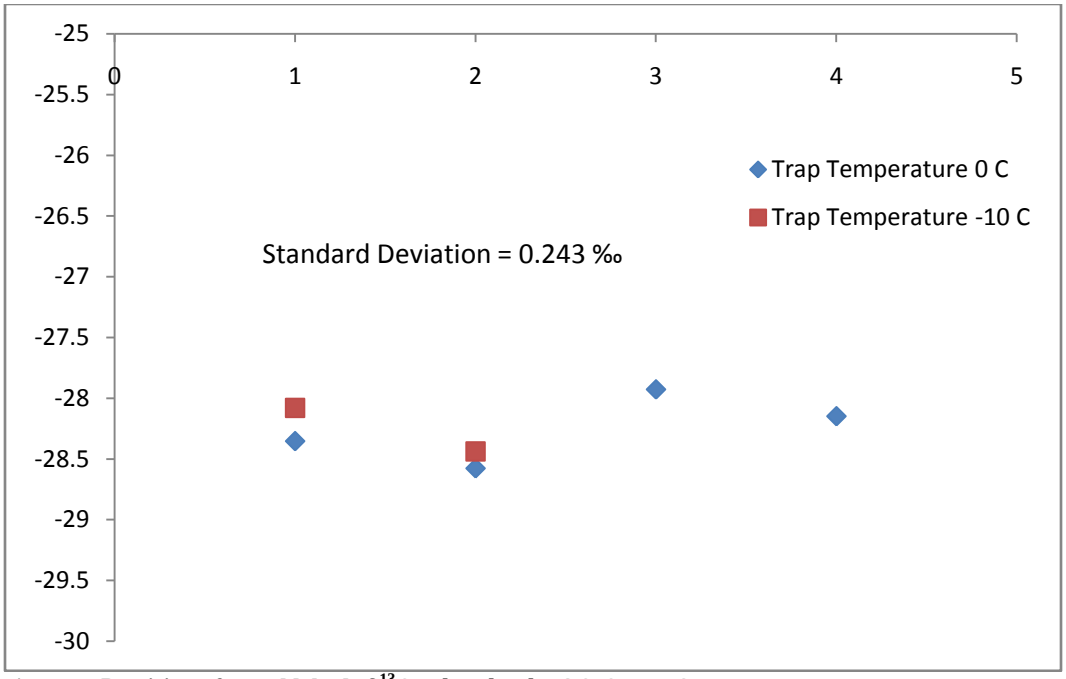

Figure 5: Precision of acetaldehyde $\delta^{13}C$ values by the GC-C-IRMS.

Repeated measurements of $\delta^{13}C$ values of 29 ppbv acetaldehyde standard by GG-C-IRMS showing precision of 0.2 ‰. $\delta^{13}C$ values are also shown to be independent of trap temperature below 0°C.

Average $\delta^{13}C$ (‰)	Standard Deviation (‰)	Number of Samples	Date
-27.931	0.472	2	3/7/2007
-26.651	0.192	6	3/20/2007
-28.253	0.243	6	3/23/2007
-28.985	0.405	15	4/14/2007
-28.264	0.969	9	4/16/2007
-27.598	0.325	5	4/19/2007
-27.944	0.500	13	4/23/2007

Statistics for Entire Data Set (3/7-4/23)
Average $\delta^{13}C$ value -28.145 ‰
Standard Deviation of $\delta^{13}C$ values 0.856 ‰

Figure 6: Summary of $\delta^{13}C$ values from repeated measurements of a 29 ppbv acetaldehyde standard between 3/20/2007 and 4/23/2007.

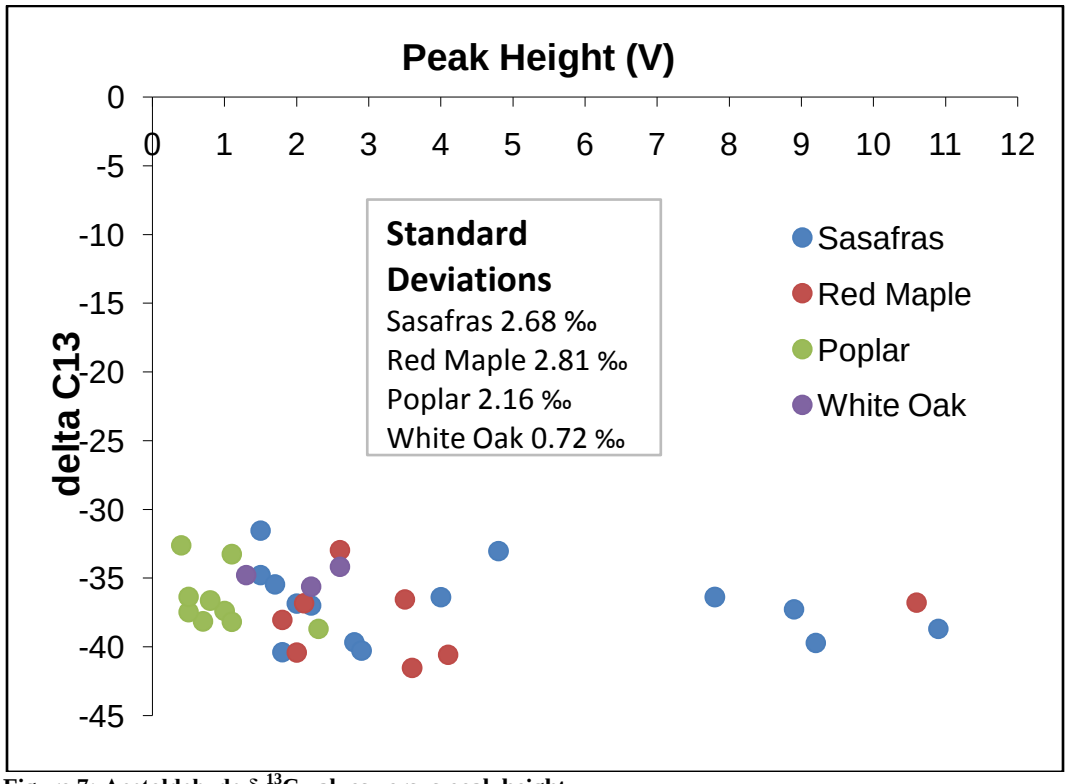

Figure 7: Acetaldehyde $\delta^{13}C$ values versus peak height.

Prior to December 2006, for a given reference CO_2 peak height (1.0 V) there is no dependence of the acetaldehyde $\delta\ ^{13}C$ values from plant samples and peak height. The variability in $\delta\ ^{13}C$ values is likely related to natural variability between leaves of the same species and between different tree species.

2.5 Proton Transfer Reaction-Mass Spectrometry (PTR-MS)

In recent years, gas chromatography separation coupled to various detection schemes of trace gas compounds has been used to quantitatively measure ultra low concentrations of hydrocarbons as low as a few parts per trillion. However, because of the low time resolution of these methods of detection, they are only useful for studying slow processes. Because the temporal and spatial concentrations of many compounds change rapidly due to fast-localized processes, these techniques are not suitable for their quantification. By coupling the concept of chemical ionization (CI) with the invention by Ferguson of the Flow Drift Tube (FDT) (Mcfarlan.M et al., 1973), a new fast analytical technique was described (Lindinger and Hansel, 1997) to overcome this problem. CI mass spectroscopy uses a primary ionized chemical (In this case hydronium ions) to ionize the sample gas molecules. In comparison to more traditional electron impact techniques (EI), CI ionizes the sample gas molecules at a lower energy, which leads to a much lower fragmentation probability. This allows for the quantification of multiple gas compounds simultaneously, whereas a complicated and overlapping mass spectrum is produced when multiple molecules are ionized by EI. Therefore, quantification of multiple VOCs by EI is difficult without prior compound separation by chromatography. Softer ionization techniques like proton transfer reactions on the other hand will produce ions with little fragmentation. Thus, most volatile compounds with a proton affinity higher than H_3O^+ can be quantified by measuring the m/z value corresponding to the molecular weight of the compound plus one. The proton transfer reactions that occur in the drift tube were designed such that the reactions have sufficient time to reach completion, as long the proton affinity of the VOC is higher than H_3O^+. Because the proton affinity of a previously protonated VOC for an additional proton is lower than that the proton affinity of H_3O^+, ions with multiple charges are not produced.

In the case of the Proton-Transfer-Reaction, a proton is transferred from the hydronium ion to the sample molecule as described by; $H_3O^+ + R \rightarrow RH^+ + H_2O$. Another advantage of this approach is that many compounds present in high concentrations in air (Ex- N_2, O_2, Ar, etc.) have a lower proton affinity than water and therefore do not show up in the mass spectrum. Lindinger points out that another advantage of this approach is the selection of molecules that are nucleophilic and contain unsaturated bonds or electronegative elements such as oxygen or nitrogen. One can also change the ion source from for example H_3O^+ to NH_4^+ to differentiate between compounds of similar proton affinity. Also, an additional buffer gas like helium, which would

dilute the sample gas, is not required because the common components of air do not react with H_3O^+ as described above. Although the parent ion is usually the dominant ion formed, most fragmentation (e.g.- for most alcohols) is due to a simple dehydration reaction (loss of a water molecule) where the percentage of ions formed is consistent. This usually occurs because protonation of oxygen makes it a better "leaving group" as a water molecule. Because the concentration of the hydronium ion is many orders of magnitude higher than the neutral sample, the reaction behaves with simple pseudo-first order kinetics where the concentration of the product ion is solely dependent upon the concentration, reaction time, and proton-affinity of the neutral species. When the proton affinity is higher than that of water (where a proton transfer reaction occurs with every collision), and a high-pressure drift tube (~2 mbars), there will be ample time for a complete reaction. This results in the concentration of the unknown gas being directly proportional to the measured signal in counts per second (cps).

The PTR-MS instrument is rapidly becoming the standard for ultra-fast acetaldehyde concentration measurements because it requires no sample preparation including pre-concentration or derivitization, has a fast response time of up to 10 Hz, and produces the unfragmented ion at m/z 45 which represents the protonated form of acetaldehyde. The response of m/z 45 to acetaldehyde was calibrated with the same dynamic dilution system used for the GC-FID. A calibration line was obtained by a linear regression of the signal at m/z 45 normalized to the primary ion at m/z 21 and plotted versus the concentration of acetaldehyde in ppbv. Other masses including m/z 33 (methanol), 37 (water), 47 (ethanol), 59 (acetone), 61 (acetic acid), and 69 (isoprene) were also monitored although no calibration standard was available to quantify their concentrations. A 10 second dwell time was set for m/z 45, a 5 msec dwell time for m/z 37, with the rest having a 2 second dwell time.

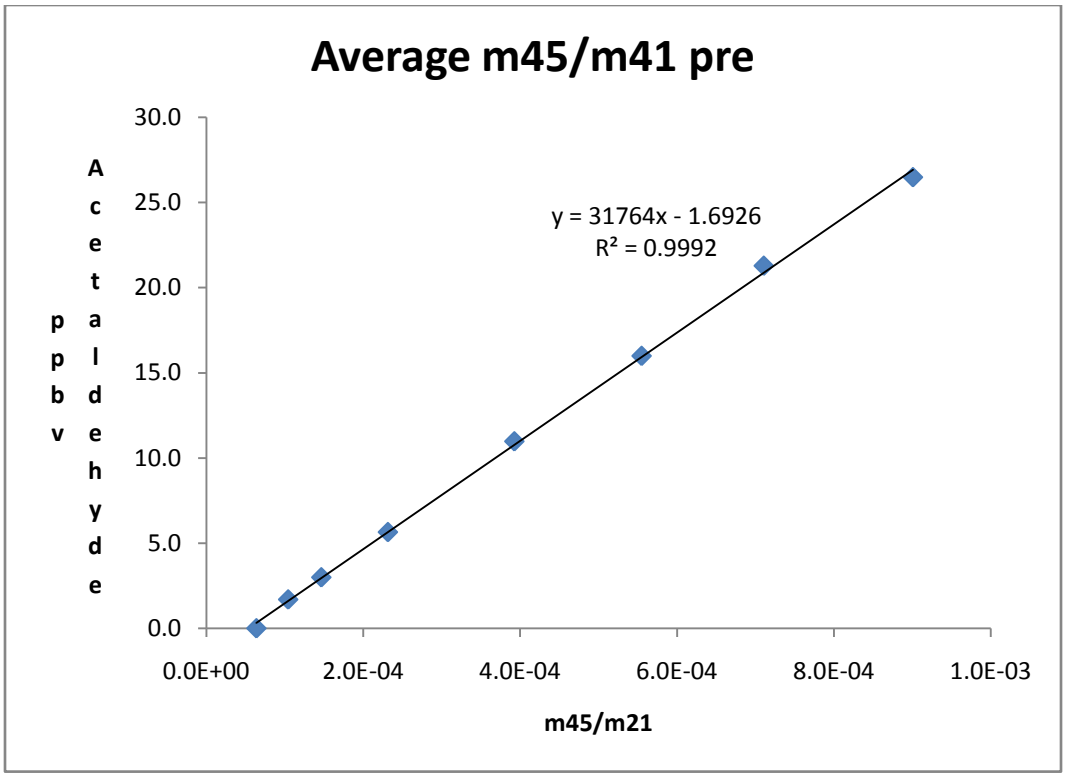

Figure 8: Example of PTR-MS calibration curve for acetaldehyde.

2.6 GC-FID

A custom built VOC pre-concentration system was coupled to an HP 6890 GC system and used to make both soil and branch enclosure flux measurements (see plumbing diagram below). The system was automated with Labview 6.0 and Chemstation 10.01. All analog and digital inputs from the pre-concentration system and outputs from the Labview 6.0 program were interfaced to a Windows 2000 computer through a Labjack U12 (Labjack, Lakewood, CO). A diaphragm pump was used to draw two liters of sample air through three feet of 1/8" Teflon tubing immersed in an ice water bath in order to remove a large amount of water vapor. The removal of acetaldehyde and other oxygenated VOCs by this process was shown to be negligible. The sample air was subsequently drawn through a VOCARB-3000 hydrocarbon trap (1/8" x 12", Sigma Aldrich) for VOC pre-concentration held at 25^{o} C with a thermoelectric cooler. All tubing and traps are composed of fused silica-lined stainless steel tubing (Restek, Bellefonte, PA). Stainless steel switching valves (VICI, Houston, TX) are heated to 100 ^{o}C and the fused silica-lined stainless steel tubing where the sample passes through is continuously heated to 200 ^{o}C by the use of heating rope (Omega). Adsorbed VOCs are then injected directly onto the GC column (0.53mm x 30m: RTX-624) by heating the VOCARB-3000 trap rapidly (30 seconds) to 200^{o} C with a helium

carrier gas flow rate of 3.0 mL min^{-1} set using a auxiliary pressure controlled valve on the 6890 GC. The two sample switching valves were configured in such a way that UHP helium was always flowing into the analytical column but could be diverted through the VOCARB-3000 trap in order to rapidly back flush the adsorbed VOCs onto the column. In order to improve separation and peak shape, a second cryofocusing trap was used which involved the emersion of a loop of the GC column in liquid nitrogen for four minutes following the injection from the VOCARB-3000 trap. This was shown to greatly lower detection limits to well below 0.5 ppbv due to the sharpening of the peaks (30 seconds to 5 seconds peak width). The GC oven (HP 6890) was held isothermally at 25^{o} C during the run (10 min) and subsequently heated to 200^{o} C for three minutes in order to "bake out" the column to prepare it for the next run. The system was leak checked by pressurizing the inlet with helium (without the GC column attached) and searched for small leaks with a helium leak detector (Restek).

The number of moles of sample gas that entered the preconcentration system was estimated from the ideal gas equation (n=PV/RT) based on the measured pressure difference in the gas expansion chamber (P) of known volume (V) and the room temperature (T). For a ten minute collection period, it was shown that approximately 2.0 liters of air was collected (at standard temperature and pressure). During calibrations with VOC standards, the number of nanomoles of standard sampled was calculated by multiplying the mixing ratio of the diluted standard (ppbv) by the moles of total air sampled. For example, if a volume mixing ratio of 10 ppbv was generated, then this is the same as 10 nmoles VOC/mole air so that multiplying 10 ppbv by the number of moles of air sampled, the number of nanomoles of VOC can be calculated. Linear calibration curves were generated by plotting nanomoles of VOC versus peak area as recorded in the Chemstation 10.01 software. In order to improve the time resolution of the system, while a sample was running on the GC column, the next sample is loaded onto the VOCARB-3000 trap. This gives a time resolution of the GC-FID system of ~20 minutes.

Note: During soil enclosure sampling at the University of Michigan Biological Station during the summer of 2005, the VOCARB-3000 traps were taken directly into the field and sample air was directly trapped on them using a small diaphragm pump (KNF) downstream of the trap. The volume passed through the trap was calculated by measuring the flow rate (~70 ml min^{-1}) and the sampling time (20 min). They were then returned to the lab, mounted on the preconcentration system and analysis was carried out as usual.

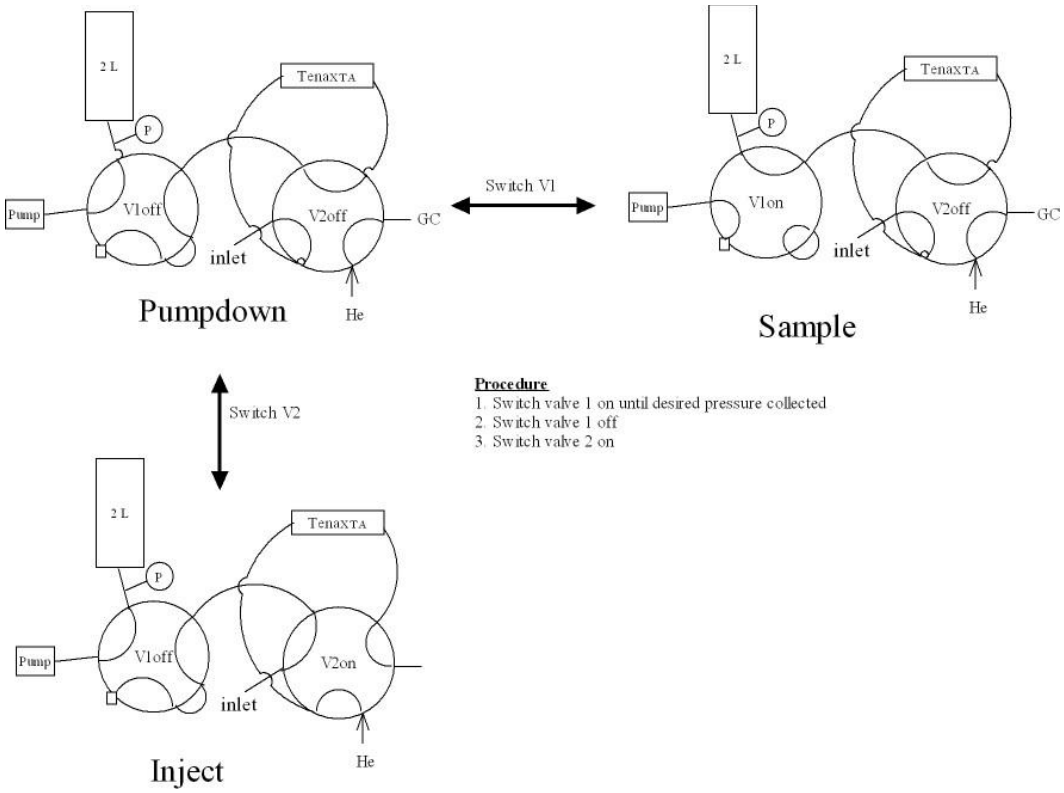

Figure 9: Plumbing diagram of the VOC pre-concentration system.

Figure 10: Picture of the GC-FID with custom built VOC preconcentration system.

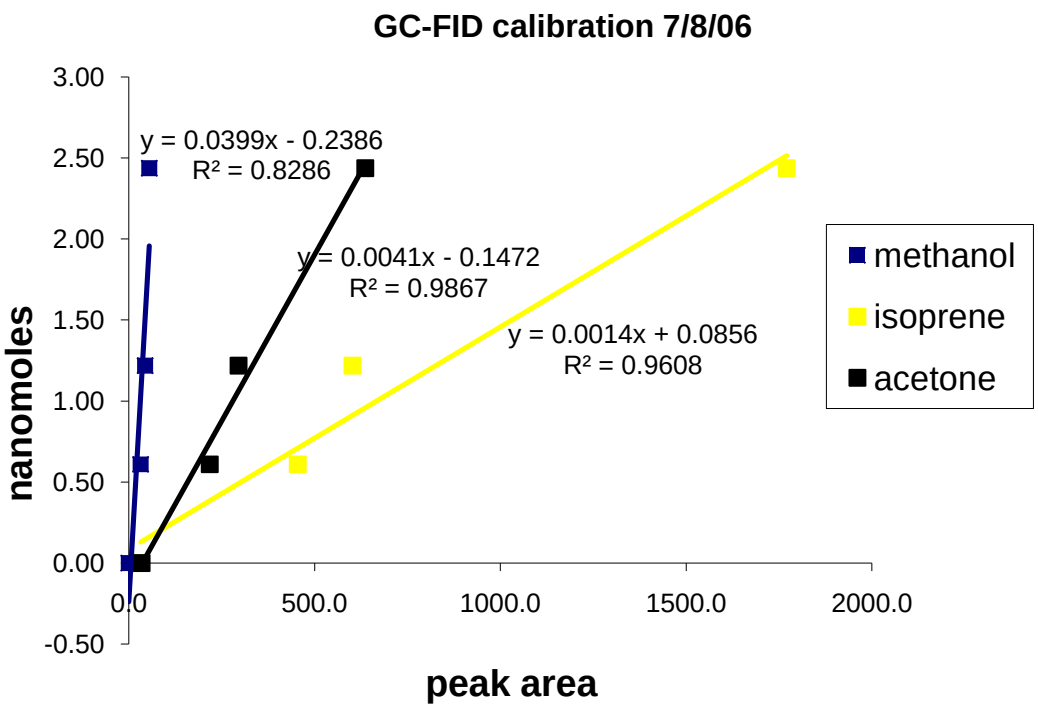

Figure 11: Example of a GC-FID VOC calibration curve at the University of Michigan Biological Station.

Note that the FID is essentially a carbon detector. Therefore the system is much more sensitive to isoprene (5 carbon atoms) than to acetone (3 carbon atoms) than to methanol (1 carbon atom). In addition, the presence of an oxygen atom further reduces the sensitivity to acetone and methanol.

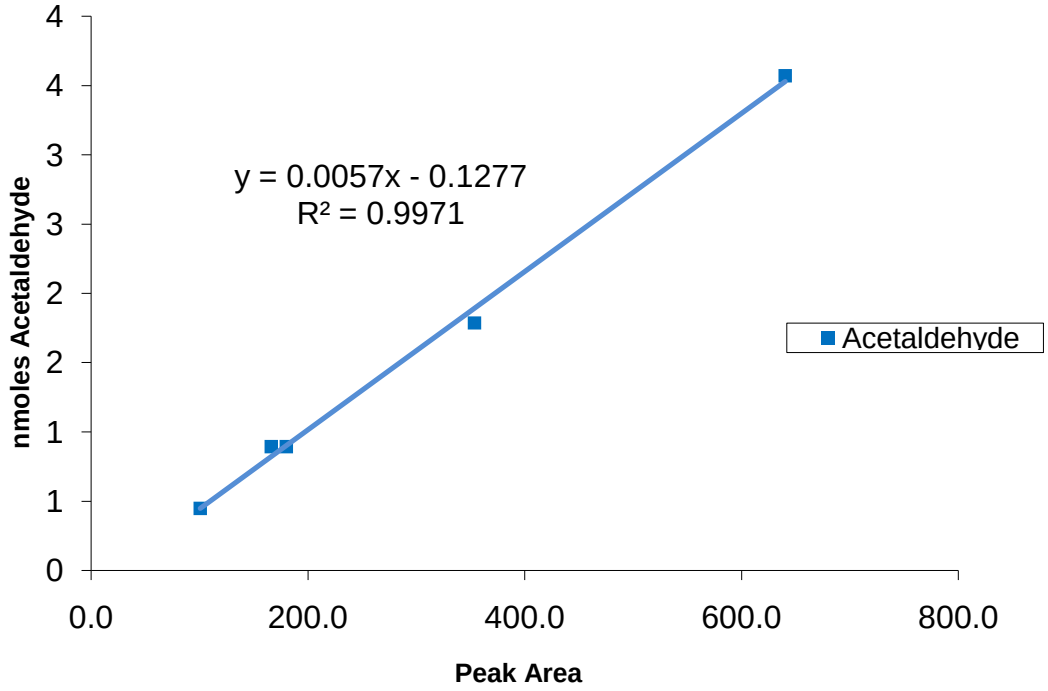

Figure 12: Example of acetaldehyde calibration curve for the GC-FID at Stony Brook University.

2.7. GC-FID Tests on Water Vapor Removal from ppbv Levels of Acetone by Experimental Membrane Module

2.7.1 Introduction

Water vapor in the atmosphere poses several technical problems for the study of Volatile Organic Compounds (VOCs). For example, the strong IR absorption band of water causes strong interference during laser based IR absorption measurements of VOCs such as formaldehyde. In addition, many analytical instruments require a preconcentration step before VOC analysis. When concentrating even small volumes of gases, large amounts of water can be collected. For example, approximately 33 mg of water is recovered from 2 liters of sample that was initially at 70 % relative humidity and at standard temperature and pressure (25^{o} C, 1 atm). Within soil enclosures during the summer of 2005 at the University of Michigan Biological Station, temperatures reached as high as 36^{o} C with 70 % relative humidity corresponding to approximately 64 mg of water in 2 L of air! These huge quantities of water could end up on the analytical column and in the detector if not removed. That much water can freeze and restrict gas flow during cryogenic steps, degrade peak shape and resolution, reduce column life, and seriously compromise performance of detectors. For example, injections of 1 mg of water into a typical benchtop mass spectrometer

will cause attenuation of analytes that co-elute with the water peak. Although previously assumed to not be sensitive to water vapor due to the use H_3O^+ as a proton transfer chemical, the sensitivity of the PTR-MS to many VOCs has now been shown to be very significant. During a temperature heating program, condensed water vapor in a gas chromatography column can rapidly expand and actually forcefully blow a flame ionization (FID) flame out, causing a complete loss of analytical information.

Therefore, the drying of an air sample while retaining the VOCs of interest is highly desirable, but technically difficult. The removal of water from VOCs in air samples is not trivial since VOCs are typically several orders of magnitude less abundant in air samples than water with amounts in the range of nanograms compared to milligrams. One approach that has been employed is the use of solid adsorbents like DriRite and silicagel. These do a good job of removing water vapor but also remove polar compounds like acetone. Another technique known as cold trap dehydration is more successful at retaining the VOCs while removing water vapor. In this method, the sample is passed into a region cooled between 0^o C and -50^o C where a fraction of the water vapor can be removed from the VOCs through condensation. If the flow rate is low enough and the surface area high enough, the emerging air can obtain dew points approaching the temperature of the cooled region. Some of the disadvantages of this technique include the use of a costly cryogen like liquid nitrogen, the lengthened analysis time and offline characteristics, the need to backflush the water trap after each sample with a dry gas to eliminate the condensed water for the next sample, and the increased "dead" volume of the analytical system.

Another approach uses Nafion Dryers to remove moisture from air samples before VOC concentration/analysis. Generally, a 1/16" OD x 4' length of DuPont engineered Nafion polymer is placed within a larger 1/8" tube. The humid air sample is passed through the smaller tubing and polar molecules such as water are transferred through the proprietary membrane to a dry air stream on the other side. Unfortunately, many compounds of interest are also lost in the Nafion dryer due to both active and passive mechanisms. For example, VOCs with OH groups are lost almost quantitatively while other water soluble compounds absorb into the membrane at rates that are dependent on the current level of hydration of the membrane making quantification difficult. Finally, since the Nafion polymer is relatively porous, low molecular weight VOCs can diffuse through it and also be lost.

Therefore, towards the goal of studying the low molecular weight polar molecules like acetone, it is highly desirable to find a system capable of dehydrating them for analysis. I contacted Membrane Technology and Research, Inc. about a membrane module that could potentially do this. Using GC-FID, I found that the membrane is capable of removing a substantial amount of water

vapor from a synthetic gas mixture containing acetone in the sub ppbv concentrations. In addition, because of the use of a vacuum pump, the acetone concentration is enhanced in the outlet of the membrane module and that the degree of dehydration and concentration enhancement is a function of flow rate of the sample through the module. This system can be set up in both a dynamic and a static configuration, with the static configuration removing the most water vapor, concentrating the acetone the greatest, but having the longest acetone residence time. Likewise the dynamic system was able to respond relatively quickly to changes in acetone concentrations while both enhancing the acetone concentration and dehydrating the sample. For the GC-FID analysis, it was determined that an input flow rate of roughly 1000 ml min^{-1} (1 Lpm) was optimal for water removal, preconcentration and low residence time. The system was later field tested on extremely humid soil enclosure plots at the PROPHET tower at UMBS and was successfully coupled to the automated GC-FID system for the continuous quantification of acetone and isoprene fluxes.

In this section, I describe the use of a novel nanofiltration membrane module based on a pore flow mechanism, that when used with a small vacuum pump can 1) Dehydrate an air sample containing both polar and non polar VOCs like acetone and isoprene 2) Preconcentrate the VOCs by up to 300% 3) Operate continuously online without the need to backflush or perform other maintenance.

2.7.2 Configuration

For lab testing, I configured the membrane module for ambient measurements such that a specific mixture of gases could be delivered at a specific rate to the inlet. The diagram of the dynamic setup is shown below. In addition, a static setup was tested in which the vent was eliminated and therefore minimized the flow through the module.

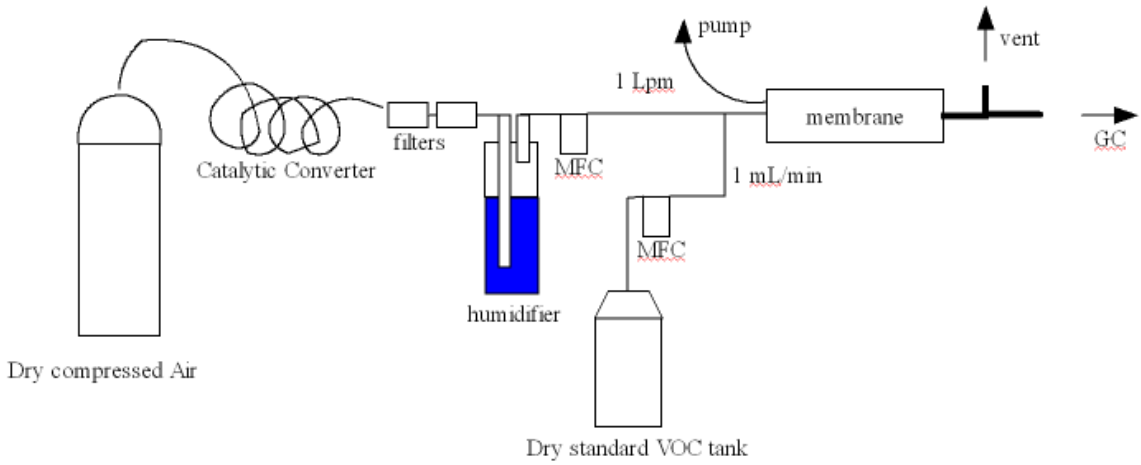

Figure 13: Diagram of the dehydration membrane setup in the trace gas analysis lab at Stony Brook University.
This system was designed for testing the dehydration capabilities of the membrane from a humidified air flow containing an acetone at 3.0 ppbv.

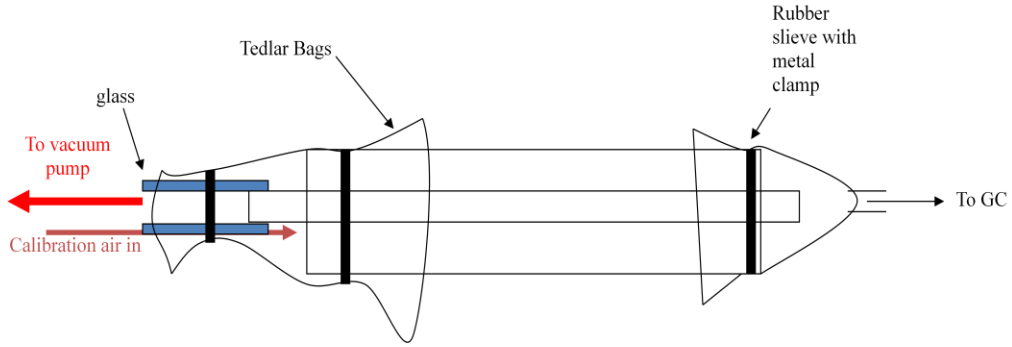

Figure 14: Plumbing diagram of the MTR membrane module.
This setup was used for testing the dehydration capabilities of the membrane while retaining acetone.

2.7.3 Results

1) Flushing the membrane: The membrane was found to initially emit acetone and so the unit was flushed with zero air overnight at an inlet flow rate of 2 Lpm. The background acetone peak was reduced in this manner to <0.2 ppbv.

2) Addition of dry acetone standard: Following this, to the zero air flow a 2 ml min^{-1} flow of acetone standard is added which produces 3.0 ppbv of acetone at the membrane's inlet. From the graph below, the concentration of acetone from the membrane's outlet reached an equilibrium concentration after 4-5 hours. (Note that the calibration system itself usually takes about 4 hours to reach a steady state acetone concentration).

3) Vacuum Pump on: Once a steady state was reached, the vacuum pump was turned on. Note that the resulting concentration at the membrane's outlet increased dramatically. This is due to the fact that acetone is too large to fit through the pores of the membrane, but the major components of air are not. Therefore, acetone is preconcentrated.

4) Addition of humid air: The introduction of water vapor into the calibration gas stream was accomplished by the addition of a humidifier before the zero air mass flow controller. Although the FID remained on after this modification, the peaks were severely tailing and sometimes double headed which indicated incomplete dehydration by the membrane. This led to anomoulsy high peak areas and so this data is not included here.

5) Reduction of flow rate: The flow rate up to this point into the membrane has been 2 Lpm. To determine if the air residence time inside the module was too low for proper dehydration for good chromatographic peak shapes, the flow rate was reduced to 1 Lpm and the acetone standard was reduced to 1 ml min^{-1} to maintain the same inlet acetone concentration (3 ppbv). When this was done, the peaks shape greatly improved and resembled the shapes of the dry samples. This indicated that the membrane was drying the air stream well enough for analysis by GC-FID. Because the concentration of acetone to the inlet didn't change, the membrane did not seem to need any more time to reach the new equilibrium concentration at the outlet. Although the acetone inlet concentration remained unchanged the new acetone concentration in the outlet almost doubled. This strongly indicates that the residence time of the VOC in the membrane module which is determined by the flow rate through the module, determines the degree of both dehydration and VOC preconcentration.

6) Turn pump off: To investigate whether the dehydration was occurring as a result of the evacuation of the membrane core by the vacuum pump, the pump was switched off. The FID was shut off after each sample as a result of overloading with water indicating that it was indeed the vacuum pump that was removing the water vapor.

7) Static setup: The vacuum pump was turned back on and the vent tee was removed after the membrane module to create a static setup. The leaks in the system allowed the calibration air to enter the Tedlar bag at the inlet only to escape through the leaks. In this case, the acetone concentrations at the outlet as measured by GC-FID greatly increased (~300% increase) and the water vapor was likely removed the most.

8) Static, dilution and blank: When converted to the static configuration, the membrane seemed to respond relatively quickly to the new acetaldehyde equilibrium at the outlet. However, once the acetone concentration was reduced to 1.5 ppbv, the concentration at the outlet quickly dropped but then very slowly decreased. An new equilibrium was not reached even after five hours (concentration still slowly decreasing). This indicates that while the static configuration is the best at sample preconcentration and dehydration, it has a long memory effect due to the lack of flushing with new sample.

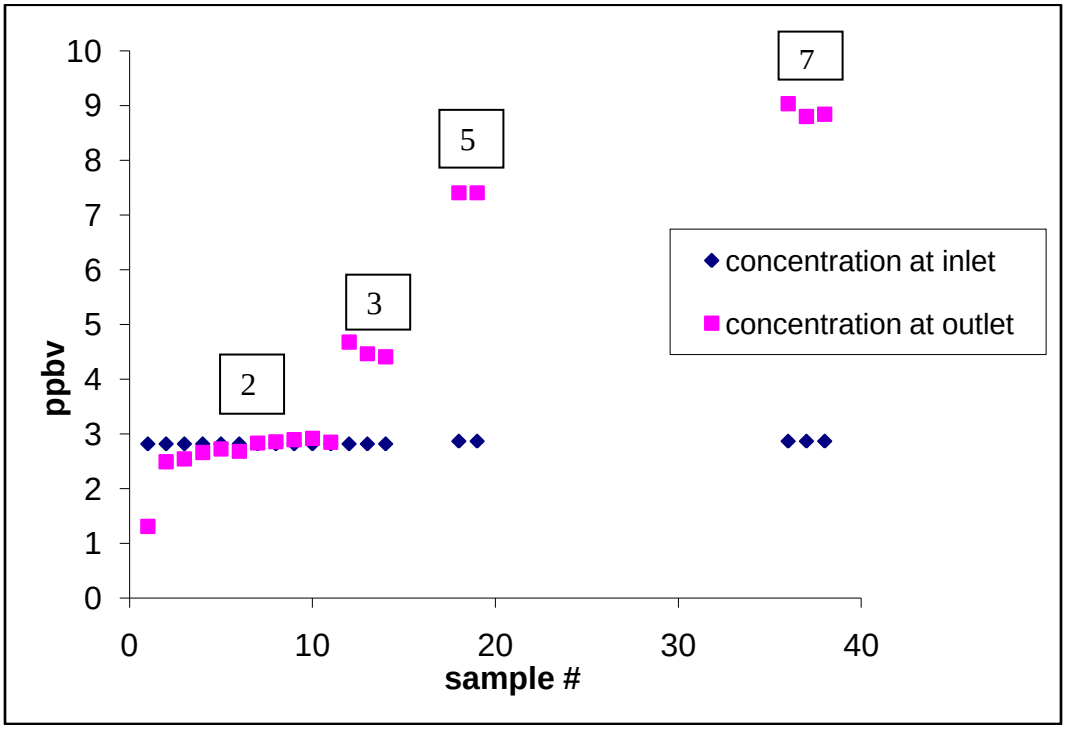

Figure 15: Preconcentration and dehydration of 3 ppbv acetone sample by MTR membrane.

2.7.4 Overview

Static Configuration

1) Likely Dries the sample the most
2) Preconcentrates acetone the most
3) Requires a long time to flush (>12hrs)

Dynamic Configuration

Flow rate of 1 Lpm is a good compromise between high water removal and high acetone preconcentration. Higher flows cause the sample to be too humid while lower flows require too long to reach new equilibrium when input concentration of acetone changes. This module may therefore be valuable in atmospheric and biospheric research of VOCs. However, field testing the module is an important next step towards commercialization of the product (see chapter 6).

Chapter 3: Ethanolic Fermentation and the Pyruvate Dehydrogenase Bypass System in Poplar Leaves under Aerobic Conditions

3.1 ABSTRACT

The production of acetaldehyde from ethanolic fermentation in plants has been well demonstrated, but considered important only in anoxic and reproductive tissues. This ancient pathway has not been considered to be important in leaves since these organs are continuously bathed in a 21% oxygen atmosphere. Previous studies have used disulfiram, an inhibitor of aldehyde dehydrogenase, to suggest that fermentation is not a source of acetaldehyde in leaves, but we find disulfiram to be ineffective at inhibiting the pyruvate dehydrogenase (PDH) bypass when delivered to plants via the transpiration stream. We suggest that ethanolic fermentation coupled with the PDH bypass system occurs under aerobic conditions in leaves. Emission rates of ethanol, acetaldehyde, and acetic acid are enhanced during photosynthesis, mechanical wounding, and light to dark transitions. We term the burst in emissions of these volatile metabolites during a light to dark transition light enhanced dark fermentation (LEDF) based on its strong analogies with light enhanced dark respiration (LEDR). Although changes in enzyme levels involved in fermentation may play a role, we suggest that enhanced emission rates of these metabolites under aerobic conditions are stimulated by the accumulation of pyruvate which allows ethanolic fermentation to compete with respiration.

3.2 Introduction

The exchange of acetaldehyde between plant canopies and the atmosphere may significantly influence air quality and climate. Unfortunately, very little is known about the biochemical pathway(s) responsible for the production and consumption of acetaldehyde in field plants. The pathways currently considered to be involved in the metabolism of acetaldehyde in plants are shown in Figure 16. The production of acetaldehyde and ethanol in plants by pyruvate decarboxylase (PDC) and alcohol dehydrogenase (ADH) during ethanolic fermentation induced by anoxia is well established (Kimmerer and Macdonald, 1987; Vartapetian and Jackson, 1997; Vartapetian et al., 1997). In modern plants, this ancient pathway is thought to supply ATP under reduced oxygen conditions. Under these conditions, pyruvate generated by glycolysis cannot be oxidized by the Krebs cycle in mitochondria and accumulates in the cytosol. The accumulating pyruvate is decarboxylated to acetaldehyde by PDC. The subsequent reduction of acetaldehyde to ethanol by ADH maintains energy production through glycolysis by regenerating the required NAD^+ during anoxic periods. When plants are reintroduced to normal aerobic conditions, mitochondrial respiration is restored and ethanolic fermentation is no longer considered to be important.

The emission rates of ethanol and acetaldehyde to the atmosphere can be greatly enhanced from plants during periods of root flooding. This enhancement is best explained by the production of ethanol in roots during ethanolic fermentation induced by anoxia. The ethanol is transported to leaves where, under aerobic conditions, it can be oxidized to acetaldehyde by the reversible ADH reaction (Macdonald and Kimmerer, 1993; Kreuzwieser et al., 1999; Kreuzwieser et al., 2001; Kreuzwieser et al., 2004). Stems and leaves of trees have been shown to constitutively express an ADH that can convert ethanol produced in anoxic roots back to acetaldehyde (Harry and Kimmerer, 1991). Such conversion is important because ethanol is toxic in high concentrations and is a reduced carbon source that will simply be lost by the plant if not oxidized to acetaldehyde. Under root flooding conditions, acetaldehyde can have emission rates as high as 225 nanomoles m^{-2} s^{-1} (Holzinger et al., 2000). While well documented in potted plants, the extent to which these processes occur in nature is unclear. During a field experiment under ambient conditions, acetaldehyde emissions from non-flooded *Picea abies* (Norway Spruce) were correlated with the flow of ethanol in the xylem, suggesting that ethanol oxidation in leaves is at least partially responsible for acetaldehyde emissions (Cojocariu et al., 2004). However, the mass flow rates of ethanol were higher in the upper regions of the tree compared with the lower regions. This is not consistent with the idea that ethanolic fermentation occurs exclusively in anoxic roots since a higher ethanol mass flow rate would be expected in the lower regions of the tree. In addition, field studies in the Amazon have failed to demonstrate higher acetaldehyde emission rates during the dry to wet season transition when roots are regularly flooded, as would be expected if anoxic roots are the dominate source of acetaldehyde emissions from leaves (Kesselmeier et al., 2002; Rottenberger et al., 2004). It is therefore uncertain whether root flooding of forested ecosystems is a significant source of acetaldehyde to the atmosphere. Also inconsistent with the view that acetaldehyde emissions from plants are ultimately derived from ethanolic fermentation in anoxic roots are the results from many laboratory and field studies which demonstrated significant acetaldehyde emissions from non-flooded potted plants and forests (Janson et al., 1999; Martin et al., 1999; Schade and Goldstein, 2002; Cojocariu et al., 2004; Hayward et al., 2004; Villanueva-Fierro et al., 2004; Cojocariu et al., 2005; Karl et al., 2005). Both ethanol and acetaldehyde emissions were observed above a ponderosa pine plantation canopy in California (Schade and Goldstein, 2002). Although root anoxia can be ruled out in these well-drained soils, simultaneous emissions of both compounds from the trees strongly suggest that ethanolic fermentation was active in these plants. In addition, Karl et al., (2002) found that light to dark transitions induce a large burst of acetaldehyde emissions from leaves under aerobic conditions. $^{13}CO_2$ fumigation showed that about half of acetaldehyde during these bursts was labeled and therefore had to

originate from very recently fixed carbon pools. These observations imply that either another biochemical pathway exists in plants for the production of acetaldehyde or that ethanolic fermentation can proceed under aerobic conditions.

Although ethanolic fermentation was thought to only occur in anoxic tissues, evidence is emerging that this process occurs under aerobic conditions in plants. Raymond et al., (1985) found high ethanolic fermentation rates in pea and maize seeds under aerobic conditions as did Joseph and Kelsey, (2004) in stem segments of Douglas-fir. In addition, Bucher et al., (1995) discovered that germinating tobacco pollen under aerobic conditions have high rates of both ethanolic fermentation and respiration. In yeast and plant pollen, ethanolic fermentation has been shown to be very important under aerobic conditions as a part of the so-called pyruvate dehydrogenase (PDH) bypass system. The PDH bypass involves the ALDH-catalyzed conversion of acetaldehyde to acetate which is then activated to acetyl CoA by acetyl CoA synthetase (ACS). The PDH bypass therefore represents an alternative to acetyl CoA production by PDH in mitochondria. If the PDH bypass system operates under aerobic conditions in leaves and other plant tissues, it may act to funnel acetate/acetyl CoA into mitochondria to support respiration and amino acid biosynthesis as well as into chloroplasts and the cytoplasm for the biosynthesis of fatty acids and terpenoids. In one study, ethanolic fermentation under aerobic conditions coupled to the PDH bypass system was very important in lipid biosynthesis in germinating tobacco pollen (Mellema et al., 2002). Although the role of ethanolic fermentation under aerobic conditions has been clearly shown in seeds and pollen, its potential role in non-reproductive plant tissue such as leaves has been overlooked. This is due in part to the results from a single study which concluded that while ethanolic fermentation and the PDH bypass is very important in pollen under aerobic conditions, its role is limited in seedlings (opdenCamp and Kuhlemeier, 1997). This conclusion was based on the use of the ALDH inhibitor disulfiram which as discussed in this paper may not be absorbed by intact plant cells/tissues, is not specific for ALDH enzymes, and is not effective against all ALDH enzymes.

In this paper, we hypothesize that ethanolic fermentation and the PDH bypass system are active in leaves under aerobic conditions and are strongly influenced by pyruvate concentrations. Under low pyruvate concentrations, PDC can't compete with PDH for pyruvate because of its much higher K_m for pyruvate (mM range for PDC compared with µM range for PDH) (Tadege et al., 1999). However, should conditions exist in leaves such that pyruvate concentrations increase, the PDC reaction may be able to compete with the PDH reaction. This may occur during photosynthesis, following light to dark transitions, and following plant stress such as mechanical wounding. We provide evidence for the coupling of ethanolic fermentation with the PDH bypass system under aerobic conditions in plants through branch level emission measurements of the volatile

metabolites acetaldehyde, ethanol, and acetic acid. This is done by observing emission rates in the dark, the light, and following light to dark transitions. We also test the ability of disulfiram to effectively inhibit the ALDH enzymes responsible for the oxidation of acetaldehyde during light to dark transitions and acetaldehyde fumigation experiments. In addition to a burst of acetaldehyde emissions, post-illumination carbon dioxide bursts also occur termed Light Enhanced Dark Respiration (LEDR) (Parys et al., 2004). We hypothesize that a connection exists between the LEDR effect and acetaldehyde emission bursts following light to dark transitions through the accumulation of pyruvate. LEDR has been shown to be a function of light intensity and duration before darkening. Therefore, we explore a possibly similar relationship for acetaldehyde by varying the duration of the light period thereby influencing the accumulation of recent photoassimilated carbon.

3.3 Materials and Methods

Branch level emissions of acetaldehyde, ethanol, and acetic acid were studied in potted poplar plants (*Populus deltoides* [S7c8 East Texas Day Neutral clone]) in the light, following a light to dark transition, and in the dark. Individuals were obtained from the University of Colorado greenhouse and the National Center for Atmospheric Research (NCAR) greenhouse in Boulder, CO. Plants were potted into 4-L plastic pots containing a commercial potting mix (MiracleGro) with Osmocote slow release fertilizers.

The flux of ethanol, acetaldehyde, and acetic acid was measured with a high sensitivity PTR-MS instrument (Ionicon, Innsbruck, Austria) from poplar branches under dark, light, and light to dark transitions in a 5 L Teflon dynamic branch enclosure. The PTR-MS instrument has been described in detail elsewhere (Lindinger and Hansel, 1997). Hydrocarbon free air was introduced into the enclosure at a flow rate of 1.0 L min^{-1} (generated by passing 1.0 L min^{-1} of room air through a catalytic converter consisting of 12" x ½" stainless steel tube packed with platinum-coated silica pellets and heated to 400^{o}C). The flow rate of hydrocarbon free air was controlled by a mass flow controller (Model FMA-A2308, OMEGA Engineering, INC., Stamford, Connecticut), and the air inside the enclosure had a residence time of approximately 5 minutes. Because the oxidation of VOCs present in room air in the catalyst contributes very little CO_2 and water vapor, the CO_2 and water vapor concentrations in the hydrocarbon free air supplied to the enclosure were essentially those of room air. For biogenic VOC concentration measurements, approximately 200 ml min^{-1} of sample air was continuously drawn out of the enclosure and into the PTR-MS through 1/8" Teflon tubing. The rest of the air flow entering the branch enclosure was vented through small leaks where the Teflon bag was tied to the branch. Mass to charge ratios 45, 47, 61, and 69 were consecutively monitored with a five second dwell

time each and correspond to the protonated form of acetaldehyde, ethanol, acetic acid, and isoprene respectively. In addition, the mass to charge ratio 37, corresponding to the protonated cluster of two water molecules, was also monitored with a 0.1 second dwell time. This signal is very sensitive to water vapor concentrations, allowing us to estimate transpiration rates. The signal for acetaldehyde was calibrated with a 2.0 ppmv (+/- 5%) gravimetrically prepared acetaldehyde standard (Apel-Riemer Inc., Denver, CO) diluted with hydrocarbon free air to 0-19.8 ppbv using a dynamic dilution system.. The net emission flux from a poplar branch placed into the enclosure was calculated from equation 1.

$$F = \frac{(ppbv_{after} - ppbv_{before}) \cdot Flow \cdot P}{gdw \cdot R \cdot T}$$

Equation 1: Calculation of branch acetaldehyde exchange rates.

Where F is the flux in nmoles/(gdw*hr), Flow is the total flow rate entering the enclosure in L/hr, P is the atmospheric pressure in atmospheres, gdw is the dry leaf mass in grams, R is the universal gas constant (0.08205 L atm K^{-1} mol^{-1}), and T is the air temperature in Kelvin. $ppbv_{before}$ and $ppbv_{after}$ are the concentration of acetaldehyde in the enclosure before and after the enclosure respectively. When hydrocarbon free air is used, $ppbv_{before}$ is assumed to be zero. Measured leaf tissue was oven dried (70 ^{o}C) and dry mass determined. Light was supplied by a 1000-W high intensity metal halide discharge lamp (Sylvania MS1000-M47) with an intensity of photosynthetically active radiation at branch height of roughly 1000 µE m^{-2} s^{-1}. Air temperatures inside the enclosure were measured with a K-type thermocouple (model KMQSS-125G-6, OMEGA Engineering, INC., Stamford, CT) and ranged between 24-25 ^{o}C in the dark and from 29-32 ^{o}C in the light. During light to dark transitions, the lamp was turned off and the branch enclosure was immediately covered with aluminum foil.

To investigate the role of prior photosynthesis on post-illumination emission rates, intact poplar branches were placed in the enclosure and three light to dark cycles were performed. The light period of the first cycle was set to 4 hours so that photosynthetic products had time to accumulate while all subsequent cycles had a light period of only ~15 minutes. All dark periods lasted for ~20 minutes.

To test the ability of disulfiram to block the oxidation of acetaldehyde by ALDH enzymes, a saturated solution of tetraethylthiuram disulfide (Disulfiram, Sigma Aldrich, St. Louis, MO) was prepared in tap water (0.65 mM) and administered to excised poplar branches via the transpiration stream. Excised branches were immediately placed in tap water and re-cut under the solution in order to maintain the transpiration flow. An excised branch in tap water was cycled through five light to dark transitions (~25 minutes in the light and ~15

minutes in the dark). Then, the tap water was removed and rapidly replaced with the disulfiram solution and five additional light to dark transitions under the same conditions were preformed. Uptake of the disulfiram solution by the excised branch was monitored by the estimated transpiration rates. These experiments were repeated with a dynamic leaf enclosure where simultaneous measurements of acetaldehyde emissions, stomatal conductance, net CO_2 exchange rates, and transpiration rates were made. The details of the leaf level measurements have been previously described (Harley et al., 2007).

To directly test the ability of disulfiram to inhibit the uptake of acetaldehyde from the atmosphere by poplar branches, an excised poplar branch in tap water was placed in the enclosure under room lighting and fumigated with 1.0 L min^{-1} of 26.5 ppbv acetaldehyde in air. An automated Teflon valve was used to switch between sampling the air before and after the enclosure and was programmed to switch after every ten cycles (~10 min). The net acetaldehyde uptake flux was calculated according to equation 1. After one hour, the tap water was replaced with disulfiram solution and the acetaldehyde uptake flux was measured for an additional six hours.

3.4 Results

The emission rates of acetaldehyde, ethanol, and acetic acid are enhanced in the light compared with the dark (Figure 17). At steady state, the emissions of acetaldehyde in the light increased by 143% relative to the dark ($5.8x10^{-7}$ ± $2.7x10^{-8}$ g gdw^{-1} hr^{-1} in the light versus $2.4x10^{-7}$ ± $2.2x10^{-8}$ g gdw^{-1} hr^{-1} in the dark). Unfortunately, calibration standards were not available for acetic acid or ethanol but the signals increased in the light by 100% and 27% respectively relative to the dark. Light to dark transitions induced large emission bursts of acetaldehyde, ethanol, and acetic acid from both excised (Figure 17) and intact (Figure 18) poplar branches. Ethanol shows a clear delay in emissions relative to acetaldehyde while acetic acid shows very similar temporal patterns to acetaldehyde.

The magnitude of the post-illumination acetaldehyde emission burst was much higher from the branch exposed to light for 4 hours prior to darkening (Figure 18) than the branch with a 25 minute light period (Figure 17, first five bursts). In addition, while the magnitudes of sequential post-illumination emission bursts were relatively consistent from the branch with a light period of ~25 minutes (Figure 17, first five bursts), the branch with a light period of ~15 minutes had sequentially lower bursts with every light to dark transition (Figure 18). For both branches, transpiration rates throughout the experiment were higher in the light than in the dark, but were consistent for all light to dark cycles carried out (data not shown).

After five light to dark transitions on an excised poplar branch in tap water, the experiment was repeated on the same branch in 0.65 mM disulfiram (Figure 17, last 5 bursts). In agreement with a previous study (Graus et al., 2004), the emission of acetaldehyde is not enhanced as would be expected under disulfiram if it effectively inhibited ALDH. Following disulfiram application, transpiration rates were unaffected (data not shown). In addition, acetic acid emissions did not decrease as would be expected from effective ALDH inhibition. When then the experiment was repeated with leaf level net CO_2 exchange rate measurements in addition to VOC emission measurements, the use of disulfiram did not affect photoassimilation rates in the light or post-illumination acetaldehyde and carbon dioxide emission bursts (Figure 19). Upon darkening, the peak in both acetaldehyde and CO_2 emission bursts occur at the same time implying a similar mechanism for both.

When elevated gas phase concentrations of acetaldehyde were introduced into the branch enclosure, acetaldehyde was taken up by the branch. When disulfiram was fed to the branch through the transpiration stream, uptake was not inhibited. For example, fumigating a control branch in tap water with 26.5 ppbv acetaldehyde for one hour resulted in a net uptake flux of $-1.0 \times 10^{-6} \pm 1.2 \times 10^{-7}$ g gdw^{-1} hr^{-1}. After replacing the tap water with the disulfiram solution, the net uptake flux over the next six hours was $-1.3 \times 10^{-6} \pm 1.2 \times 10^{-7}$ g gdw^{-1} hr^{-1}.

3.5 Discussion

The higher emission rates of acetaldehyde, ethanol, and acetic acid in the light compared with the dark may be attributed to increased ethanolic fermentation and PDH bypass rates under enhanced pyruvate concentrations (Figure 17). During photosynthesis, pyruvate accumulates in the cytoplasm due to the export of Calvin Cycle intermediates from chloroplasts, continued glycolysis in the cytoplasm, and a partial inhibition of mitochondrial respiration in the light (Raghavendra et al., 1994). Because the branch enclosure used in this study was not temperature controlled, we were unable to separate light from temperature effects on the emission rates, and it is likely that an increase in temperature also stimulates emissions. Using a temperature controlled leaf cuvette, Karl et al., (2005) demonstrated that the acetaldehyde compensation point increases with temperature. This may be due to an increase in photosynthetic and glycolytic rates and therefore increased ethanolic fermentation rates as temperatures increase.

Following a light to dark transition, the emission of ethanol is delayed relative to acetaldehyde (Figure 18). This may be due to the higher water solubility of ethanol relative to acetaldehyde and/or the kinetics of acetaldehyde reduction to ethanol by ADH. The continued emissions of ethanol after acetaldehyde emissions have returned to background levels may be related to the fact that ethanol is a “dead end” product which accumulates in the aqueous phase

and can only be emitted to the atmosphere or further metabolized by conversion back to acetaldehyde. Because acetic acid is even more water soluble than ethanol, it would be expected to accumulate to considerable levels and display a delayed emission pattern even more so than ethanol if not readily metabolized. Assuming that all of the acetic acid is produced from the oxidation of acetaldehyde, the similar temporal patterns of these two species indicates that acetaldehyde is rapidly converted to acetic acid which is then activated to acetyl CoA. In leaf fumigation experiments with extremely high concentrations of acetaldehyde (over 3000 ppbv) strong uptake of acetaldehyde continued for 8 hours with no visible damage to the leaf (Kondo et al., 1998), consistent with the continuous operation of effective acetaldehyde sinks.

These results suggest that the production of ethanol supplied to leaves via the transpiration stream is not restricted to anoxic roots. It is possible that ethanolic fermentation under aerobic conditions occurs in many plant organs which could contribute to the production of acetaldehyde in leaves. Therefore, the supply of ethanol to leaves contributes to the production of acetaldehyde and therefore also must influence the compensation point. This could contribute to the variability in acetaldehyde compensation point values with height due to different supplies of ethanol from the transpiration stream.

The reduced fluxes of acetaldehyde, ethanol, and acetic acid from sequential light to dark transitions shown in Figure 18 indicate that the accumulation of photoassimilated carbon during the previous light period is an important source of acetaldehyde during these events. This is supported by the fact that isoprene emissions, which are known to be mainly fueled by recent photoassimilated carbon (Delwiche and Sharkey, 1993; Karl et al., 2002), are not given enough time in the light (~15 min) to recover to pre-darkened conditions (data not shown). However, when the light period for an excised branch (Figure 17) was increased to ~25 minutes, more consistent acetaldehyde bursts occurred after darkening. In addition, a similar recovery of isoprene emissions during the light occurred, further suggesting that the source of acetaldehyde during light to dark transitions is related to the accumulation of recent photosynthetic products (data not shown).

If ethanolic fermentation can occur simultaneously with mitochondrial respiration and photosynthesis, as we suggest, how do plants integrate their carbon and energy metabolism? Studies have shown that elevated pyruvate concentrations activate the alternative oxidase pathway (AOX) in mitochondria (Day et al., 1994). Therefore the AOX pathway is very important during times when pyruvate and reduced equivalents accumulate. These conditions arise under aerobic conditions in plants when there is an imbalance between upstream respiratory carbon metabolism and downstream electron transport (Vanlerberghe, 1997; Vanlerberghe and McIntosh, 1997). This imbalance can occur during

changes in the supply or demand for carbon, reducing power, or ATP. For example, elevated pyruvate concentrations may be associated with light to dark transitions and this may in turn activate the AOX pathway. The regulation of the AOX pathway by pyruvate can help integrate fermentation and respiratory carbon metabolism with electron transport in plant mitochondria (Vanlerberghe and McIntosh, 1997). Stimulation of the AOX pathway by pyruvate is critical in limiting the activity of ethanolic fermentation under aerobic conditions. The link between AOX pathway activity, pyruvate accumulation, and ethanolic fermentation was demonstrated using plants lacking the AOX pathway. Under aerobic conditions where the cytochrome oxidase (COX) pathway was limiting respiration, both pyruvate and ethanol accumulated to substantial levels (Vanlerberghe et al., 1995).

When Arabidopsis leaves are switched from light to darkness, the expression of more than 790 genes is altered indicating a massive shift in cellular processes (Kim and von Arnim, 2006). In addition, light to dark transitions modify the activity of important enzymes already present such as pyruvate dehydrogenase (PDH) in chloroplasts and mitochondria. During the light, the basification of chloroplast stroma leads to the activation of its PDH while mitochondrial PDH becomes less active due to reversible phosphorylation (Tovar-Mendez et al., 2003). Therefore in the light, fatty acid biosynthesis proceeds in chloroplasts whereas respiration in mitochondria is reduced (Tcherkez et al., 2005). In contrast, in the dark mitochondrial PDH activity increases while chloroplastic PDH becomes less active. Therefore, following a light to dark transition, it is likely that pyruvate concentrations in the cytoplasm dramatically increase because 1) The conversion of pyruvate in chloroplasts to acetyl CoA by PDH is rapidly inhibited whereas mitochondrial PDH takes longer to become active, 2) Malate that accumulated in the cytoplasm during photosynthesis due to reduced mitochondrial respiration in the light is rapidly decarboxylated by malic enzyme to pyruvate upon darkening. If the cytosolic concentration of pyruvate rapidly increases upon darkening, ethanolic fermentation may be important for preventing acidification of the cytoplasm (Harry and Kimmerer, 1991), since decarboxylation of pyruvate by PDC leads to the pH neutral species acetaldehyde and carbon dioxide. This process is termed the pyruvate overflow mechanism and Karl et al., (2002)) attempted to demonstrate its role in the bursts of acetaldehyde measured during light to dark transitions. They argued that light to dark transitions enhance the rate of the PDC reaction in the cytoplasm due to the transient accumulation of pyruvate. They demonstrated that inhibitors of mitochondrial respiration and pyruvate transport which are expected to increase pyruvate concentrations in the cytoplasm induced acetaldehyde emissions although non-specific inhibition was noted. Graus et al., (2004) also demonstrated that the emissions of acetaldehyde by plant leaves were greatly enhanced when

the PDH reaction in mitochondria was inhibited. These studies provide strong evidence that pyruvate decarboxylation by PDC occurs in leaves under aerobic conditions and that its rates are strongly influenced by pyruvate concentrations.

When Graus et al., (2004) attempted to enhance emissions of acetaldehyde during light dark transitions by using disulfiram to inhibit acetaldehyde consumption by ALDH, acetaldehyde emissions were not enhanced as they expected. They concluded that light to dark transitions do not produce acetaldehyde by the pyruvate overflow mechanism, and suggested instead that acetaldehyde emitted is due to the leaf response to wounding because of the simultaneous emissions of the Green Leaf Volatiles (GLVs). Although small emissions of GLVs were detected by PTR-MS in the current study (data not shown), their magnitude was very low and became undetectable with subsequent light to dark transitions. Nonetheless, our results do suggest that a small amount of membrane damage occurs during light to dark transitions as would be expected since physical changes are associated with these transitions in chloroplasts. However, even if disulfiram did fully inhibit the oxidation of acetaldehyde by ALDH, ethanolic fermentation as a source of acetaldehyde during light to dark transitions cannot be ruled out; regardless of what the source of acetaldehyde is during light to dark transitions, inhibiting its consumption by ALDH should always result in enhanced emissions. These results call into question the effectiveness of disulfiram as an ALDH inhibitor.

The ability of disulfiram dissolved in an aqueous solution and supplied to excised leaves via the transpiration stream to completely and specifically inhibit all ALDH enzymes responsible for acetaldehyde oxidation was not observed in this study. Although disulfiram has been shown to be a potent inhibitor of mammalian ALDH enzymes, it may not be able to completely inhibit all plant ALDH enzymes which have been found in chloroplasts, mitochondria, and the cytosol. Our observations are supported by various complementary studies. For example, during *in vitro* acetaldehyde oxidation assays with two mitochondrial ALDH enzymes from maize (RF2A and RF2B), Liu and Schnable, (2002) demonstrated that only RF2B is significantly inhibited by disulfiram (90%) whereas RF2A is not (20%). Grover and Laties, (1981) also demonstrated that disulfiram is not specific for ALDH since it also inhibits the alternative respiratory pathway in isolated mitochondria but not in intact cells or tissues possibly due to a lack of absorption. Although opdenCamp and Kuhlemeier, (1997) showed that disulfiram effectively kills tobacco pollen presumably by inhibiting ALDH and therefore the PDH bypass, its application to seedlings had little visible effect. Although they concluded that the PDH bypass may not be important in seedlings, it is also possible that disulfiram was not taken up by the plant cells, was inactive on all forms of ALDH present, and/or was not specific for ALDH. The non-specific nature of disulfiram was also revealed by its ability

to inhibit lipooxygenase enzymes (Stelzig et al., 1983) and the photosynthetic electron transport chain in thylakoid membranes (Blubaugh and Govindjee, 1988) effectively inhibiting photosynthesis (Bown et al., 1984). Therefore, the ability of disulfiram supplied to plants via the transpiration stream to effectively and selectively inhibit ALDH enzymes responsible for acetaldehyde oxidation seems highly unlikely. This conclusion is supported by the results from an acetaldehyde compensation point study on holly oak and poplar branches (Jardine et al., 2007). Acetaldehyde compensation points did not significantly increase in disulfiram treated branches relative to tap water controls in either the light or dark. Therefore, it can be concluded that disulfiram supplied to branches via the transpiration stream is ineffective at blocking the oxidation of acetaldehyde by ALDH which may occur in the cytosol, mitochondria, and chloroplasts.

There is a significant enhancement in respiration measured by CO_2 evolution from leaves following a light to dark transition, termed light-enhanced dark respiration (LEDR). This is thought to be based on the interaction between newly assimilated carbon in chloroplasts and respiration in mitochondria (Raghavendra et al., 1994; Parys et al., 2004; Parys and Jastrzebski, 2006; Barbour et al., 2007). Following a light to dark transition, a major switch is made between chloroplasts and the mitochondria for ATP production in plant cells. Upon darkening, respiration rates suddenly increase several fold over background dark respiration rates. Although the height of the LEDR peak upon darkening is correlated with the cumulative amount of photoassimilated carbon during the preceding light period (Atkin et al., 1998), the specific metabolic source of the respired carbon is uncertain. One possibility is that during the light period, malate accumulates because of the suppression of mitochondrial respiration. Malate can be made in the cytosol during the light period from bicarbonate and phosphoenolpyruvate (catalyzed by PEP carboxylase). As supported by new stable carbon isotope measurements of the evolved CO_2 upon darkening, an NAD^+ dependent malic enzyme may rapidly decarboxylate malate to pyruvate (Barbour et al., 2007). This enzyme has been found both in the cytosol as well as mitochondria (Wedding, 1989) and so darkening may lead to a rapid buildup in pyruvate leading to bursts in both ethanolic fermentation and respiration. This mechanism is supported by the simultaneous emission bursts of CO_2 and acetaldehyde following darkening (Figure 19) measured in this study. This is consistent with the light to dark transition experiments by (Karl et al., 2002) with plants labeled with 99% $^{13}CO_2$. During these experiments, nearly equal amounts of both labeled and unlabeled acetaldehyde emissions occurred. This suggests that the pyruvate is derived from both recent photosynthetic products (malate) as well as cytosolic sources (glycolysis of sugars) following a light to dark transition. We term the burst in acetaldehyde and ethanol emissions measured here during a light to dark transition the Light Enhanced Dark Fermentation (LEDF) effect. Although

it has not been directly measured, the rapid increase in pyruvate concentrations following a light to dark transition is supported by the finding that LEDR is strongly dependent upon the activity of the alternate respiration pathway in mitochondria. Treatment of Z. *mays* with an inhibitor of AOX caused a substantial reduction in post illumination respiration (Parys and Staszewski, 1992).

The results presented here clearly demonstrate that acetaldehyde emission rates can be significantly enhanced during light to dark transitions if enough time is spent in the light and in the dark. The time in the light may be necessary to accumulate photosynthetic products and the time in the dark may be necessary for the LEDR and LEDF processes to occur. This situation may occur in nature for example when clouds pass overhead after periods of full sunlight. This may significantly enhance local acetaldehyde emissions to the atmosphere and therefore strongly affect regional atmospheric chemistry. Future work could attempt to demonstrate these processes in the field by quantifying ecosystem scale flux measurements of carbon dioxide, acetaldehyde, ethanol, and acetic acid and relate this to changes in solar illumination.

In a separate paper (Jardine et al., 2007), stable carbon isotope analysis of acetaldehyde emissions induced by a stress event like leaf desiccation provides evidence that ethanolic fermentation rates are stimulated by stress. This is consistent with a small but growing base of literature suggesting that ethanolic fermentation rates are stimulated following a stress event such as pathogen attack, dehydration, and mechanical wounding. For example Kimmerer and Kozlowski, (1982) found that the leaves of plants produce ethanol and acetaldehyde under aerobic conditions following a number of stresses including ozone, sulfur dioxide, and desiccation. This may be due to the accumulation of pyruvate due to damage to mitochondria and/or to an increase in PDC and ADH gene expression following stress (Tadege et al., 1999; Moyano et al., 2004). Recent evidence suggests that acetaldehyde produced from ethanolic fermentation may be important in defense gene activation and the hypersensitive response in plants under pathogen attack (Tadege et al., 1998).

3.6 Conclusions

The metabolic origin of acetaldehyde emitted into the atmosphere by plants is currently unknown but has been generally considered to be due to the production of ethanol in anoxic roots followed by transport to leaves and oxidation to acetaldehyde. However, this is not consistent with current knowledge of acetaldehyde emissions from forests. In the current study, we present evidence that ethanolic fermentation coupled to the PDH bypass system occurs under aerobic conditions in leaves of terrestrial C3 plants and that the rates are

controlled in part by pyruvate concentrations. We demonstrate that under aerobic conditions acetaldehyde, ethanol, and acetic acid are emitted from branches during photosynthesis and following a light to dark transition. In addition, in a separate paper we support the role of ethanolic fermentation during plant stress (Jardine et al., 2007). The balance between fermentation and respiration under aerobic conditions in plants is controlled at multiple levels including gene expression, pyruvate concentrations, and the activity of the alternative oxidase pathway (AOX).

Among the many functional reasons for the coupling of ethanolic fermentation and the PDH bypass under aerobic conditions in plants are 1) to help integrate the carbon metabolisms of photosynthesis, respiration, and fermentation, 2) to provide substrate (acetyl CoA) for the biosynthesis of lipids (fatty acids and terpenoids), 3) to help prevent the acidification of the cytosol, and 4) to maintain the production of ATP during periods of impaired mitochondrial function. These coupled pathways lead to both the emissions of acetaldehyde to the atmosphere via the PDC reaction and its uptake via the ALDH reaction. Therefore, the relative rates of these reactions may strongly influence the acetaldehyde compensation point and therefore the exchange flux with the atmosphere.

Light to dark transitions lead to a considerable burst in emissions of all three metabolites, a process which we term light enhanced dark fermentation (LEDF) based on its strong analogies with the light enhanced dark respiration (LEDR) effect. In particular, both the LEDF and the LEDR effect are dependent on previous photosynthetic rates and appear to be stimulated by the rapid accumulation of pyruvate after darkening. We also address previous doubts over the role of ethanolic fermentation in aerobic conditions in leaves by investigating the ability of disulfiram to interfere with acetaldehyde metabolism. In particular, for the first time we directly test the ability of disulfiram to inhibit ALDH enzymes in plants by fumigating plants with elevated levels of gas phase acetaldehyde and measuring the effect of disulfiram on acetaldehyde uptake rates. The results demonstrate that disulfiram does not appear to interfere with the reaction catalyzed by ALDH since 1) no clear suppression of acetaldehyde uptake rates could be detected relative to control plants, and 2) light to dark transitions on disulfiram treated poplar branches did not increase acetaldehyde emissions relative to control plants as expected. Assuming that acetaldehyde oxidation by ALDH is the major sink for acetaldehyde in branches, it can be concluded that disulfiram supplied to branches via the transpiration stream is unable to effectively inhibit ALDH enzymes.

3.7 Acknowledgments

We would like to kindly thank Ray Fall at the University of Colorado at Boulder for providing poplar trees for this experiment and for the many fruitful

discussions about acetaldehyde. We also would like to thank Eric Apel at NCAR for providing the acetaldehyde gas standards and the NSF-funded Biosphere Atmosphere Research and Training (BART) program for providing the financial assistance for this work. The National Center for Atmospheric Research is operated by the University Corporation for Atmospheric Research under the sponsorship of the National Science Foundation.

3.8 Figures

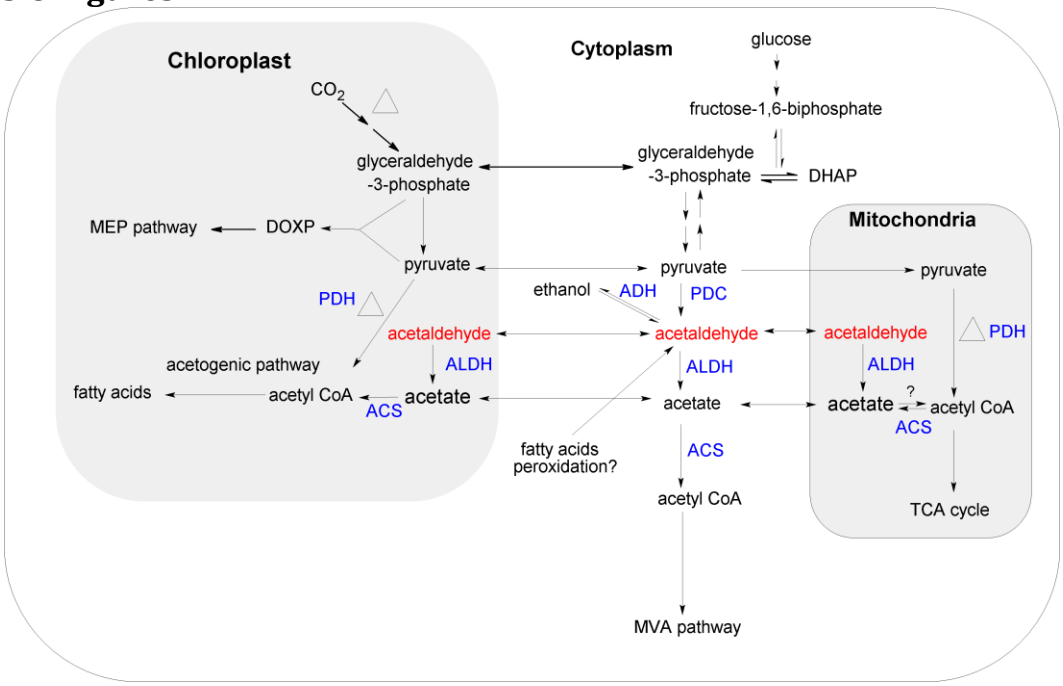

Figure 16: Possible biochemical sources and sinks of acetaldehyde in plant leaves.
Acetaldehyde is produced by ethanolic fermentation in the cytoplasm and consumed by the PDH system to produce acetyl CoA. Acetyl CoA may then help fuel respiration in the mitochondria, lead to terpenoid biosynthesis via the Mevalonate pathway (MVA) or fatty acid biosynthesis via the acetogenic pathway. Triangles indicate reactions associated with a large kinetic isotope effect. During plant stress, a new possible source of acetaldehyde has recently been suggested from lipid peroxidation reactions (Jardine et al., 2007). Enzymes involved in the metabolism of acetaldehyde include alcohol dehydrogenase (ADH), pyruvate decarboxylase (PDC), pyruvate dehydrogenase (PDH), acetyl-CoA synthetase (ACS), and aldehyde dehydrogenase (ALDH).

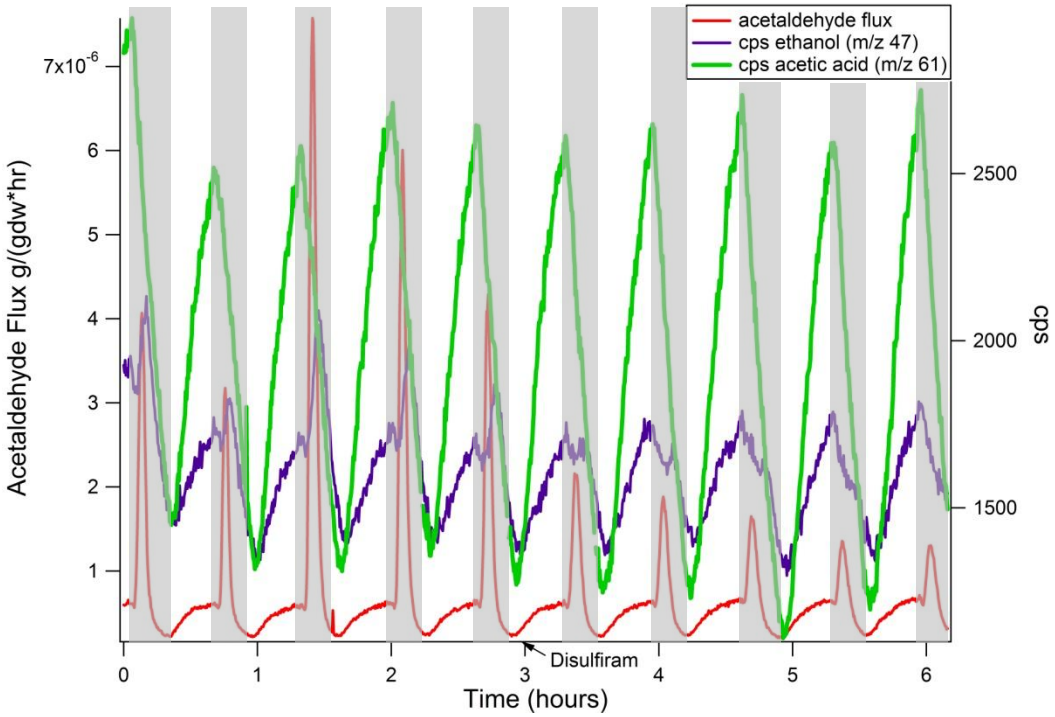

Figure 17: VOC emissions following ten light to dark transitions on an excised poplar branch in tap water. After 3 hours, 0.65 mM disulfiram was applied through the transpiration stream.

The results demonstrate that at steady state the emissions of acetaldehyde, ethanol, and acetic acid are enhanced during the light compared with the dark. In addition, light to dark transitions lead to a large transient burst in emissions of these metabolites. However the magnitudes of acetaldehyde emission bursts under disulfiram are not enhanced as expected. The light period was set to ~25 minutes in order for isoprene emissions to recover to pre-darkening levels (data not shown).

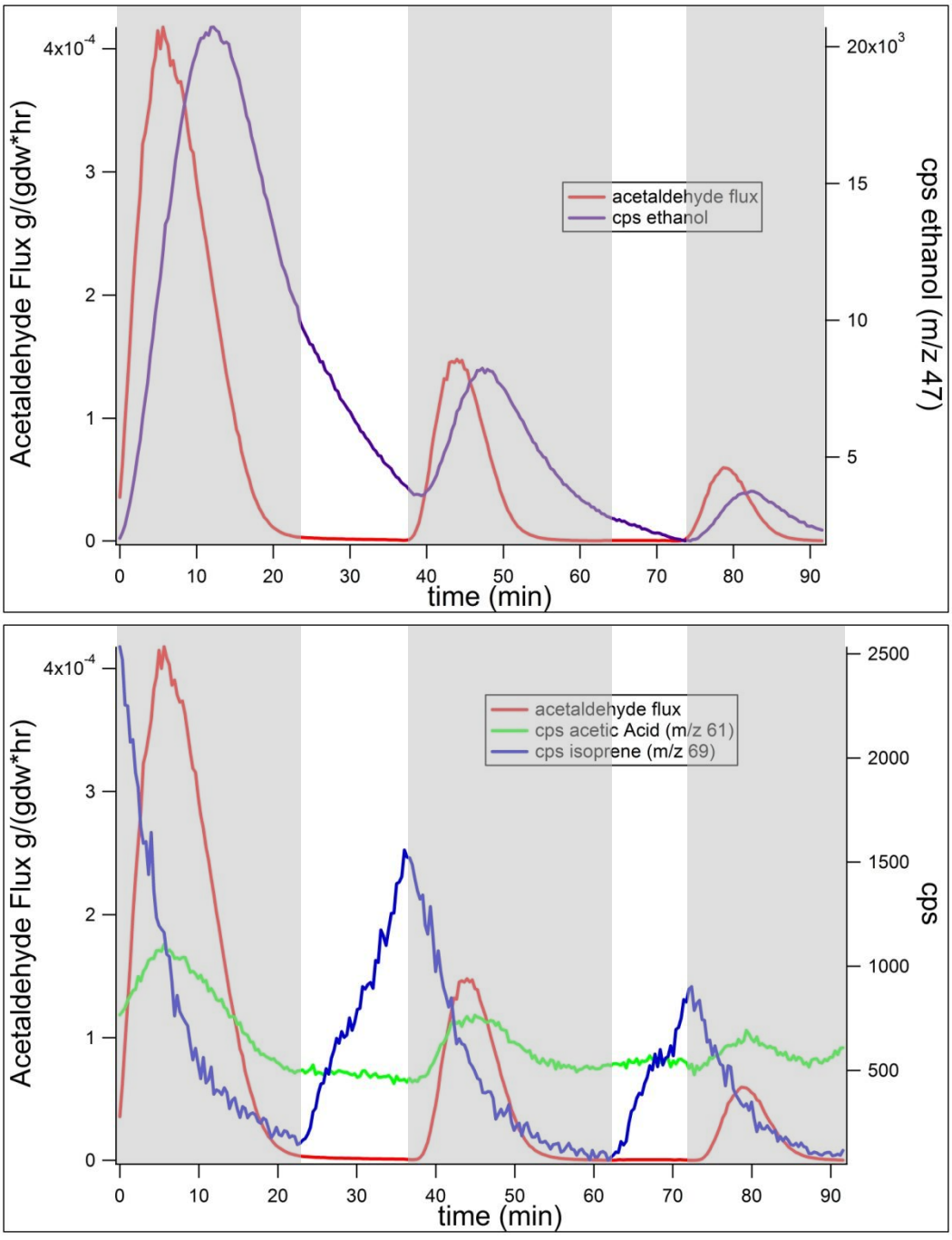

Figure 18: Light to dark transitions showing large emissions of acetaldehyde, ethanol, and acetic acid from an intact poplar branch. The light was turned off between 0-20, 37-58 and 74-95 minutes.

A poplar branch was exposed to four hours of light prior to darkening. Emissions of ethanol show a clear delay relative to acetaldehyde while acetic acid has very similar temporal patterns to acetaldehyde. The

reduced fluxes of acetaldehyde from sequential light to dark transitions indicate that the accumulation of photoassimilated carbon is an important source of acetaldehyde during these events. This is supported by the fact that isoprene emissions, which are known to be mainly fueled by recent photoassimilated carbon, are not given enough time in the light to recover to pre-darkened conditions (data not shown). Transpiration rates throughout the experiment were higher in the light than in the dark, but were consistent for all three light to dark cycles.

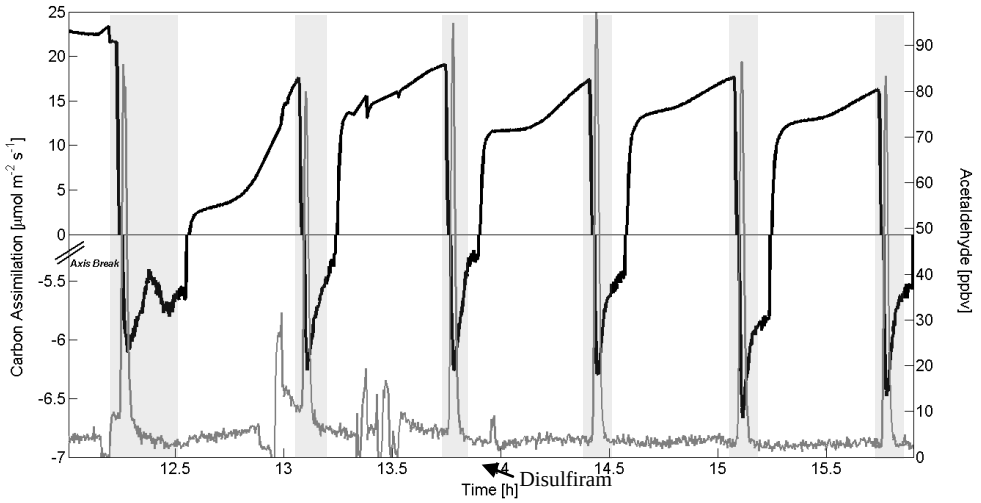

Figure 19: Six light to dark transitions on an excised poplar branch showing leaf level CO2 and acetaldehyde exchange rates without (first three transitions) and with (last three transitions) disulfiram.

The tight temporal coupling of acetaldehyde and carbon dioxide emission bursts supports the hypothesis that the LEDF and LEDR processes are both dependent on the concentration of pyruvate.

Chapter 4: Acetaldehyde Production in Plants: Stress induced peroxidation of fatty acids?

4.1 ABSTRACT

We investigated the pathway(s) responsible for the production of acetaldehyde during biotic and abiotic stresses in plants by studying variations in the stable carbon isotope composition of acetaldehyde that is produced under stress. Under an anoxic environment, C3 leaves produced acetaldehyde with a similar carbon isotopic composition to C3 bulk biomass. In contrast, the initial emission burst following mechanical wounding was 5 to 12 ‰ more depleted in ^{13}C than emissions under anoxia. During the drying process, a second large enhancement in emission rates occurred and was also ^{13}C depleted. However, in between and after these high emission rates, lower emission rates of acetaldehyde occurred that had similar $\delta^{13}C$ values to bulk C3 biomass. Our observations provide the first evidence that under stress, acetaldehyde depleted in ^{13}C is produced from fatty acid peroxidation reactions initiated by the accumulation of reactive oxygen species (ROS). Emissions of acetaldehyde with similar $\delta^{13}C$ values to bulk biomass in between the wounding and drying process may be due to an increase in ethanolic fermentation rates stimulated by the wounding process. Continued emissions with similar $\delta^{13}C$ values to bulk biomass after drying may be due to decomposition processes characteristic of decaying litter.

4.2 Introduction

The emission of acetaldehyde from plant canopies to the atmosphere may significantly influence air quality and climate. Although its metabolic origin remains uncertain, acetaldehyde is emitted into the atmosphere from plants during a wide variety of stresses and may play important roles in plant defense against stress. Acetaldehyde is a potent antibiotic and its emission from damaged tissue may help prevent infections (Utama, 2002). Acetaldehyde may also activate the expression of plant defense genes (Tadege et al., 1998). Enhanced acetaldehyde emissions have been observed following mechanical wounding, desiccation, freeze thaw events, herbivore attack, ozone fumigation, high light, high temperature, and many other biotic and abiotic stresses (Kimmerer and Kozlowski, 1982; de Gouw et al., 1999; Fall et al., 1999; Karl et al., 2001; Karl et al., 2001; Cojocariu et al., 2005; Karl et al., 2005; Loreto et al., 2006). Although a small amount of this acetaldehyde can be attributed to what was present in the transpiration stream, another source is likely (Fall, 2003).

The stimulation of respiration rates following mechanical wounding is well documented in plants and it appears that both lipids and carbohydrates are used as substrates. For example, using potato slices, Jacobson et al., (1970) suggested that immediately following wounding, lipids are the respiratory substrate but that subsequently a switch is made to carbohydrates. As reviewed by Tadege et al., (1999), there is also evidence emerging that various stresses increase ethanolic fermentation rates and that a switch from respiration to

ethanolic fermentation can accompany stress under aerobic conditions. For example, the expression of PDC and ADH enzymes involved in ethanolic fermentation increased dramatically under abiotic stress in Arabidopsis (Dolferus et al., 1994; Dolferus et al., 1994). However, the ubiquitous production of acetaldehyde from plants under stress cannot be used to conclusively demonstrate the switch to ethanolic fermentation since other pathways for producing acetaldehyde may exist. Graus et al., (2004) suggested that another possible source of acetaldehyde is the conversion of acetyl-CoA to acetaldehyde, although there is currently no known mechanism in plants for this reaction, and the pool size of acetyl-CoA is too small to account for the acetaldehyde observed. Although the reduction of acetyl-CoA to acetaldehyde by an acetaldehyde dehydrogenase has been discovered in a protist (Sanchez, 1998), a comparable enzyme has not been found in plants. Halliwell and Gutteridge, (1999) suggested that free radical peroxidation of membrane fatty acids may lead to the production of acetaldehyde, although there is no experimental evidence to support this hypothesis. In this paper, we investigate the pathway(s) responsible for the production of acetaldehyde during biotic and abiotic stresses in plants by studying variations in the stable carbon isotope composition of acetaldehyde that is produced under stress.

Knowledge of the intermolecular distribution of carbon isotopes among organic compounds is a powerful emerging tool in the area of biosphere atmosphere interactions. As discussed by Augusti and Schleucher, (2007), changes in the relative abundance of the stable carbon isotopes in plant metabolites can be directly related to their metabolic origin. There are two major reactions in plants that strongly alter the carbon isotope composition of plant matter. The first is the carboxylation of ribulose-1,5-bisphosphate during photoassimilation and the second is the decarboxylation of pyruvate to acetyl-CoA by pyruvate dehydrogenase (PDH) during biosynthetic and energy related processes such as lipid biosynthesis and respiration. During photoassimilation, along with kinetic isotope fractionation during carbon dioxide diffusion, carboxylation by RuBisCO is the major cause of the depletion in ^{13}C in bulk plant matter relative to atmospheric carbon dioxide. Because plants derive virtually all their carbon from photoassimilation, the large discrimination against $^{13}CO_2$ strongly influences the $\delta^{13}C$ value of plant bulk biomass. However, photosynthesis and diffusion alone cannot explain the uneven distribution of carbon isotopes among cellular metabolites (intermolecular variability).

Evidence for intermolecular variations in the carbon isotope content of plant matter was first provided by Park and Epstein, (1961) who discovered that the lipid fraction of plants was significantly depleted in ^{13}C when compared with bulk biomass. Deniro and Epstein, (1977) demonstrated the role of pyruvate decarboxylation by PDH on the ^{13}C depletion of lipids. Compounds produced

from PDH-derived acetyl-CoA such as fatty acids are depleted in ^{13}C relative to bulk biomass. For example Ballentine et al., (1998) found that fatty acids from C3 plants are on average 6.5‰ more depleted in ^{13}C than bulk biomass. In contrast, compounds that are produced from ethanolic fermentation and the PDH bypass system such as acetaldehyde, ethanol, and acetic acid are not as depleted in ^{13}C. For example when Hobbie and Werner, (2004) surveyed the literature on ethanolic fermentation by C3 plants, they found that the ethanol (and therefore acetaldehyde) produced during fermentation was between 1-2 ‰ depleted in ^{13}C relative to the parent carbohydrate.

In this study, we hypothesize that acetaldehyde produced from ethanolic fermentation in C3 leaves will have a similar $\delta^{13}C$ value to bulk biomass. Likewise, processes that produce acetaldehyde from the decomposition of bulk biomass such as during leaf decay will also carry the $\delta^{13}C$ signature of bulk biomass. However, if acetaldehyde is derived from carbon pools depleted in ^{13}C such as fatty acids, then it will be similarly depleted in ^{13}C. To test this hypothesis, we performed stable carbon isotope ratio measurements of gas phase acetaldehyde emitted from various C3 tree species under anoxic conditions, during mechanical wounding and desiccation, as well as during leaf decay. In addition, emission rate measurements of acetaldehyde were made with high temporal resolution during mechanical wounding, anoxia, and re-aeration.

4.3 Materials and Methods

4.3.1 Plants

Potted poplar (*Populus deltoides*, clone #ST109) individuals were obtained from the Stony Brook University greenhouse (Stony Brook, NY). Plants were potted into 4-L plastic pots containing a commercial potting mix (MiracleGro) with Osmocote slow release fertilizers. White oak (*Quercus rubra*), red maple (*Acer rubrum*), and sassafras (*Sassafras albidum*) branches were obtained from plants in the forest surrounding the Marine Science Research Center at Stony Brook University. Post-senescent red maple leaves were obtained from the forest floor during early December.

4.3.2 Acetaldehyde $\delta^{13}C$ measurements

$\delta^{13}C$ measurements of gas phase acetaldehyde were made without the need for derivitization by coupling traditional cryogenic preconcentration of VOCs from ambient air (Greenberg and Zimmerman, 1984) to a gas chromatograph-combustion-isotope ratio mass spectrometer (GC-C-IRMS) system. A custom VOC pre-concentration system was built in order to preconcentrate gas phase acetaldehyde as well as separate it from N_2, O_2, Ar and trace species including H_2O and CO_2. All tubing and traps were composed of fused silica-lined stainless steel tubing (Restek, Bellefonte, PA) or Teflon. Stainless steel switching valves

(VICI, Houston, TX) were heated to 100 ^{o}C and tubing through which the sample passed was heated to 200 ^{o}C. The sample was drawn into the preconcentration system by a diaphragm pump (Pfeiffer Vacuum, Nashua, NH) connected to a mass flow controller (Omega, Stamford, CT) at 250 mL min^{-1} for 10 minutes resulting in a sampled volume of 2.5 L. The air sample first passed through a 3 foot coil of 1/8" O.D. Teflon tubing held at 0 ^{o}C in order to condense a large percentage of the water vapor. In contrast to alternate drying methods using solid adsorbents, this technique did not affect the concentration of acetaldehyde. We assume that carbon isotope fractionation during the partitioning of acetaldehyde into the condensed water during this step is insignificant, by analogy with the results of Johnson and Dawson, (1993) who found that the equilibrium carbon fractionation associated with the partitioning of gaseous formic acid into an aqueous phase is negligible. They concluded that the carbon isotope signature of oxygenated organics is not affected by wet deposition. Following drying, the sample was passed through a hydrocarbon trap (1/4" O.D. x 9" Silcosteel tube packed with TENAX-TA (Sigma-Aldrich)) held at -50 ^{o}C. Hydrocarbon trap temperatures above 0 ^{o}C were shown to strongly fractionate acetaldehyde due to incomplete trapping efficiency (acetaldehyde breakthrough).

The concentrated sample was then injected directly onto the GC column (0.53mm x 30m: RTX-624) by rapidly heating the hydrocarbon trap to 200 ^{o}C for five minutes while back-flushing with 1.0 ml min^{-1} UHP helium. After the injection, the preconcentration system was continuously back-flushed with UHP helium at a flow rate of 25 ml min^{-1} until the next sample was ready for collection. In order to improve peak separation and shape, we employed a cryofocusing trap consisting of two small loops at the beginning of the GC column, immersed in liquid nitrogen. The cryofocusing trap was rapidly heated by removing the liquid nitrogen bath. Following sample injection, the GC oven (6890 GC, Agilent Technologies, Santa Clara , CA) was maintained at 25 ^{o}C for 10 min and then rapidly heated to 200 ^{o}C for two minutes to "bake out" the GC column. Eluents of the GC column then underwent oxidation to water and carbon dioxide in an alumina tube held at 950 ^{o}C and packed with CuO, NiO, and Pt wires. The oxidation products then passed through a Nafion drying membrane (Permapure Inc., Toms River, NJ), and chromatographic peaks were introduced into an isotope ratio mass spectrometer (IRMS) (Finnigan Delta Plus; Finnigan MAT, Bremen, Germany) through an open split system providing ~0.5 mL min^{-1} to the ion source. Prior to the arrival of the acetaldehyde peak at the IRMS, three injections of a carbon dioxide standard of known isotopic composition (-42.7 ‰) were performed in order to calibrate the δ^{13}C measurement. The pressure of the reference carbon dioxide was adjusted prior to the run to approximately match the expected peak height of the sample. Peaks were identified based on retention time relative to calibration standards (acetaldehyde, methanol, acetone, isoprene).

Isotope data is expressed using the conventional δ notation in units of per mil (‰):

$$\delta^{13}C = \frac{R_{sample} - R_{standard}}{R_{standard}} \cdot 1000$$

where R is the ratio of the peak area for m/z 45 ($^{13}CO_2$) to m/z 44 ($^{12}CO_2$) for sample and standard (V-PDB-CO_2). The $\delta^{13}C$ values were calculated by the ISODAT NT 2.0 software and a manual correction based on a linear dependence of $\delta^{13}C$ on the difference in peak heights between the reference carbon dioxide peak and the VOC derived carbon dioxide peak was applied when necessary. The precision of the instrument was between 0.2 and 1.0 ‰ (V-PDB) determined by multiple measurements of a 30 ppbv acetaldehyde standard diluted in zero air with a dynamic dilution system. Due to losses at the split (50 %) and IRMS sensitivity, the minimum acetaldehyde concentration needed to produce a 1.0 volt peak for an accurate $\delta^{13}C$ measurement was determined to be ~10 ppbv. Peaks smaller than 1.0 V were not included in the analysis.

4.3.3 Ethanol oxidation

In order to demonstrate the ability of tree leaves to oxidize ethanol in the transpiration stream to acetaldehyde, a 0.5% solution of commercial ethanol in tap water was supplied via the transpiration stream to excised leaves of white oak exposed to full sunlight for 2 hours. 4-5 leaves were then removed from the ethanol solution and placed in a static enclosure filled with outdoor air and connected to the GC-C-IRMS system. $\delta^{13}C$ values of the acetaldehyde in the headspace was measured every 30 minutes and the experiment was repeated four times. Because commercial ethanol is derived from C4 plants, its $\delta^{13}C$ value is likely to be between -11 ‰ and -14 ‰ (Ishida-Fujii et al., 2005).

4.3.4 Ethanolic fermentation under anoxia and re-aeration

In order to obtain the carbon isotope signature of acetaldehyde emitted from ethanolic fermentation, excised red maple and white oak leaves were exposed to anoxic conditions during three replicate experiments per species. 4-5 leaves were placed in a polyethylene bag filled with approximately 15 L of UHP helium in order to induce fermentation. The static enclosure was connected to the GC-C-IRMS system and $\delta^{13}C$ measurements were made approximately every 30 minutes. Control experiments were also performed with empty bags filled with UHP helium.

In order to investigate the role of re-aeration on acetaldehyde emissions following anoxic conditions, in two replicate experiments poplar branches were placed in a 5 L dynamic Teflon branch enclosure and UHP nitrogen was added at a flow rate of 1.0 L min^{-1}. After emission rates of acetaldehyde stabilized (30-60 min), UHP nitrogen was replaced with 1.0 L min^{-1} of hydrocarbon free air. While

$\delta^{13}C$ measurements of acetaldehyde were not available, the emission rates of acetaldehyde, ethanol, and acetic acid were measured with a proton transfer reaction-mass spectrometer (PTR-MS) as described by (Jardine et al., 2008).

4.3.5 Mechanical wounding

3-5 excised leaves from a single species were mechanically wounded by ripping the leaf in half by hand, and then placed in a 15 L polyethylene bag filled with UHP hydrocarbon free air. The enclosure was immediately connected to the GC-C-IRMS instrument and $\delta^{13}C$ measurements were made approximately every 30 minutes. Control experiments were also performed with empty polyethylene bags filled with a similar volume of UHP zero air. The experiment was repeated 11, 11, 9, and 14 times for red maple, white oak, poplar and sassafras respectively. For emission rate measurements using the PTR-MS, mechanically wounded poplar leaves were placed in a dynamic enclosure, purged with 1.0 L min^{-1} flow of hydrocarbon free air; 0.2 L min^{-1} was continuously drawn into the PTR-MS.

4.3.6 Leaf desiccation

In order to investigate the sources of acetaldehyde during leaf desiccation, during three replicate experiments, 4-5 excised poplar leaves were mechanically wounded by ripping the leaves in half to accelerate drying and placed in a 5 L dynamic Teflon branch enclosure. Dry UHP hydrocarbon free air was then continuously added to the enclosure at a flow rate of 0.5 L min^{-1} with a residence time in the enclosure of ~10 minutes. The enclosure was connected to the cryogenic preconcentration system coupled to the GC-C-IRMS instrument and $\delta^{13}C$ measurements were made approximately every 30 minutes for up to 8 hours. Control experiments with an empty enclosure were also performed prior to introducing the leaves.

4.3.7 Leaf decay

Approximately ~50 post-senescent red maple leaves were collected from the forest floor during December, placed in a polyethylene bag and incubated for ~ 1 hour in order to accumulate acetaldehyde in the headspace sufficient for carbon isotope analysis by GC-C-IRMS. Five replicate experiments were preformed.

4.4 Results

White oak leaves successfully converted 0.5% commercial ethanol in the transpiration stream to acetaldehyde, which accumulated in the static enclosure over time (data not shown). The strong enhancement in ^{13}C of acetaldehyde emitted from ethanol oxidation relative to fermentation shown in Figure 20 is due to the fact that the commercial ethanol was derived a C4 plant, and not to

fractionation during the conversion of ethanol to acetaldehyde (Ishida-Fujii et al., 2005). However, these results clearly demonstrate that acetaldehyde can be produced from the oxidation of ethanol in the transpiration stream. The acetaldehyde emitted from mechanically wounded white oak leaves was more depleted in ^{13}C by up to 12 ‰ relative to acetaldehyde emitted during ethanolic fermentation under anoxia.

Figure 21 presents a summary of the ranges of acetaldehyde $\delta^{13}C$ values measured from the various species studied here and compared with a previous study (Keppler et al., 2004). For all species studied, $\delta^{13}C$ values of acetaldehyde arising from ethanolic fermentation during anoxia are very similar to those from decaying leaf litter as well as those from acetaldehyde emitted during leaf heating experiments (Keppler et al., 2004). All are very similar to the carbon isotope signature of bulk biomass of C3 plants as measured by Keppler et al., (2004) which suggests that they are all derived from components with carbon isotopic composition similar to bulk biomass. In contrast, acetaldehyde emitted from mechanical wounding of leaves is depleted in ^{13}C with a similar depletion for the four different broadleaf C3 tree species studied. The $\delta^{13}C$ values of acetaldehyde emitted from mechanical wounding are 5-12 ‰ more depleted in ^{13}C than acetaldehyde emitted during ethanolic fermentation.

There is a large enhancement in acetaldehyde emissions during wounding/desiccation experiments with poplar leaves in a dynamic enclosure (Figure 22). The initial wounding event leads to enhanced acetaldehyde emissions rates which give way to much larger and sustained emissions during the drying process. These emissions are strongly depleted in ^{13}C relative to bulk C3 biomass. Although lower in magnitude, emissions of acetaldehyde with $\delta^{13}C$ values similar to bulk C3 biomass occur before and after the large emission burst from the drying process. High temporal resolution PTR-MS emission rate measurements (Figure 23) demonstrate that mechanical wounding leads to a rapid burst of acetaldehyde emissions and that enhanced emission rates occur even one hour after wounding. During this experiment, emissions from additional wounding during the drying process were not observed and the wounded leaf tissue did not show signs of dehydration after one hour in the enclosure.

Figure 24 illustrates the large enhancement in acetaldehyde emissions under anoxic conditions followed by a very large burst in emissions immediately following re-aeration. In order to investigate the role of ethanol oxidation in generating the acetaldehyde burst following re-aeration, ethanol, acetaldehyde, and acetic acid emission rates were monitored in a duplicate experiment (Figure 25). At approximately 0.25 hours, the branch was placed in the enclosure and the apparent enhancement in acetic acid emissions during this time is likely due to room air entering into the enclosure. Emission rates of acetaldehyde, ethanol, and acetic acid increase under anoxia indicating that both ethanolic fermentation and

acetaldehyde oxidation to acetic acid by ALDH occur under these conditions. Upon re-aeration, acetaldehyde emissions greatly increase for roughly 0.5 hour. During the anoxic period as well as during re-aeration, the emission rates of acetic acid parallel those of acetaldehyde. This indicates that the oxidation of acetaldehyde to acetic acid by ALDH occurs under both aerobic and anaerobic conditions. In contrast, while acetaldehyde and ethanol emissions generally increase in parallel under anoxia, upon re-aeration ethanol emission rates decrease rapidly while acetaldehyde emissions rates increase. When acetaldehyde emissions begin to decline, ethanol emissions slightly recover. Later, both acetaldehyde and ethanol emissions decline in parallel to background levels. These results suggest that under anoxia, both ethanol and acetaldehyde are being produced from fermentation of carbohydrates. Upon re-aeration, some of the acetaldehyde produced must be at the expense of ethanol as suggested by previous authors. Finally, emissions of both species decline because of a switch from fermentation back to respiration under aerobic conditions.

4.5 Discussion

The results presented here imply that during mechanical wounding, desiccation, and possibly other plant stresses, there exists a metabolic pathway that produces acetaldehyde from a source of carbon depleted in ^{13}C (Figure 26). There is a large carbon isotope fractionation during the production of acetyl CoA from pyruvate by pyruvate dehydrogenase (PDH) (Deniro and Epstein, 1977), and because fatty acids are derived from acetyl CoA via the acetogenic pathway, they are also depleted in ^{13}C. For example, individual fatty acids isolated from the C3 plant eucalyptus were 5-11 ‰ more depleted in ^{13}C relative to bulk biomass (Ballentine et al., 1998). The similar range of ^{13}C depletion for acetaldehyde emitted from wounded leaves and fatty acids leads us to hypothesize that fatty acids are a source of acetaldehyde emissions from stressed plants. Graus et al., (2004) suggested that the conversion of acetyl CoA to acetaldehyde represents an additional possible source. Although consistent with the depletion in ^{13}C of acetaldehyde emitted following leaf wounding and the known depletion in ^{13}C of acetyl CoA, no mechanism is known for this conversion. In addition, the emission rates of acetaldehyde following wounding are very high and it is not clear whether the pools of acetyl-CoA in plants could sustain the high emission rates observed in Figure 23. Roughan, (1997) measured total acetyl-CoA concentrations in chloroplasts freshly isolated from spinach and pea leaves and found values between 10 and 20 μM. Future work should establish whether leaf acetyl-CoA concentrations are high enough to account for the measured acetaldehyde emissions following wounding and if a mechanism exists for its conversion to acetaldehyde. However, following wounding, the drying process leads to a very large enhancement in emissions that is sustained for a long period of time relative

to the emissions from the initial wounding event (de Gouw et al., 1999). The total amount of acetaldehyde emitted is much larger than the initial wounding event making the role of acetyl-CoA conversion to acetaldehyde more doubtful.

Plant phospholipids contain polyunsaturated fatty acids derived from acetyl-CoA such as linoleic and linolenic acid which are highly susceptible to oxidation due to the presence of multiple double bonds between carbon atoms. Wagner et al., (1994) concluded that the oxidizability of lipids increases linearly with their extent of unsaturation. The generation of large oxidative bursts is known to be a general response of plants to stress such as ozone damage, high light, desiccation, pathogen attack, and mechanical damage (Cazale et al., 1998; Langebartels et al., 2002; Kotchoni and Gachomo, 2006). Interestingly, these same stresses also induce the emission of acetaldehyde. The rapid increase in the concentrations of Reactive Oxygen Species (ROS) such as superoxide, hydrogen peroxide, singlet oxygen, and the hydroxyl radical may have direct and indirect roles in the stress response such as acting as an antibiotic agent and controlling gene expression. However it is still unclear how ROS are perceived in order to elicit a range of stress responses. Many oxygenated VOCs important for atmospheric chemistry such as formaldehyde, acetone, and acetaldehyde are major products of lipid peroxidation by ROS (Dennis and Shibamoto, 1990; DeZwart et al., 1997; Enoiu et al., 2000; Orhan et al., 2006; Shibamoto, 2006). Although extensively used as biomarkers for lipid oxidation in animals including humans, their production in stressed plants via this mechanism has not been demonstrated. To our knowledge, the carbon isotope data presented here provides the first evidence for acetaldehyde emissions derived from the peroxidation of membrane fatty acids during plant stress, and satisfies three constraints. The source of acetaldehyde is only active during stress events; it is depleted in ^{13}C relative to bulk biomass, and constitutes a pool sufficiently large to sustain observed emission rates. In model plant membrane systems, Barclay and McKersie, (1994) found that increased concentrations of free linoleic acid and linolenic acid as opposed to the corresponding membrane associated phospholipids increased aldehyde production during lipid peroxidation reactions with ROS. Since stress can induce the massive release of fatty acids from plant membranes as a part of the octadecanoid pathway (Farmer and Ryan, 1992), the potential for peroxidation reactions is large. For example, during the initial stages of the drying process a large amount of fatty acid peroxidation may occur which then gives way to decomposition reactions of the dried bulk biomass (Warneke, 1999). The role of fatty acid peroxidation in producing acetaldehyde immediately following mechanical wounding is supported by many studies which discovered that a very rapid burst of oxidants accompanies stress. For example, within 30 seconds of stem cutting, leaves experienced an ROS burst that lasted for over 3

minutes (Dong and Xu, 2006). In another study, the cutting of leaf blades induced an immediate ROS burst (Le Deunff et al., 2004).

However, carbon isotope and emission data (Figure 22 and Figure 23) also suggests that an increase in ethanolic fermentation rates stimulated by the wounding and drying processes may occur. This is consistent with a small but growing base of literature suggesting that ethanolic fermentation rates are stimulated following a stress event such as pathogen attack, dehydration, and mechanical wounding. For example Kimmerer and Kozlowski, (1982) found that the leaves of plants produce ethanol and acetaldehyde under aerobic conditions following a number of stresses including ozone, sulfur dioxide, and desiccation. This may result from the accumulation of pyruvate due to damage to mitochondria and/or to an increase in PDC and ADH gene expression following stress (Tadege et al., 1999; Moyano et al., 2004).

In high concentrations, acetaldehyde can have dangerous effects on cellular processes by releasing zinc from zinc containing enzymes (Hao and Maret, 2006). Additional sinks of acetaldehyde are likely to exist in plants due to its high reactivity. For example, acetaldehyde readily form adducts with proteins, phospholipids, and DNA (Niemela et al., 1995; Shibamoto, 2006). The significance of these potentially harmful reactions to the overall sink of acetaldehyde is not known. In addition, the presence of acetaldehyde itself in excessive amounts leads to the production of reactive oxygen species and lipid peroxidation (Zhang et al., 1996; Novitskiy et al., 2006) which is a major cause of liver damage in alcoholic humans. Excessive damage due to the accumulation of ROS and toxic lipid peroxidation products such as aldehydes is prevented by ALDH enzymes. The expression of several ALDH enzymes are induced under stresses such as wounding, osmotic stress, dehydration, etc. (Kirch et al., 2004). These are known as ‘turgor responsive’ or ‘stress’ ALDH enzymes. For example, (Kotchoni et al., 2006) showed that the *Arabidopsis thaliana* genes ALDH3I1and ALDH7B4 are transcriptionally activated by abiotic stress and protect plants against oxidative damage and lipid peroxidation during abiotic stress events. Both chloroplastic ALDH3I1 and cytoplasmic ALDH7B4 enzymes help protect against damage by reducing both reactive oxygen species such as hydrogen peroxide and aldehydes produced during lipid peroxidation reactions following plant stresses such as dehydration. In human cells, acetaldehyde induced the production of ROS and cellular apoptosis but was alleviated by the overexpression of an ALDH gene (Li et al., 2006). The simultaneous occurrence of ROS, lipid peroxidation products such as aldehydes, and their detoxification by ALDH enzymes under stress supports the hypothesis presented here that lipid peroxidation leads to acetaldehyde production in stressed plants.

As suggested by others (Zuckermann et al., 1997; Tsuji et al., 2003), the results from Figures 24 and 25 support the role of ethanol peroxidation/oxidation

as a source of acetaldehyde upon re-aeration of anoxic tissue. The carbon isotope signature of the acetaldehyde burst following re-aeration was not obtained during this study, although this information is critical for determining the source(s) of acetaldehyde upon re-aeration. If the majority of acetaldehyde produced during re-aeration of anoxic tissue is from the peroxidation of fatty acids, then it should be depleted in ^{13}C. Future work should focus on these experiments as well as characterizing the carbon isotope signature of acetaldehyde emitted from other stress conditions in order to determine if the results obtained from wounding and desiccation are a general feature of plant stress. In addition, the carbon isotope composition of acetaldehyde emitted in the light and following light to dark transitions should be carried out in order to verify the hypothesis that ethanolic fermentation is the dominant source of acetaldehyde during normal unstressed conditions (Jardine et al., 2008). If ethanolic fermentation is the major pathway contributing to acetaldehyde production as proposed, then it should have a $\delta^{13}C$ value very similar to bulk biomass.

4.6 Conclusions

In this paper, we characterized the stable carbon isotope composition of acetaldehyde emitted from plants under various conditions. We found that the carbon isotopic composition of acetaldehyde emitted from C3 leaves during ethanolic fermentation and leaf decay is similar to the signature of acetaldehyde emitted from leaf heating and bulk C3 biomass (Keppler et al., 2004). However, mechanical wounding and desiccation of leaves releases acetaldehyde depleted in ^{13}C to a similar extent as in fatty acids. We propose that immediately following a stress such as mechanical wounding, the rapid accumulation of reactive oxygen species leads to fatty acid peroxidation reactions that produce acetaldehyde as a secondary product. Following the initial emission burst, lower acetaldehyde emissions with similar $\delta^{13}C$ values to bulk C3 biomass supports the idea that enhanced ethanolic fermentation rates are stimulated by the wounding process. As the leaves begin to dry out, massive amounts of membrane damage occurs leading to additional and more sustained fatty acid peroxidation. Once dry, the enzymatic machinery can no longer function yet continuous low level emissions of acetaldehyde with a $\delta^{13}C$ signature similar to that of bulk leaf biomass occur mainly due to general decomposition processes characteristic of decaying litter. Finally, while our observations support the role of ethanol peroxidation as a source of acetaldehyde following re-aeration of anoxic tissue, we suggest fatty acid peroxidation reactions may also contribute to this burst.

4.7 Acknowledgments

We would like to kindly thank the NSF funded Biosphere Atmosphere Research and Training (BART) program for providing the financial assistance for completing this work. We also would like to thank Jim Greenberg and Eric Apel

at NCAR for helping with instrument development and for providing gas standards. This work was supported by NSF grant ATM 0303727 (JE Mak), the NSF-funded Biosphere Atmosphere Research and Training (BART) program, and the Atmospheric Chemistry Division at NCAR. The National Center for Atmospheric Research is operated by the University Corporation for Atmospheric Research under the sponsorship of the National Science Foundation.

4.8 Figures

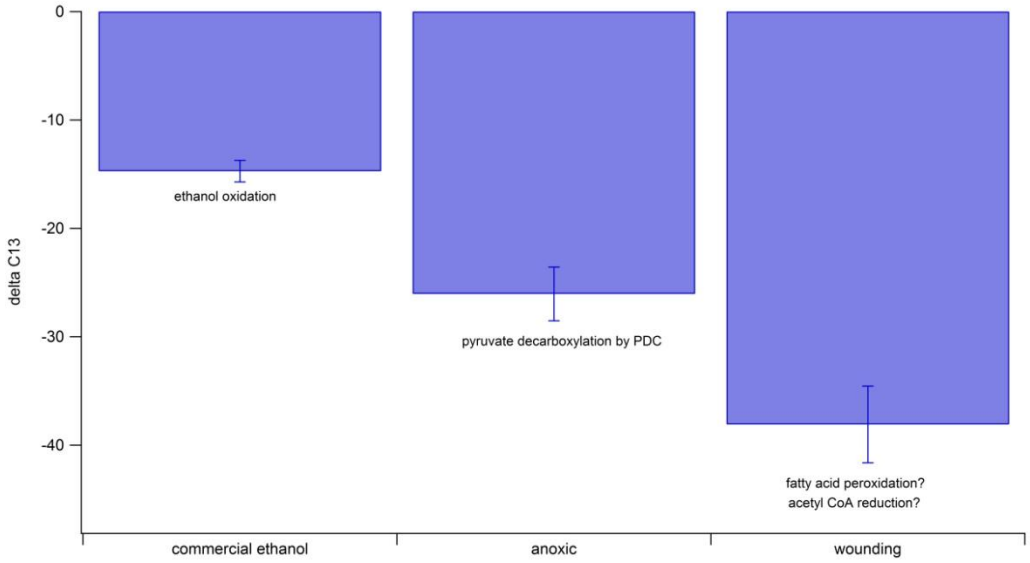

Figure 20: Stable carbon isotope ratios of acetaldehyde emitted from white oak (*Quercus rubra*) leaves under three different conditions.
Acetaldehyde derived from the oxidation of commercial ethanol in leaves is enriched in 13C because it is derived from C4 plants and not to fractionation during its production in leaves. Acetaldehyde emissions from mechanically wounded leaves are depleted in 13C by up to 12 ‰ relative to emissions under anoxia.

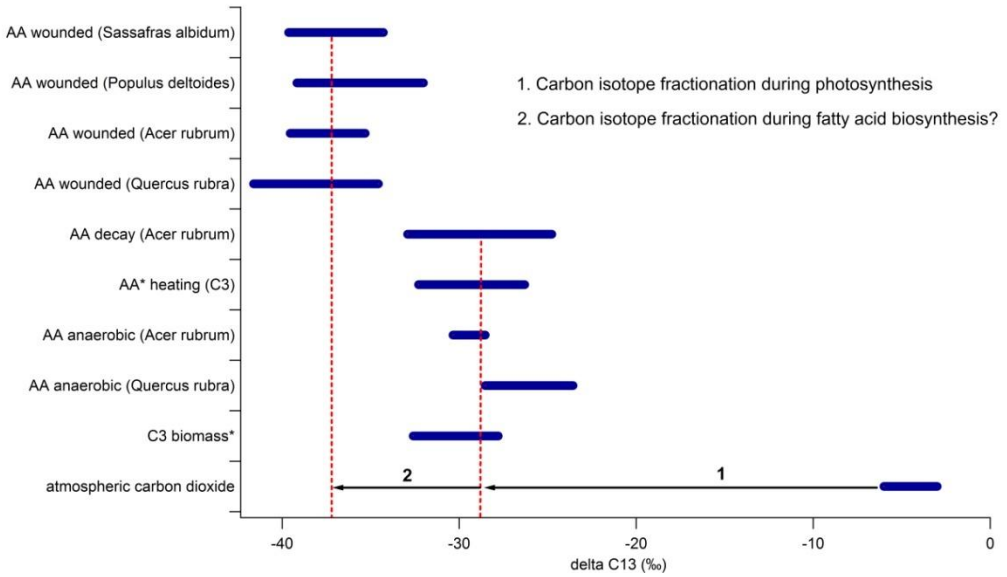

Figure 21: Ranges of δ ^{13}C values of atmospheric carbon dioxide, C3 biomass, and acetaldehyde emitted under various conditions.
There is a large carbon isotope fractionation associated with the fixation of carbon during photoassimilation by C3 plants. Acetaldehyde emissions from various C3 leaves have δ ^{13}C values similar to bulk biomass except for during leaf wounding which releases ^{13}C depleted acetaldehyde (* Data from (Keppler et al., 2004)).

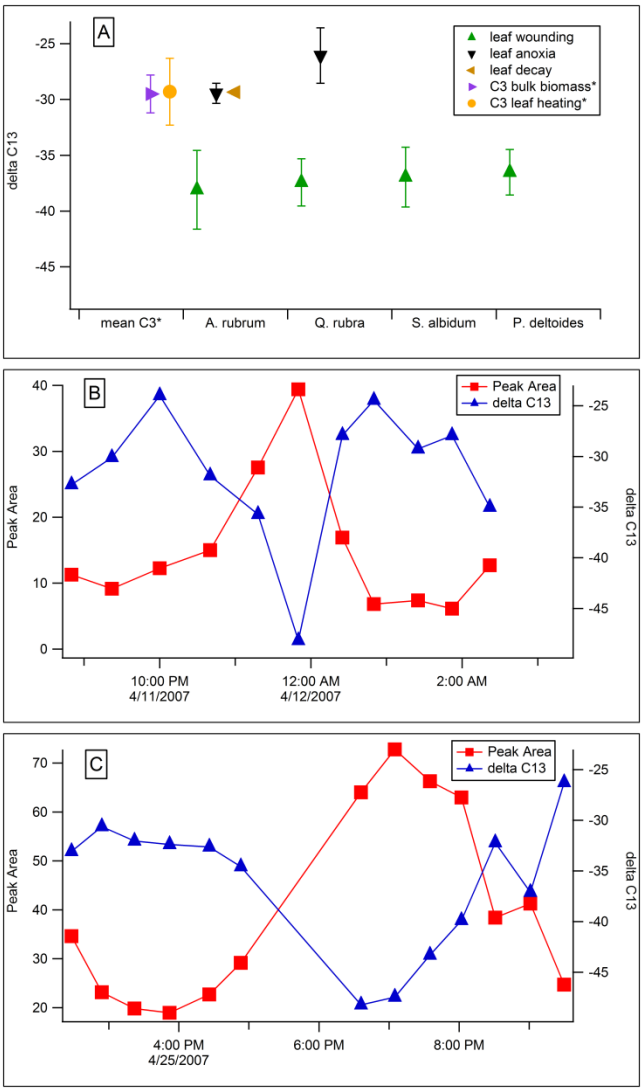

Figure 22: Time course of acetaldehyde emission rates and δ13C values during wounding/desiccation of poplar leaves.

(a) Summary of acetaldehyde emissions from leaf decay, leaf heating, and from leaves under anoxic conditions. Leaf heating and bulk biomass data is from Keppler et al., (2004). (b) and (c) Wounding/desiccation experiments with poplar in a dynamic enclosure demonstrates that acetaldehyde emissions are enhanced immediately following mechanical wounding (beginning of experiment) and are depleted in ^{13}C relative to bulk biomass. The drying process leads to a second much larger enhancement in emissions that is sustained for a longer period of time relative to the emissions from the initial wounding event. These emissions are also strongly depleted in ^{13}C. Although lower in magnitude, emissions of acetaldehyde with similar $\delta^{13}C$ values to bulk biomass also occur in between and after the burst in emissions from the initial wounding event and the drying process.

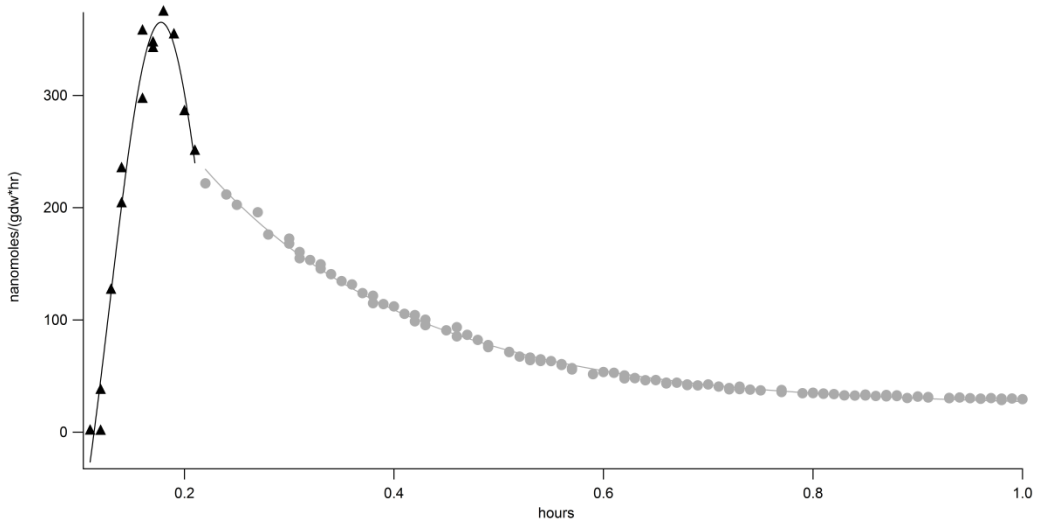

Figure 23: Acetaldehyde emission rates from mechanically wounded poplar leaves as measured by PTR-MS.

$\delta^{13}C$ values of acetaldehyde emitted during the first hour following wounding suggests that two distinct sources appear to be responsible for acetaldehyde production (Figure 3). The first leads to a rapid burst of acetaldehyde emissions and is possibly related to the peroxidation of fatty acids. The second source may be caused by an increase in ethanolic fermentation rates known to be stimulated by the wounding process.

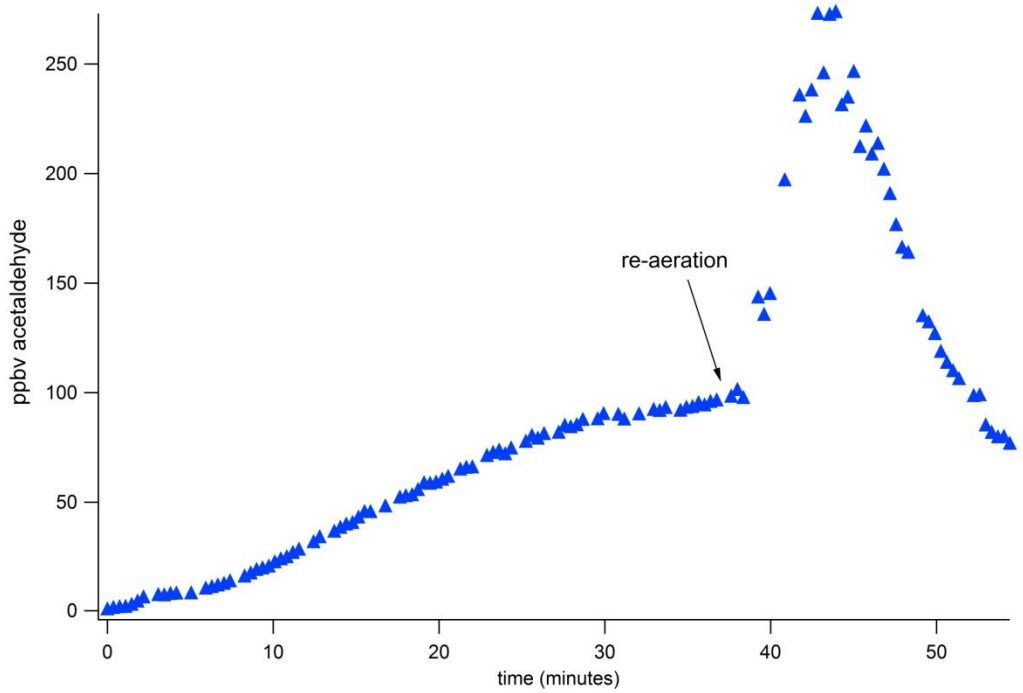

Figure 24: The emission rates acetaldehyde under anoxia and re-aeration.

Anoxic conditions were imposed at the beginning of the experiment (time = 0 min) and emission rates greatly increased because of the increased rate of ethanolic fermentation. Upon re-aeration in hydrocarbon free air, a large burst of acetaldehyde emissions was observed.

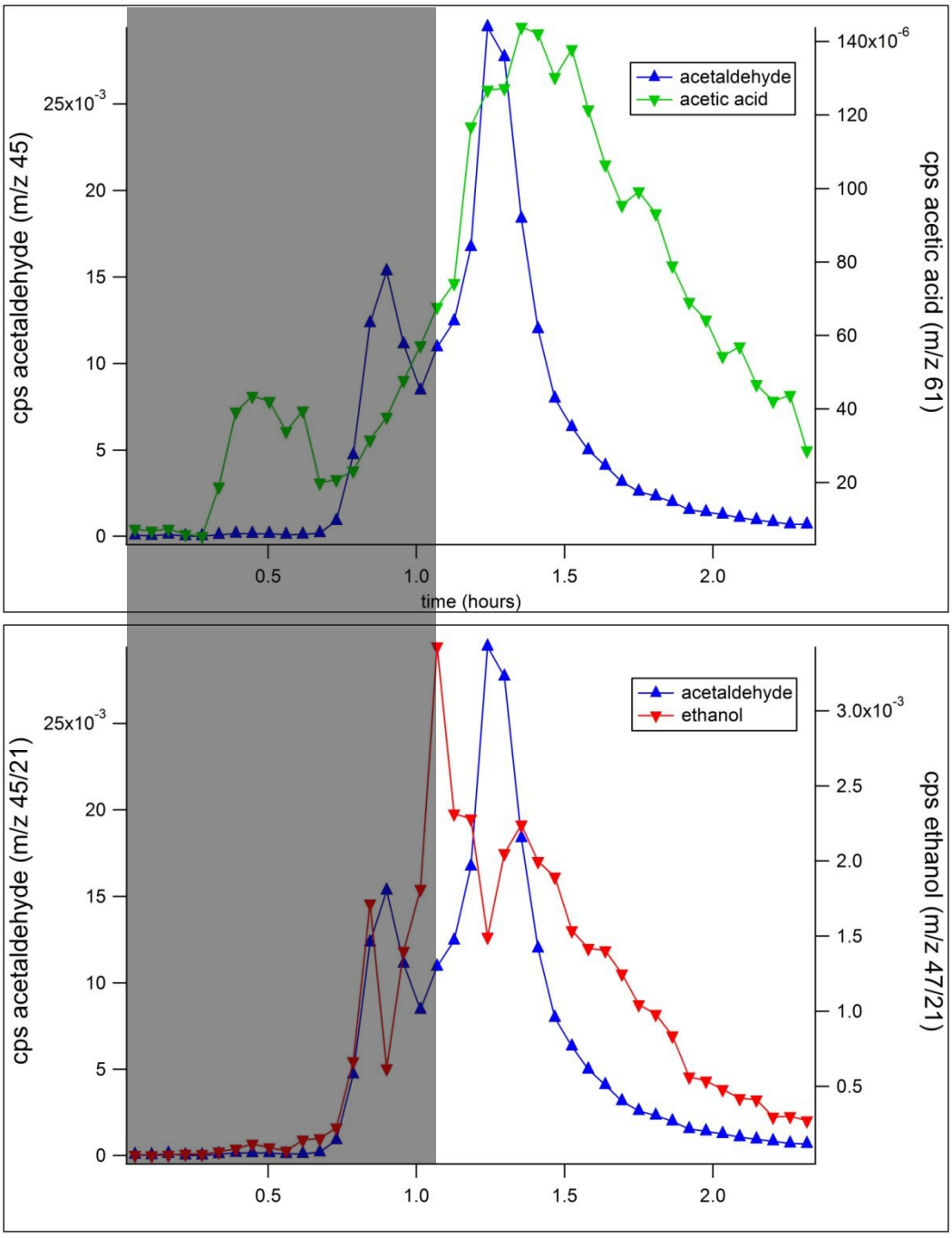

Figure 25: Acetaldehyde, acetic acid, and ethanol emissions were monitored from a poplar branch under anoxia with subsequent re-aeration.

At approximately 0.25 hours, the branch was placed in the enclosure and the apparent enhancement in acetic acid emissions during this time may be due to room air entering the enclosure. During the anoxic period (grey

area) as well as during re-aeration, the emission rates of acetic acid generally parallel those of acetaldehyde. In contrast, while acetaldehyde and ethanol emissions generally parallel each other under anoxia, upon re-aeration ethanol emission rates decrease while acetaldehyde emissions rates increase. When acetaldehyde emissions begin to decline, ethanol emissions slightly recover. Later, both acetaldehyde and ethanol emissions declined in parallel to background levels.

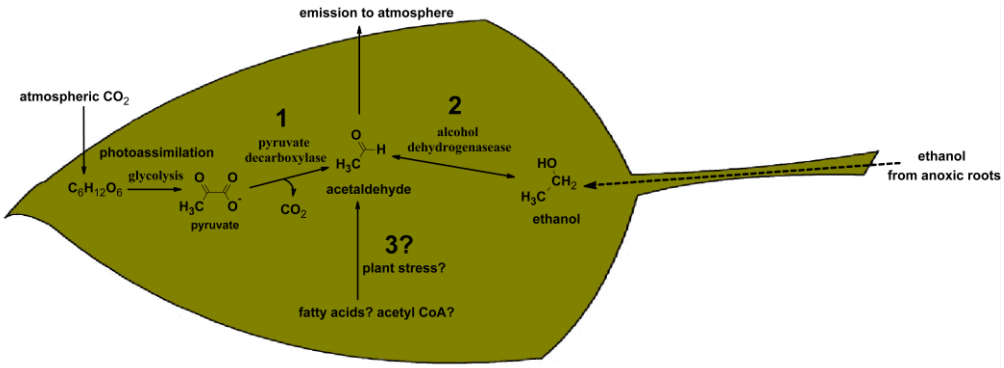

Figure 26: Biochemical pathways involved in the production of acetaldehyde in plants.

Although acetaldehyde is known to be emitted into the atmosphere from plants, very little is known about the pathways that give rise to its formation. Currently there are two known processes that may influence acetaldehyde emission rates and involves ethanolic fermentation within leaves and in other tissues (Jardine et al., 2008). Carbon isotope data presented here suggest that a third pathway for acetaldehyde production in plants exists and is related to the stress response.

Chapter 5: Plant physiological and environmental controls over the exchange of acetaldehyde between forest canopies and the atmosphere

5.1 ABSTRACT

We quantified fine scale sources and sinks of gas phase acetaldehyde in two forested ecosystems in the US. During the daytime, canopy tops behaved as a net source while at lower heights, reduced emission rates and even net uptake was observed. At night, uptake generally predominated throughout the canopies. Net ecosystem emission rates were inversely related to foliar density which influenced the extinction of light and therefore the acetaldehyde compensation point in the canopy. This is supported by branch level studies revealing a higher compensation point in the light than in the dark for poplar (*Populus deltoides)* and holly oak (*Quercus ilex*) implying a higher light sensitivity for acetaldehyde production relative to consumption. The view of stomata as the major pathway for acetaldehyde exchange is supported by the strong linear correlations between branch transpiration rates and acetaldehyde exchange velocities for both species. Natural abundance carbon isotope analysis of gas-phase acetaldehyde during branch fumigation experiments revealed a significant kinetic isotope effect of 5.1 ± 0.3‰ associated with the uptake of acetaldehyde by poplar branches. Similar experiments with dead poplar leaves showed no fractionation or uptake of acetaldehyde, confirming that this is only a property of live leaves. This implies that the cuticle resistance is large and can probably be ignored. We suggest that acetaldehyde belongs to a potentially large list of plant metabolites where stomatal conductance can exert long term control over both emission and uptake rates due to the presence of both source(s) and sink(s) which strongly buffers large changes in concentrations in the substomatal airspace due to changes in stomatal conductance. We conclude that the exchange of acetaldehyde between plant canopies and the atmosphere is fundamentally controlled by the compensation point which is a function of light and temperature, the ambient acetaldehyde concentrations, and stomatal conductance.

5.2 Introduction

Acetaldehyde is considered to be a hazardous air pollutant by the USEPA and can lead to the production of other harmful air pollutants such as ozone and peroxyacetyl nitrates (PAN). As recently reviewed by Seco et al., (2007), significant quantities of acetaldehyde are emitted by plants to the atmosphere (Janson et al., 1999; Martin et al., 1999; Schade and Goldstein, 2001; Hayward et al., 2004; Villanueva-Fierro et al., 2004). However, the ability of plants to also act as a sink for acetaldehyde has become increasingly clear (Rottenberger et al., 2004; Karl et al., 2005). Our understanding of how environmental and plant physiological variables influence acetaldehyde exchange rates with the atmosphere is in its infancy. This is largely because information on the processes that produce and consume acetaldehyde in plants, the mechanism by which acetaldehyde exchanges with plants (cuticle, stomata, or surface), and the role of

environmental variables such as light and temperature on these processes is limited. Recently, it was suggested that under non-stressed aerobic conditions, acetaldehyde is produced in leaves during ethanolic fermentation and activated to acetyl-CoA by the pyruvate dehydrogenase bypass system. However, there is much discrepancy in the literature on the importance of various environmental and physiological controls of acetaldehyde exchange with the atmosphere. Unless these controlling factors are clearly understood, a quantitative understanding of the role of the biosphere in the tropospheric budget of acetaldehyde will not be possible.

Within-canopy flux studies of acetaldehyde are extremely rare, but experiments measuring concentration gradients have been used to imply a flux. For example in Germany, Muller et al., (2006) measured lower concentrations within the canopy than above the canopy. They attributed this to emissions and photochemical production of acetaldehyde in the upper canopy with deposition in the lower canopy. Rottenberger et al., (2004) also measured similar vertical concentration profiles in the Amazon and attributed it to photochemical production above the canopy and strong uptake by the vegetation within the canopy. At a highway site in Finland, a large drop in acetaldehyde concentration from directly above the highway (over 10 ppbv) to two forested sites located immediately adjacent to the highway (under 2 ppbv) could not be explained by dilution from mixing alone and plant uptake was implied (Viskari et al., 2000). By directly measuring the exchange of acetaldehyde using branch enclosures, Cojocariu et al., (2004) found that acetaldehyde was emitted by spruce (*Picea abies*) trees in the field and that the emission rates increased with height in the canopy. When ecosystem exchanges of acetaldehyde were measured over an Alfalfa field, a complex pattern emerged of deposition in the mornings and evenings and emissions during the day (Warneke et al., 2002). Because of the use of eddy covariance, exchange rates could not be estimated at night. By characterizing the structure of the fields of acetaldehyde concentration and air turbulence, Karl et al., (2004) used an inverse Lagrangian dispersion model (Raupach, 1989) in an old growth forest in Costa Rica. The results show a complex source/sink exchange pattern that varied not only with time but also with height.

Using a similar technique in North Carolina, US, during the day, emissions occurred at the top of the canopy while strong uptake occurred within the canopy with the highest uptake coinciding with the highest leaf area index (Karl et al., 2005). During the night, the overstory was a net sink while the understory was a small net source.

Currently, these emission/uptake patterns and their temporal and vertical dependences cannot be explained. However it is clear that a complex interaction of physical, chemical, and biological processes influenced by the environment

must responsible. In this study, we further examine the results from Karl et al., (2005) and compare them with new in-canopy source/sink estimates and process-based laboratory studies.

Because plants both produce and consume acetaldehyde, exchange with the atmosphere can proceed in either direction. For all leaves, there exists a compensation point (Kesselmeier, 2001) defined as the ambient concentration at which the net exchange between a plant and the atmosphere is zero. When ambient acetaldehyde concentration is below the compensation point, acetaldehyde is emitted from leaves; when ambient levels exceed the compensation point, it is taken up. Compensation points reflect the relative rates of production and consumption processes within plants. When production predominates, the compensation point is high, and vice versa. Unfortunately, acetaldehyde compensation point measurements are extremely rare. From fumigation studies on potted Norway Spruce, Cojocariu et al., (2004) found the acetaldehyde compensation point is about 6 ppbv. Lower compensation point was measured for two drought deciduous Amazonian tree species in the field during the wet season of 0.56 ppbv (*Hymeneae courbaril*) and 0.32 ppbv (*Apeiba tibourbou*) (Rottenberger et al., 2004). However, the authors also discovered that the acetaldehyde compensation point for these two species greatly increased to 1.12 ppbv and 1.11 ppbv respectively during the dry season. In a series of laboratory studies, acetaldehyde compensation points were measured to be 0.8 ppbv for *Quercus pubescens* and 1.5 ppbv for *Quercus ilex* (Kesselmeier, 2001). While species composition and leaf age may have some influence on compensation point (Rottenberger et al., 2005), recent evidence suggests that environmental variables like temperature is also important (Karl et al., 2005). Acetaldehyde compensation points for potted Loblolly Pine (*Pinus taeda*) increased exponentially from 2.5 ppbv at 25^{o}C to 4.3 ppbv at 30^{o}C. This implies that production is more sensitive to temperature than consumption in plants.

A simple gas diffusive resistance model can be used to examine the controls over the exchange of acetaldehyde at the branch level between plants and the atmosphere (Rottenberger et al., 2004). This model relates the total resistance of the branch to the exchange of acetaldehyde to boundary layer and leaf resistances acting in series according to equation 1.

$$\frac{1}{R_t} = \frac{1}{R_b + R_l} \quad (1)$$

where R_t is the total resistance to acetaldehyde exchange, R_b is the boundary layer resistance, and R_l is the result of stomatal and mesophyll resistance acting in series and in parallel with cuticle resistance. (equation 2).

$$\frac{1}{R_l} = \frac{1}{R_s + R_m} + \frac{1}{R_{ct}} \quad (2)$$

However, the boundary layer resistance which is associated with a small stagnant film of air just over the surface of the leaf is small relative to R_l and can

be ignored in a well mixed branch enclosure (Kondo et al., 1998). Therefore, the total resistance of the branch to the exchange of acetaldehyde is approximately equal to the total leaf resistance (equation 3).

$$\frac{1}{R_t} \approx \frac{1}{R_l} = \frac{1}{R_s+R_m} + \frac{1}{R_{ct}} \quad (3)$$

During fumigation experiments with extremely high concentrations of acetaldehyde, Kondo et al., (1998) observed that trees with higher transpiration rates had higher uptake rates and when light levels were varied, a linear relationship was discovered between transpiration rates and uptake rates. Uptake was measured continuously for up to 8 hours at ambient concentrations as high as 3000 ppbv with no visible damage to the plants. This strongly suggests that a biological removal process rather than a physical deposition process was responsible for uptake since a continuous removal process is required for such a large and sustained sink. In addition, chemical reactions with the leaf surface are unlikely since the surface is mainly composed of inert alkanes (waxes). Even at the extremely high ambient concentrations of acetaldehyde used in this study, no uptake was observed in the dark. This implies that adsorption to the leaf surface or through the cuticle is insignificant and that the cuticle resistance must be extremely high. Therefore, the total leaf resistance to acetaldehyde exchange is only a function of stomatal and mesophyll resistances acting in series (equation 4). The authors concluded that uptake of acetaldehyde occurs through the stomata and that it is rapidly metabolized within the plant. This implies that the mesophyll resistance is small and that the stomatal resistance is the most important factor determining the resistance to acetaldehyde exchange.

$$\frac{1}{R_l} = \frac{1}{R_s+R_m} \quad (4)$$

In a recent study in the Amazon, acetaldehyde deposition predominated during branch enclosure measurements on broad leaf tree species under ambient conditions (Rottenberger et al., 2004). The authors argued that the uptake of acetaldehyde cannot be explained by its dissolution into leaf water due to its poor water solubility (Henry's law constant of 7.00 Pa m^3 $mole^{-1}$), which would lead to a high mesophyll resistance. They suggested that high metabolic consumption processes within leaf tissue maintains the concentration gradient between the atmosphere and the intercellular airspace, leading to a low mesophyll resistance. Although no significant correlation could be found between branch level acetaldehyde exchange rates and stomatal conductance, resistance modeling supported the idea that stomatal uptake is the most important sink. By regressing the ambient acetaldehyde concentrations against the acetaldehyde exchange flux, two important pieces of information were obtained. The first is the compensation point (x-intercept) and the second is the slope defined as the acetaldehyde exchange velocity v_e which equals one over the total leaf resistance (equation 5).

$$v_e \approx \frac{1}{R_l} \approx \frac{1}{R_s + R_m} \quad (5)$$

The stomatal resistance for acetaldehyde R_s can be estimated from measurements of stomatal resistance for water vapor corrected for differences in molecular diffusivities. This allowed the authors Rottenberger et al., (2004) to estimate the importance of R_m. During the wet season, the total leaf resistance R_l was roughly the same as the estimated stomatal resistance for acetaldehyde R_s. This implies that R_m during these conditions is close to zero and can be ignored from the analysis and supports the idea that acetaldehyde is rapidly consumed upon entering the plant. This means that the acetaldehyde exchange velocity is roughly equal to the stomatal conductance for acetaldehyde ($1/R_s$) supporting the idea that it is the main pathway for acetaldehyde exchange with the atmosphere. Moreover, during the dry season the total leaf resistance remained essentially unchanged while the estimated stomatal resistance for acetaldehyde increased for both species investigated. From this the authors concluded that during the dry season when ambient acetaldehyde concentrations are higher (2-4 ppbv), deposition onto or diffusion through the cuticle is significant. However, the deposition mechanism for acetaldehyde remains highly uncertain because resistance model estimates are based on surface resistance parameterization models which are mainly built on theoretical considerations. Kondo et al., (1998) did not see uptake of acetaldehyde in the dark from any species studied even at ambient acetaldehyde concentrations three orders of magnitude higher than as measured in the dry season in the Amazon (3000-4000 ppbv). Another possibility is that instead of a leaf surface sink, the mesophyll resistance may have increased significantly from the wet to dry season. The role of stomatal conductance for acetaldehyde in controlling its exchange rate between the atmosphere was further supported by Rottenberger et al., (2005) who found that for the deciduous Amazonian tree species *Hymenaea courbaril*, acetaldehyde exchange rates were high for mature leaves with high stomatal conductance and low for young leaves with low stomatal conductance.

Confusingly, there are many studies that indicate a lack of stomatal influence on exchange rates. For example, when Dindorf, (2000) measured acetaldehyde uptake in leaves of *Quercus ilex* before and after inducing stomatal closure with abscisic acid, there was no significant change in acetaldehyde uptake rates. Other studies concluded that acetaldehyde emissions were not correlated with any physiological parameters including stomatal conductance (Kesselmeier et al., 1997; Martin et al., 1999; Kesselmeier, 2001). When ethanol was supplied to poplar leaves, promoting production of acetaldehyde in a reaction catalyzed by alcohol dehydrogenase, no correlation could be found between stomatal conductance and acetaldehyde emissions, where variation in conductance was induced either by absicisic acid or by varying light (Kreuzwieser et al., 2001). The authors concluded that acetaldehyde emissions are primarily controlled by

biochemical production mechanism within the plant. This was the same general conclusion of Cojocariu et al., (2004) who found no significant correlation of acetaldehyde emissions with stomatal conductance. However, these authors did find a strong correlation between acetaldehyde emission, photosynthesis and transpiration rates.

In a few field studies, the forest canopy has been observed to be a net source of acetaldehyde during the day but a net sink during the night (Karl et al., 2004; Karl et al., 2005). When vertically resolved fluxes were estimated, during the daytime net emissions occurred in the upper canopy while net uptake occurred deeper within the canopy (Karl et al., 2005). These results cannot be explained assuming a fixed acetaldehyde compensation point because the ambient concentrations are typically higher during the day than during the night which would tend to increase uptake rates during the day and emission rates at night. Therefore, it is likely that diurnal trends of radiation and temperature influence the rates of acetaldehyde production and consumption in plants, which determine the compensation point. Several studies show a clear diurnal emission pattern from plants in both laboratory and field settings (Kreuzwieser et al., 2000; Schade and Goldstein, 2001; Karl et al., 2002; Karl et al., 2004; Cojocariu et al., 2005). In addition, a strong relationship between acetaldehyde emission rates and temperature has been found in several studies (Schade and Goldstein, 2002; Cojocariu et al., 2004; Hayward et al., 2004). On the other hand, other experiments found no clear relationship between acetaldehyde emissions and temperature (Kesselmeier et al., 1997; Martin et al., 1999; Kesselmeier, 2001; Villanueva-Fierro et al., 2004). The effect of light is equally uncertain with some studies showing a clear dependence on exchange rates with photosynthetic light intensity (Kondo et al., 1998; Kreuzwieser et al., 2000) and others finding no such relationship (Kesselmeier, 2001; Kreuzwieser et al., 2001; Schade and Goldstein, 2002; Cojocariu et al., 2004).

In this study, ambient acetaldehyde concentrations were varied over a wide range (0-30 ppbv) and branch compensation points were determined in the dark and the light. The effect of stomatal conductance was investigated by measuring branch level transpiration rates which varied from branch to branch and from dark to light conditions. In addition, to better understand the role of stomatal conductance on the exchange of acetaldehyde with the atmosphere, the carbon isotope composition of gas phase acetaldehyde was studied during branch fumigation experiments. It is well known that during photosynthesis, carbon dioxide uptake occurs exclusively through the stomata. During this process, the "heavier" isotopologues of carbon dioxide containing ^{13}C are discriminated against (see review by Farquhar et al., (1989)). The major components of the discrimination are physical and chemical kinetic fractionation processes, including diffusion through plant stomata and within the plant and carboxylation

reactions. We hypothesized that if plant stomata are the dominant pathway of acetaldehyde exchange, then the heavy isotopologues of acetaldehyde will also be discriminated against during uptake. We further hypothesized that the fractionation is only due to diffusional processes and not to chemical processes such as the oxidation of acetaldehyde to acetate. If this is the case, the kinetic isotope effect should be on the same order as that for diffusion of acetaldehyde in air. Assuming that once the acetaldehyde enters the plant it is not returned to the atmosphere, then the kinetic isotope effect due to diffusion in air can be estimated according to equation 6 adopted from Johnson and Dawson, (1993).

$$\alpha = \sqrt{\frac{M44 + Mair}{M45xMair} x \frac{M45xMair}{M45 + Mair}} \quad (6)$$

Where M44, M45, and Mair represent the molecular weight of the acetaldehyde isotopes and air respectively. The value for α in this case is 1.0044 corresponding to a 4.4 ‰ fractionation. In other words, at steady state the acetaldehyde remaining in the air stream passing over a branch should be 4.4 ‰ more enriched in ^{13}C than the initial source. Therefore, if the measured kinetic isotope effect during the uptake of acetaldehyde is near 4.4 ‰, this would provide strong evidence to support the role of stomatal exchange. If dry deposition onto the surface of leaves were the dominant mode of acetaldehyde deposition to plants, it might also fractionate the acetaldehyde in a similar manner due to molecular diffusion through the stagnant air near the leaf surface (boundary layer resistance). However, this may only be a temporary sink since an equilibrium may be quickly established where no net deposition or emission occurs. Therefore, long term uptake and fractionation would indicate a stomatal sink. We employ dead leaves which possess similar surface area but lack a biochemical sink mechanism to help discriminate between physical and biological processes. If deposition to external surfaces dominates acetaldehyde removal, then similar uptake rates and associated kinetic isotope effects should be observed for both live and dead poplar branches.

5.3 Methods

Potted poplar individuals (*Populus deltoides*, clone #ST109) used for estimating the kinetic isotope effect associated with acetaldehyde uptake were obtained from the Stony Brook University greenhouse. Additional poplar (*Populus deltoides* [S7c8 East Texas Day Neutral clone]) and holly oak (*Quercus ilex*) individuals used for acetaldehyde compensation point studies were obtained from the National Center for Atmospheric Research greenhouse, (Boulder, CO). Plants were potted into 4-L plastic pots containing a commercial potting mix (MiracleGro) with Osmocote slow release fertilizer.

5.3.1 Branch compensation point measurements

The concentration of acetaldehyde was measured with a high sensitivity proton transfer reaction mass spectrometer (PTR-MS) instrument (Ionicon, Innsbruck, Austria) from poplar branches in a 5.0 L Teflon dynamic branch enclosure. Hydrocarbon free air was introduced into the enclosure at a flow rate of 1.0 L min^{-1} (generated by passing 1.0 L min^{-1} of room air through a catalytic converter consisting of 12" x ½" stainless steel tube packed with platinum-coated silica pellets and heated to 400^{o}C). The flow rate of hydrocarbon free air was controlled by a mass flow controller (Model FMA-A2308, OMEGA Engineering, INC., Stamford, Connecticut), and the air inside the enclosure had a residence time of approximately 5.0 minutes. For acetaldehyde concentration measurements, approximately 200 ml min^{-1} of sample air was continuously drawn out of the enclosure and into the PTR-MS through 1/8" Teflon tubing. The rest of the air flow entering the branch enclosure was vented through small leaks where the Teflon bag was tied to the branch. The PTR-MS instrument has been described in detail elsewhere (Lindinger and Hansel, 1997). Mass to charge ratio 45 was monitored with a 30 second dwell time and corresponds to the protonated form of acetaldehyde. In addition, mass to charge ratio 37, corresponding to the protonated cluster of two water molecules, was monitored with a 0.1 second dwell time. This signal is very sensitive to water vapor concentrations, allowing us to estimate transpiration rates. During branch compensation point measurements, 0-15 ml min^{-1} of a 2.0 ppmv acetaldehyde standard (± 10% accuracy) was diluted with 1.0 L min^{-1} of hydrocarbon free air to generate acetaldehyde concentrations between 0 and 30 ppbv. The mixture was added to the branch enclosure and an automated Teflon valve was used to switch between sampling the air before and after the enclosure. The air before the enclosure was used to calibrate the acetaldehyde concentration measurements by regressing the incoming acetaldehyde concentrations against the signal at m/z 45 normalized to m/z 21. The sample switching valve was programmed to switch after every ten PTR-MS measurement cycles (~ 10 min). During one cycle, the mass to charge ratios 21, 37, 45, and 69 were sequentially measured (~1 min). The net exchange flux of acetaldehyde was calculated using equation 7.

$$Flux = \frac{(ppbv_{after} - ppbv_{before}) \cdot Flow \cdot P}{gdw \cdot R \cdot T} \cdot \frac{10^{-9} mole}{nanomole} \cdot \frac{44g}{mole} \qquad (7)$$

where Flux is the net flux rate in g gdw^{-1} hr^{-1}, Flow is the total flow rate entering the enclosure in L hr^{-1}, P is the atmospheric pressure in atmospheres, gdw is the dry leaf weight, R is the universal gas constant (0.08206 L atm K^{-1} mol^{-1}), and T is the air temperature in Kelvin. The total relative error in calculating the concentration difference $E_{\Delta C}/\Delta C$ is the sum of errors associated with uncertainty

in the concentration of the standard and the precision of the concentration measurements (equation 8).

$$\frac{E_{\Delta C}}{\Delta C} = \underbrace{\sqrt{\left(\frac{E_{after}}{\Delta C}\right)^2 + \left(\frac{E_{before}}{\Delta C}\right)^2}}_{calibration} + \underbrace{\frac{\sqrt{E_{after}^2 + E_{before}^2}}{\overline{\Delta C}}}_{measurement} \quad (8)$$

The relative error for each concentration calculation due to uncertainty in the concentration of the standard is set to 10% (calibration error). The measurement error is the standard deviation of the concentration measurement during each measurement period. The absolute error in the calculated exchange rates (E_{ex}, in g gdw^{-1} hr^{-1}) is calculated according to the error propagation method (equation 9).

$$E_{ex} = Flux\sqrt{\left(\frac{E_{\Delta C}}{\Delta C}\right)^2 + \left(\frac{E_{Flow}}{Flow}\right)^2 + \left(\frac{E_P}{P}\right)^2 + \left(\frac{E_{gdw}}{gdw}\right)^2 + \left(\frac{E_T}{T}\right)^2} \quad (9)$$

The relative errors were set to enclosure flow rate (E_F/Flow = 0.10), pressure (E_P/P = 0.10), temperature (E_T/T = 0.10), and the leaf dry weight (E_{gdw}/gdw = 0.005).

Acetaldehyde emissions thus represent a positive flux, while deposition to the leaf is represented as a negative flux. The flux was allowed to stabilize for at least one hour before switching to the next concentration. Once the concentrations stabilized, the PTR-MS signals were averaged and the difference in concentrations between the incoming and outgoing air was calculated. Light was supplied by a 1000-W high intensity metal halide discharge lamp (Sylvania MS1000-M47) with an intensity of photosynthetically active radiation at branch height of roughly 1000 µE m^{-2} s^{-1}. Air temperatures inside the enclosure were measured with a K-type thermocouple (model KMQSS-125G-6, OMEGA Engineering, INC., Stamford, CT) and ranged between 24-25 ^{o}C in the dark and from 29-32 ^{o}C in the light. For dark measurements, the lamp was turned off and the branch enclosure was covered with aluminum foil. Compensation point measurements were performed on four poplar branches in the light and six in the dark. For holly oak, five compensation point measurements were performed in the light and one in the dark.

5.3.2 Estimating the Kinetic Isotope Effect Associated with Acetaldehyde Uptake

To estimate the kinetic isotope effect associated with the uptake of acetaldehyde by poplar branches, a 39.2 ppbv acetaldehyde standard was generated by mixing 0.5 Lpm of commercial UHP hydrocarbon free air with 10 ml min^{-1} of a 2.0 ppmv acetaldehyde standard. This mixture was introduced into a 5 L dynamic branch enclosure made of Teflon and had a residence time of ~10

minutes. A gas chromatography-combustion-isotope ratio mass spectrometer (GC-C-IRMS) system with a custom cryogenic VOC preconcentration system as described in chapter 2 was used to alternately analyze the stable carbon isotope composition of acetaldehyde before and after the dynamic branch enclosure. After obtaining several blank samples without a branch (~30 minutes/sample), the poplar branch was introduced into the enclosure. Although the branch was exposed to only the very low light levels of room light, transpiration rates were not zero as evidenced by the large amount of water trapped in the water trap. Control experiments were also performed with dead poplar leaves. The precision of the instrument (one standard deviation) was calculated from repeated measurements of the 39.2 ppbv standard to be between 0.2‰ and 1.0‰.

The kinetic isotope fractionation factor α associated with the uptake of acetaldehyde was determined as in Miller et al., (2001) from the slope (b) of the regression of $\delta^{13}C$ values of the remaining reactant acetaldehyde on the natural logarithm of the fraction of remaining reactant (ln *f*) using equations 9 and 10. rf and ro refer to the reactant at f and the initial reactant. It is then reported as ε, the deviation from unity using equation 11 (in units of per mil). The quantity f was calculated from the acetaldehyde peak areas before and after the enclosure using equation 12, where PA is the acetaldehyde derived carbon dioxide peak area for m/z 44 as measured by GC-C-IRMS for samples before and after the enclosure.

$$b = \frac{\delta^{13}C_{rf} - \delta^{13}C_{ro}}{\ln f} \tag{9}$$

$$\alpha = \frac{1000}{b + 1000} \tag{10}$$

$$\varepsilon = (\alpha - 1) \cdot 1000 \tag{11}$$

$$f = \frac{PA_{before} - PA_{after}}{PA_{before}} \tag{12}$$

2.3 Canopy Scale Gradients

Continuous vertical gradients of acetaldehyde concentrations were obtained at a hardwood forest in Northern Michigan at the PROPHET Tower (at the University of Michigan Biological Station, UMBS), during July 25-August 14, 2005. Similar measurements were also obtained at a Walnut Orchard in central California as a part of the Canopy Horizontal Array Turbulence Study field experiment ([1]CHATS) during May 10th to June 15th. At both field sites, a

[1] http://www.eol.ucar.edu/rtf/projects/CHATS/isff/

Proton-Transfer-Reaction Mass Spectrometer was used for gradient measurements of selected VOCs including acetaldehyde. Using this method, acetaldehyde concentrations could be measured at m/z 45 with an accuracy of ± 20% and a detection limit of 50 pptv for a 5 s integration time. The instrument was operated at 2.3 mbar drift pressure and 540 V drift voltage and calibrated using a multicomponent ppmv VOC standards. (VOC standard contained a mixture of methanol, acetonitre, acetaldehyde, acetone, isoprene, methyl vinyl ketone, methyl ethyl ketone, benzene, toluene, m,o,p xylenes and camphene).
In California, the instrument sequentially sampled six independent ¼" inch Teflon (PFA) sampling lines mounted at 1.5, 4.5, 9, 11, 14 and 23 m on a 30 m tall Rohn Tower. A valve switching system changed sampling lines every 5 minutes giving a complete profile every 30 minutes. Gradients were calculated from the 5 minute averages. High flow rates through the sampling lines resulted in delay times of less than 8-12 seconds, measured by spiking a VOC pulse at each sampling inlet.
At UMBS in Michigan, air was pulled through a single Teflon line (O.D. =1/4") from the top of the sampling tower at a high flow rate (~15 L min^{-1}), reducing the pressure inside the line to 400 mbar in order to avoid water condensation, minimize memory effects and assuring a fast response time (see Karl et al., (2004) for details of this site). The overall delay time was ~6 s, measured by introducing an isoprene and acetone pulse at the top of the tower. The gradient sampling inlet line was attached to a pulley controlled by an automated winch, and ambient acetaldehyde concentrations were made continuously between 7.5 m to 28.5 m height. The canopy line moved at a constant speed of 0.2 m/s resulting in a complete profile approximately every 1.75 min.
Source/sink profiles for both field sites were computed according to equation 7, with C (concentration vector), Cref (concentration at top of canopy), D (dispersion matrix and S (source/sink vector).

$$\boldsymbol{C - C_{ref} = \vec{D} \cdot S} \qquad (7)$$

Parameterization of the dispersion matrix (21 concentration layers and 5 source/sink layers) was based on an inverse Lagrangian model with transport time-scales constrained by within-canopy turbulence measurements (Raupach, 1989).

5.4 Results and Discussion

5.4.1 Branch Results

Figure 27 and Figure 28 illustrate the acetaldehyde compensation point measurements for poplar and holly oak branches, respectively. When acetaldehyde-free air was used, emissions were observed from all branches. Increasing the acetaldehyde concentration entering the enclosure invariably resulted in a reduction in emission rates and eventually to net uptake of

acetaldehyde in many cases. The concentration at which the net flux is zero represents the compensation point. In the dark, the acetaldehyde compensation point for poplar branches was between 1 and 3 ppbv. However, measurements in the light showed much higher compensation points (>12 ppbv) with values not often reached by ambient acetaldehyde concentrations in the troposphere. Ambient concentrations at the surface typically ranges between 0.1 ppbv and 6.0 ppbv although have been observed as high as 23 ppbv in Mexico City (Baez et al., 1995). The variability of acetaldehyde compensation points seen for the different branches in the light may partly be due to the variable amount of dry biomass (1.0-7.0 gdw) which likely resulted in a variable amount of leaf shading. Similar measurements on Holly Oak branches revealed a similar pattern in the light with very high compensation points (>22 ppbv). In the dark, acetaldehyde exchange rates were very low and the precise compensation point was difficult to determine.

The slope of the relationship between acetaldehyde exchange rate and ambient acetaldehyde concentration is defined as the exchange velocity. A strong linear correlation between branch transpiration rates and exchange velocities was found for both species (Figures 29 and 30). While acetaldehyde exchange velocities tended to be smaller for holly oak than for poplar (Figure 31), so did transpiration rates. For example, while poplar branches were able to maintain non-zero transpiration rates and therefore significant acetaldehyde exchange velocities during the dark, holly oak branches displayed very low transpiration and acetaldehyde exchange velocities in the dark. While the range of acetaldehyde exchange velocities for poplar is comparable to those for Loblolly Pine (Karl et al., 2005), those of holly oak are the lowest yet reported. Relative to exchange velocities measured here for poplar, Rottenberger et al., (2004) reported higher acetaldehyde exchange velocities for two Amazonian overstory species while those of the understory species is comparable (Figure 5).

During fumigation experiments where the carbon isotopic composition of headspace acetaldehyde was measured by GC-C-IRMS, the uptake of 39.5 ppbv acetaldehyde by dead poplar leaves did not occur (Figure 32, top row). In addition, the isotopic composition of acetaldehyde was not affected by entering the enclosure. In contrast, when a live poplar branch was placed in the enclosure, strong acetaldehyde uptake and carbon isotope fractionation occurred (Figure 32 second row). The remaining acetaldehyde in the headspace became enriched in ^{13}C with time signifying the preferential uptake of the lighter acetaldehyde isotopologues by the poplar branch (CH_3CHO over $^{13}CH_3CHO$, $CH_3{}^{13}CHO$, and $^{13}CH_3{}^{13}CHO$). The second experiment was designed to test the long term sink ability of poplar branches in order to completely rule out a simple physical deposition process (Figure 32 third row). A surface deposition process would be expected to saturate the leaf surface and subsequently establish an equilibrium

condition which would no longer act as a net sink. The branch remained a strong sink for acetaldehyde for over 15 hours with continuous carbon isotope fractionation of acetaldehyde.

Data from all branch measurements (two branches) were pooled and a kinetic isotope effect was calculated to be to be 5.1 ± 0.3 ‰ (Figure 33). At steady state conditions, the fraction of the gas phase acetaldehyde remaining in all experiments was ~0.4 in both experiments which is close to the ideal value of 0.5 needed to minimize errors in kinetic isotope effect (KIE) calculations based on the analysis of the remaining reactant.

5.4.2 Canopy Results

Average ambient acetaldehyde concentrations were separated into daytime (7:00 AM-7:00 PM, local time) and night time components (7:00 PM-7:00 AM) and show clear vertical gradients in California, Michigan, and North Carolina (Figure 34). During the daytime in Michigan, the average concentration (0.99 ± 0.20 ppbv) was the highest at 28.5 m and steadily declined within the canopy to 0.95 ± 0.19 ppbv at the lowest sampled height of 7.5 m. A similar pattern was observed in North Carolina during the daytime where the average concentration (0.63 ± 0.13 ppbv) was the highest at 18.6 m and steadily declined within the canopy to 0.59 ± 0.12 ppbv at 0.5 m. In contrast, the walnut orchard in California displayed a different concentration profile during the day. The lowest concentration (3.34 ± 0.67 ppbv) occurred at a height of 23 m and increased to 3.44 ± 0.69 ppbv at a height of 4.5 m.

At night, the concentrations in all field sites (Michigan, North Carolina, and California) decreased with decreasing height. In Michigan, the concentrations decreased from 0.83 ± 0.17 ppbv at 28.5 m to 0.75 ± 0.15 ppbv at 7.5 m. In North Carolina, the concentrations decreased from 0.20 ± 0.4 ppbv at 18.6 m to 0.18 ± 0.04 ppbv at 0.5 m. In California, the concentrations decreased from 2.97 ± 0.59 ppbv at 23 m to 2.94 ± 0.59 ppbv at 1.5 m. Although different background levels of acetaldehyde existed at each site, the maximum change in concentration throughout the canopies during the day or night was small (< 0.1 ppbv).

During the daytime, when the fine scale source/sink distributions of acetaldehyde were estimated by inverse modeling, similar patterns emerged between the three canopies at the top, but showed important differences deeper in the canopies (Figure 34). Corresponding with the first peak in leaf area index (LAI) at the top of the canopies, a strong net emission of acetaldehyde occurred. The magnitude of these net emissions declined with decreasing height in the canopies. In California, the emissions declined to near zero near the ground (1.5 m). However in the taller canopies of Michigan and North Carolina, a transition to a net sink occurred. With an additional decrease in canopy height, the magnitude of the net sink decreased

to near zero in both Michigan and North Carolina. At night, the canopies mainly behaved as a net sink.

5.5 Discussion

The experiments presented here were designed to gain insight into the processes influencing the exchange of acetaldehyde with vegetation. The very low acetaldehyde uptake rates by Holly Oak branches in the dark with very low transpiration rates indicates that deposition to leaf surfaces is not a significant sink for acetaldehyde even at ambient concentrations as high as 27 ppbv. Moreover, fumigation of dead poplar leaves with 39.5 ppbv acetaldehyde did not result in significant uptake or carbon isotope fractionation of the gas phase acetaldehyde. These results further support the idea that the cuticle resistance to acetaldehyde is extremely large and can be ignored. Therefore, we assume that the measured acetaldehyde exchange velocities are a function of stomatal and mesophyll resistances only (equation 4).

Although acetaldehyde compensation point measurements in the literature are rare, they have been generally considered to be constant for a given species with only relatively small dependencies on season (Rottenberger et al., 2004) and leaf age (Rottenberger et al., 2005). However, evidence suggests that changing environmental variables such as an increase in temperature may significantly increase the acetaldehyde compensation point (Karl et al., 2005). The much higher compensation points measured here using branch enclosures in the light compared with the dark suggests that solar radiation also has a large impact on acetaldehyde exchange rates. This is consistent with a recent finding that acetaldehyde production from ethanolic fermentation is stimulated more than its consumption with increasing temperature and light levels (chapter 3). While compensation points measured here in the dark (1-3 ppbv) are comparable to those previously reported in the literature, those in the light far exceed any previously published values (>12 ppbv for poplar and >22 ppbv for holly oak). This may be because previous measurements were performed on leaves exposed to relatively low light levels.

The strong correlation between acetaldehyde exchange velocities and transpiration rates in the light and dark for both poplar and holly oak provides strong evidence for the role of stomatal resistance in controlling the magnitude of both emission and uptake fluxes between plants and the atmosphere. This is because the stomatal resistance to both acetaldehyde and water vapor begins to decrease as the stomata open. Although mesophyll resistance may be significant, it is not expected to correlate with transpiration rates. Therefore, the increase in exchange velocity with increasing transpiration rates must be due to a decrease in stomatal resistance. We suggest that stomatal resistance does not affect the acetaldehyde compensation point but rather its exchange rate with the

atmosphere. Therefore a small stomatal resistance value leads to a large slope of the compensation point curve (exchange velocity) with high emission rates at ambient concentrations below the compensation point and high uptake rates at ambient concentrations above the compensation point.

In the dark, while poplar branches were able to maintain significant transpiration rates and acetaldehyde exchange velocities, those of holly oak were very small. This indicates that holly oak stomata close while those of poplar remain open during the night. New evidence suggests that like poplar, many plant species do not fully close their stomata at night (Dawson et al., 2007), particularly in ecosystems that are not water-limited. The strong uptake of acetaldehyde at night from whole ecosystems and from shade leaves during the day (Karl, 2005) may therefore be a result of a low compensation point in the dark/shade and non-zero stomatal conductance.

If acetaldehyde exchange with plants occurs primarily via stomata, then fluxes to and from leaves may be expressed according to Fick's law as $Flux = \frac{\Delta P}{R_s + R_m}$, where R_s and R_m are stomatal and mesophyll resistance to acetaldehyde respectively and ΔP is the partial pressure difference between the substomatal cavities and the atmosphere (Niinemets and Reichstein, 2003). ΔP is positive if the concentration in the substomatal cavities is higher than in the atmosphere, leading to net emission, and negative when it is lower, which results in net uptake. No net exchange occurs at the compensation point where ΔP is zero. Stomatal resistance then can modulate the magnitude of the fluxes if and only if ΔP and stomatal conductance are at least somewhat independent of each other. That is, if an increase in stomatal resistance leads to a simultaneous and proportional increase in ΔP due to the accumulation of acetaldehyde during continuous production, there will be no long term stomatal control over acetaldehyde emission rates. This is the case for compounds like isoprene (Fall and Monson, 1992) that lack a significant biological sink. In this well studied system, when stomatal resistance increases, the pressure gradient (ΔP) increases to overcome the new stomatal limitation. Therefore, ΔP and R_s are not independent of each other and so there is a lack of stomatal control over emission rates. For more water soluble compounds like methanol, while stomatal resistance can influence the short term exchange rates due to the transient sink/source of dissolving/evaporating into/from leaf water, no long term control over emission rates exist (Niinemets and Reichstein, 2003). Like isoprene, this is due to the fact that the emission driving force ΔP is dependent on the stomatal resistance such that over time ΔP will increase to compensate for any decrease in stomatal resistance and the net emission flux will be unchanged.

In contrast, we propose that long term stomatal control over exchange rates exists for volatile metabolites such as acetaldehyde that have both significant sources and sinks within plants. The internal partial pressure of acetaldehyde is

strongly buffered against large changes in stomatal resistance. For example, if net acetaldehyde emissions are occurring and stomatal resistance increases, then concentration inside the leaf will tend to increase due to the reduction of a loss process (emission). However, if the internal concentration of acetaldehyde increases, then the rate of the sink will also increase thereby preventing a large increase in acetaldehyde concentrations and therefore ΔP. Likewise, if net acetaldehyde uptake is occurring and stomatal resistance increases, then internal acetaldehyde concentrations will decrease some due to the reduction of a source (uptake). However, because continuous production from internal sources and the fact that the internal concentration cannot drop below 0 ppbv, it does not decrease enough to overcome the stomatal limitation and maintain a constant uptake rate.
This is in contrast to a recent modeling study which suggested that, if the net production of acetaldehyde is unaffected by stomatal closure, emission rates should be diminished only briefly by stomatal closure; continuous production would lead to rapid increases in the acetaldehyde concentration in the substomatal cavity, overcoming the reduction in stomatal conductance and restoring the original flux (Niinemets and Reichstein, 2003). However, this model is incomplete as it does not include the biological sink(s) for acetaldehyde in plants and therefore the driving force to overcome the stomatal limitations does not necessarily occur. We suggest that like acetaldehyde, exchange rates of a potentially large group of other volatile metabolites such as formaldehyde, formic acid, ethanol, and acetic acid with both a biological source and a sink are also likely to be under stomatal control. However, this model fails to take into account possible feedback inhibition on production as concentrations increase or increased activity of metabolic sinks.

Further evidence that acetaldehyde uptake is largely due to internal metabolic sinks comes from the finding that there was little to no deposition to dead poplar leaves, and that there was no change in the carbon isotopic composition of acetaldehyde. In contrast, acetaldehyde was strongly taken up and fractionated with a KIE of 5.1‰ by live poplar branches. This is close to the expected value of 4.4 ‰ due to diffusion in air which supports the idea that carbon isotope fractionation of acetaldehyde mainly occurs during diffusion into and within the plant. It may be possible to use the fractionation of acetaldehyde during uptake to separate uptake from emissions. This would be based on the fact that net uptake rates would enrich ambient acetaldehyde in ^{13}C while net emission rates would tend to enrich it in ^{12}C. Similar to what has been done for carbon dioxide using Keeling type plots (Bowling et al., 2001); it may be possible to use ambient measurements of $\delta^{13}C$ of acetaldehyde to partition net ecosystem flux measurements into gross uptake and emission fluxes.

Because the ambient concentrations of acetaldehyde measured in this study (0.18-3.44 ppbv) are typically much less than the compensation points

measured for poplar and holly oak in the light, net emissions are expected from sun lit leaves. This was the case for the upper canopies during the day. Because solar radiation can be rapidly extinguished in a forest canopy, the compensation points are expected to decrease with height. This can lead to a reduction in emission rates and even to net uptake if the compensation point drops below the ambient acetaldehyde concentration as was the case in Michigan and North Carolina. This suggests that well watered shade leaves can be a significant sink for tropospheric acetaldehyde. However, because of the extremely low concentrations at night in North Carolina near the bottom of the canopy, the understory behaved as a small net source. At the walnut orchard in California, a lack of significant uptake deeper in the canopy may be related to its short height and rather open nature (with trees well separated from each other) of the canopy in California. This likely increased the percentage of sunlit versus shade leaves which increased the compensation point (Figure 35).

By summing up the flux contributions of each layer within the canopy, it appears that that a lower foliar density results in higher net emissions due to a higher ratio of sun to shade leaves. Consistent with this idea, the low canopy density in California was a net source of acetaldehyde throughout the canopy although emission rates decreased with decreasing canopy height to a minimum of close to zero near the ground. In contrast, the higher density canopies in North Carolina and Michigan allowed for a switch to be made from a net source to a net sink with decreasing canopy height thereby allowing the lower canopy to recapture some of the emissions from the upper canopy, thereby reducing net emission rates and potentially acting as a net sink.

5.6 Conclusions

There is currently no consensus in the literature on the mechanism or the controls of acetaldehyde exchange with plants. Some articles conclude that the compensation point together with the ambient concentrations determine the exchange rates. Others point to the role of biochemical production and consumption as the dominating factor while others indicate that environmental factors such as temperature and light are the most important. Still other articles consider stomatal conductance to strongly influence acetaldehyde exchange rates while others find no dependence on this. The role of surface deposition/emission versus stomatal exchange also remains highly uncertain.

In this paper, we argue that acetaldehyde exchange rates with plants are fundamentally controlled by three variables: 1) The acetaldehyde compensation point which is a function of light and temperature 2) ambient acetaldehyde concentrations 3) stomatal conductance to acetaldehyde. We suggest that the opening and closing of plant stomata does not have a large affect on internal acetaldehyde concentrations due to continuous production and consumption

processes. We therefore argue that unlike isoprene, the driving force for acetaldehyde exchange with plants (ΔP) is independent of stomatal resistance allowing stomatal behavior to strongly influence exchange velocities.

The results presented here suggest a possible strategy for modeling the exchange of acetaldehyde between plant canopies and the atmosphere. Acetaldehyde fluxes could be calculated from various vertical layers within a model based on Fick's law. Fluxes could be calculated with knowledge of the ambient acetaldehyde concentration, the acetaldehyde exchange velocity, and the compensation point. In order to parameterize such a model, an empirical relationship between the acetaldehyde compensation point as a function of both light and temperature would be needed. Future laboratory and field research on acetaldehyde should focus on this goal. Possible intrinsic differences between these relationships for different plant species as well as height within the canopy (sunlit versus shade leaves) should also be investigated.

Should primary and secondary anthropogenic sources of acetaldehyde increase in the future, the biosphere may act to buffer large increases in tropospheric concentrations due to a decrease in plant emissions and an increase in plant uptake rates. Fumigation studies with extremely high concentrations of acetaldehyde indicates that uptake rates do not saturate until ambient concentrations of 200-1000 ppbv (Kondo et al., 1998). Higher anthropogenic primary and secondary sources have likely contributed to the high regional ambient background concentration of acetaldehyde in California (> 3 ppbv). Unfortunately, the lower canopy leaf area density of the walnut orchard appears to have further degraded regional air quality. High net emissions during the day due to the lack of significant uptake deeper in the canopy may lead to increased regional acetaldehyde pollution. In contrast, dense forests in non-water limited ecosystems such as in Michigan and North Carolina may be effective sinks for tropospheric acetaldehyde pollution. These forests may therefore effectively mitigate regional air pollution through the net uptake of acetaldehyde. However, future predicted increases in surface temperatures and landscape changes associated with a reduction in foliar density will likely increase compensation points, thereby worsen regional air pollution.

5.7 Acknowledgements

This work was supported by NSF grant ATM 0303727 (JE Mak), the NSF-funded Biosphere Atmosphere Research and Training (BART) program, and the Atmospheric Chemistry Division at NCAR. The National Center for Atmospheric Research is operated by the University Corporation for Atmospheric Research under the sponsorship of the National Science Foundation. We would

like to kindly thank Eric Apel at NCAR for providing gas standards and Ray Fall at CU, Boulder for our many discussions on oxygenated VOCs.

5.8 Figures

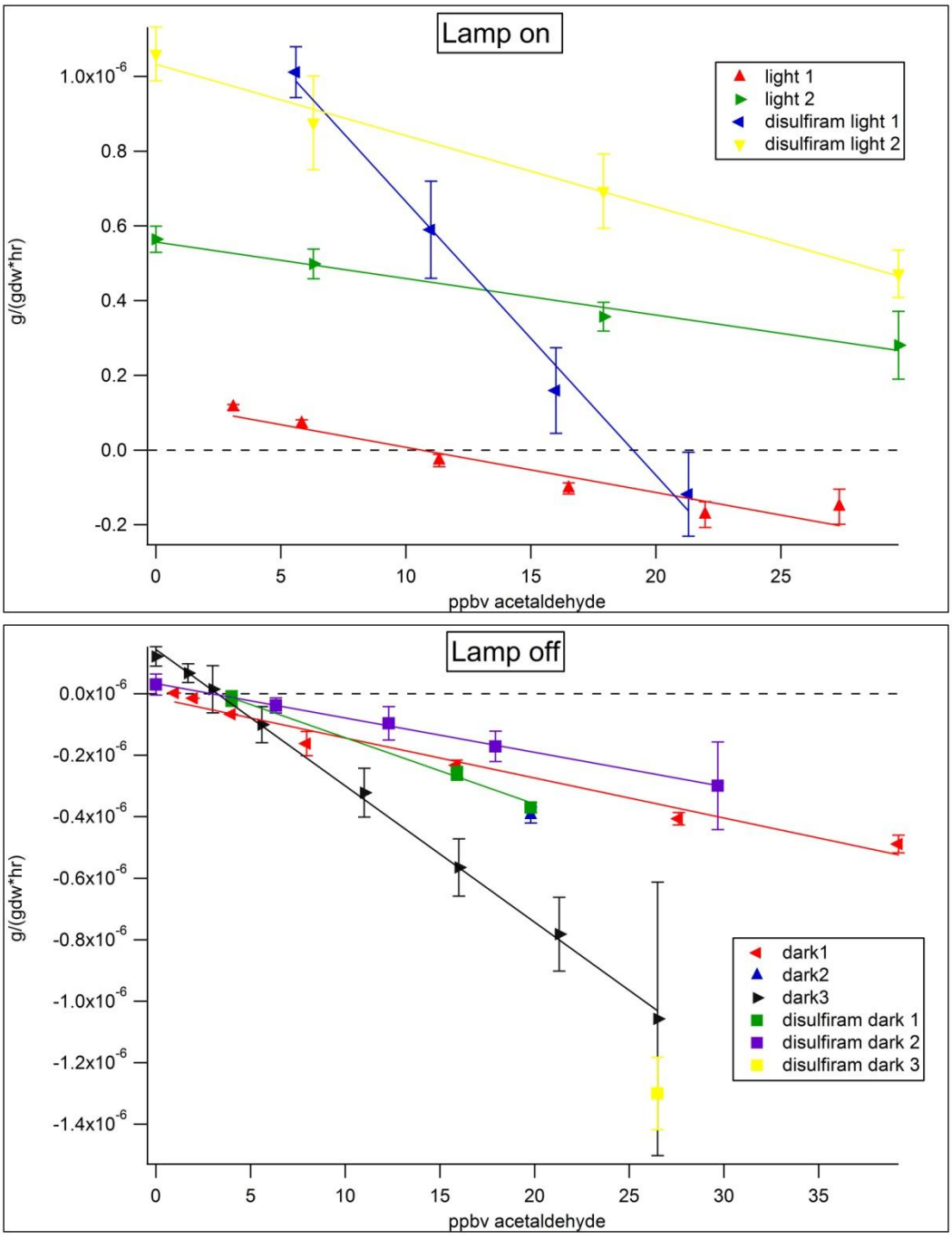

Figure 27: Example of compensation point measurements for acetaldehyde with Poplar branches (Populus deltoides) measured by PTR-MS during light and dark conditions. Branch level flux measurements (y-axis) are plotted versus incoming acetaldehyde concentrations (x-axis).

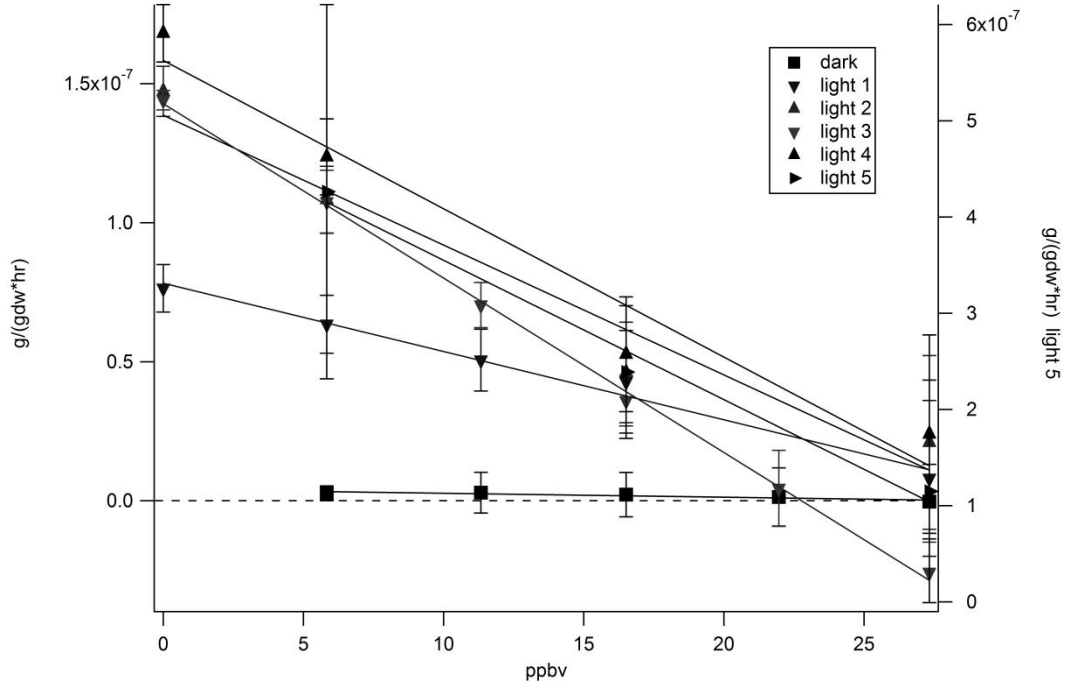

Figure 28: Example of compensation point measurements for acetaldehyde with Holly Oak branches (Quercus ilex) measured by PTR-MS during light and dark conditions. Branch level flux measurements (y-axis) are plotted versus incoming acetaldehyde concentrations (x-axis).

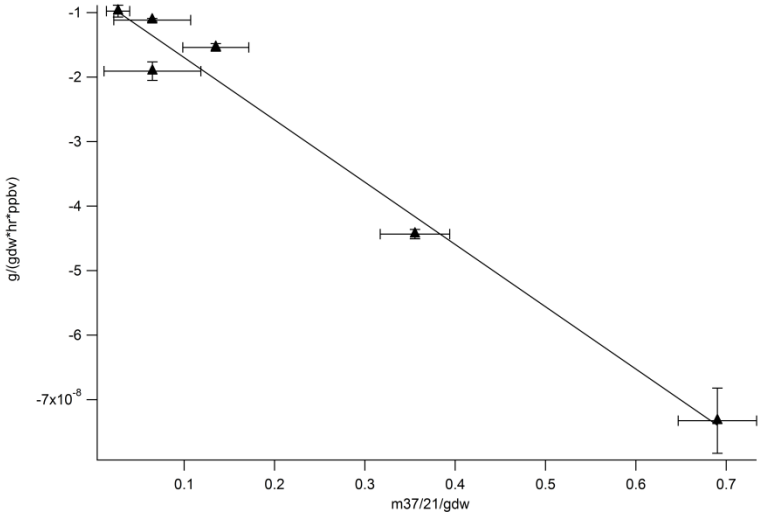

Figure 29: Measured acetaldehyde exchange velocities for Poplar branches are related to transpiration rates. Branch level exchange velocities (y-axis) are plotted versus incoming acetaldehyde concentrations (x-axis).

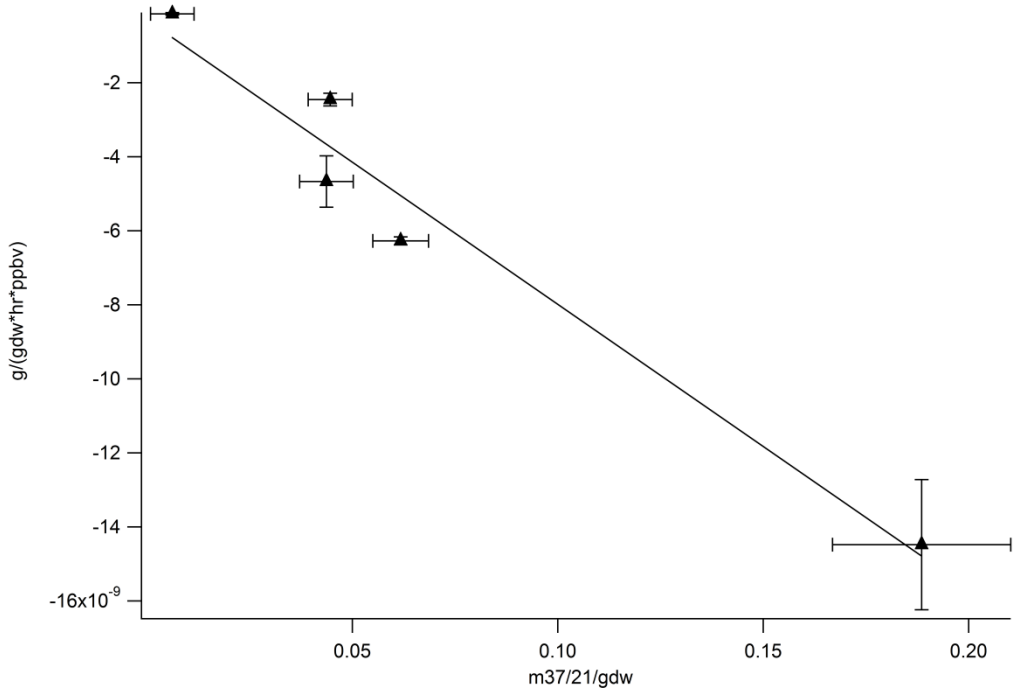

Figure 30: Measured acetaldehyde exchange velocities for Holly Oak branches are related to transpiration rates. Branch level exchange velocities (y-axis) are plotted versus incoming acetaldehyde concentrations (x-axis).

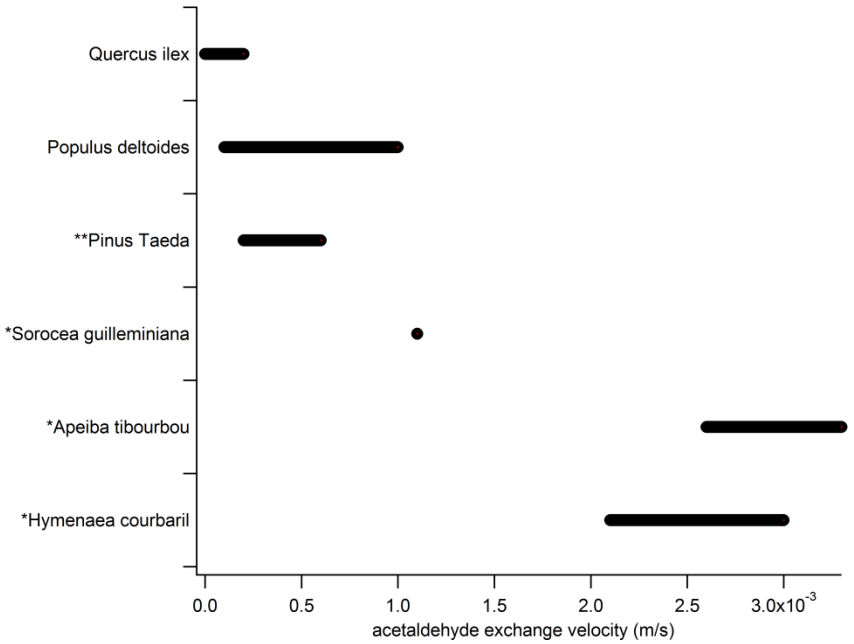

Figure 31: Ranges of acetaldehyde exchange rates (m/s) measured from this study (Q. ilex and P. deltoids), Karl et al., (2005) (P. Taeda), and Rottenberger et al., (2004) (S. guilleminiana, A tibourbou, and H. courbaril).

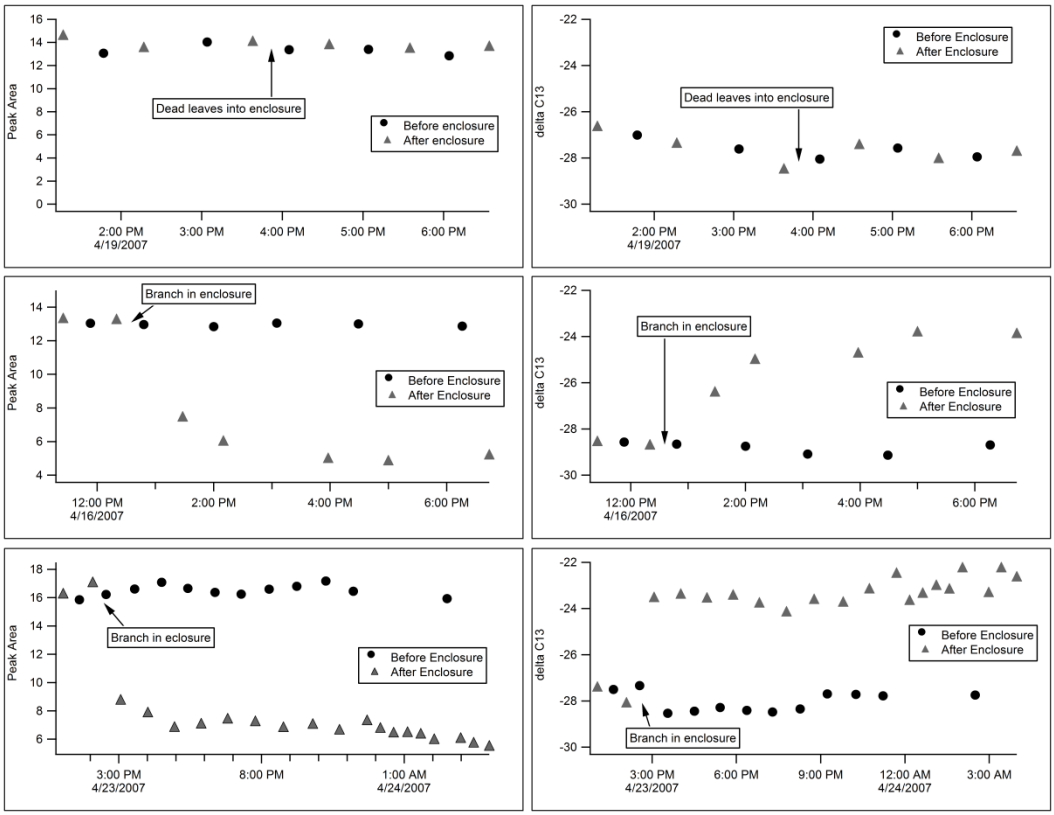

Figure 32: Carbon isotope fractionation of headspace acetaldehyde during fumigation experiments. GC-C-IRMS peak areas (first column) as well as their corresponding δ 13C values (second column) are plotted versus time during acetaldehyde fumigation experiments in a dynamic branch enclosure.

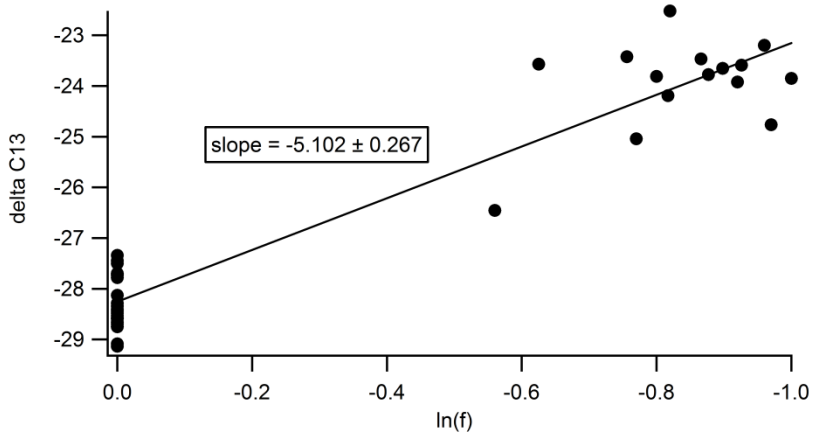

Figure 33: Estimation of the Kinetic Isotope Effect associated with the uptake of acetaldehyde by poplar branches. The δ 13C value of gas-phase acetaldehyde in the headspace of the branch enclosure

(y-axis) plotted against the natural logarithm of the fraction of remaining reactant (x-axis). The slope this relationship is defined as the kinetic isotope effect in units of per mil (‰).

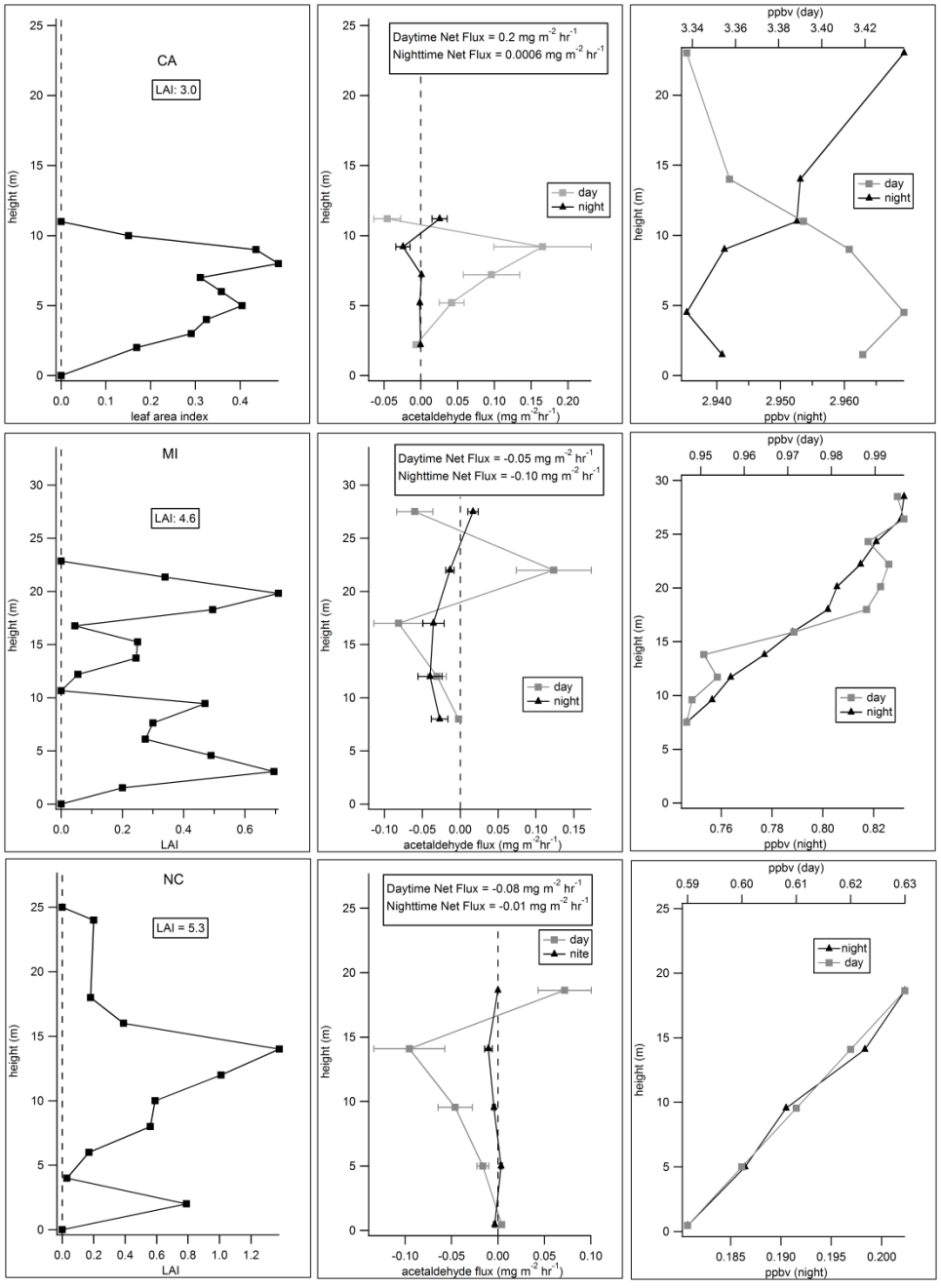

Figure 34: Fine scale vertical profiles of leaf area index (first column), net acetaldehyde source/sink strength (second column), and ambient concentrations (third column) measured from towers in California (CA), Michigan (MI), and North Carolina (NC). Data from North Carolina is from Karl et al., (2005). Double dashed line is approximate canopy height.

Figure 35: Overhead image of Walnut orchard in California demonstrating the openness of the canopy. During the daytime, a large percentage of the leaves appear to be sunlit.

Chapter 6: The Exchange of Volatile Organic Compounds between Litter/Soil and the Atmosphere

6.1 ABSTRACT

Live vegetation is known to be a strong source of isoprene and acetone to the atmosphere while being both a source and a sink for acetaldehyde. However, the role of soil and decaying litter in the exchange of these compounds under ambient conditions is uncertain. In this study, we measured the stable carbon isotope ratios of acetaldehyde emitted from senescent leaf litter as well as the exchange rates of acetaldehyde, acetone, and isoprene under ambient conditions from various soil plots at the University of Michigan Biological Station (UMBS) during the summers of 2005 and 2006. Based on carbon isotope data, we find that the ability to consume and therefore fractionate acetaldehyde is rapidly lost by red maple leaves as they transition from senescence to decay during the fall but is present again in buds produced during early spring. Therefore leaf senescence and decay are a strong source of acetaldehyde to the atmosphere both because of increased production due to decomposition processes and the loss of biological sink(s). UMBS soil plots lacking litter displayed no net exchange of acetaldehyde but behaved as a sink for acetone and isoprene. To our knowledge, this is the first report of isoprene and acetone uptake rates by soils under ambient conditions which is presumably mediated by microbial activity. While soil plots containing litter remained as a sink for isoprene, emissions of acetaldehyde were observed which increased with the amount of litter present. Plots with litter showed a complex pattern for acetone exchange with net uptake during the night and net emissions during the day. These results are consistent with the formation of a large vertical acetone concentration gradient during the night. The litter alone was found to emit acetone and acetaldehyde but not a source or a sink of isoprene. These results suggest that the litter source of acetone is much more temperature sensitive than the soil sink. So, while isoprene is consumed by soils and acetaldehyde is produced from decaying litter, the exchange of acetone is influenced by both processes. The magnitude of both emission and uptake fluxes are linearly correlated with temperature although the magnitude of these exchange rates is only on the order of a few percent of the total canopy scale fluxes measured previously at UMBS (Karl et al., 2004).

6.2 Introduction

The role of soils and litter in the exchange of VOCs with the atmosphere including acetone, acetaldehyde, and isoprene under ambient conditions is uncertain. This is partially due to 1) The lack of knowledge of sources and sinks in litter/soils 2) The lack of significant air turbulence near the surface undermining exchange estimates by inverse modeling 3) The use of zero air in soil/litter enclosures during flux measurements, eliminating the chance of uptake and maximizing emission rates.

Under ambient conditions in the Amazon, Rottenberger et al., (2005) discovered that live leaves are net sinks for acetaldehyde while senescent leaves are a net source and are associated with a net negative carbon dioxide balance. This implies that the biological sink for acetaldehyde is lost during senescence while production through decomposition processes begins. However, not only has this not been verified, the timing of these processes are not known. In chapter 4, it was demonstrated that the uptake of acetaldehyde by live vegetation is associated with a significant carbon isotope effect. Therefore, we hypothesized that if elevated gas phase concentrations of acetaldehyde are present with live vegetation in a static enclosure, the $\delta^{13}C$ values of acetaldehyde in the headspace should become strongly ^{13}C enriched over time in parallel with the consumption of the acetaldehyde. This can be explained by the kinetic isotope effect during uptake in combination with Raleigh distillation during acetaldehyde pool depletion in the headspace. We attempt to verify this following the mechanical wounding of white oak and red maple leaves in a static enclosure. This technique is then used with red maple leaves to study the temporal pattern of the loss of the biological sink(s) following senescence. The importance of this transition is then studied in a hardwood forest in Northern Michigan by measuring fluxes of acetaldehyde and other VOCs from the soil and litter.

Direct flux measurements of VOCs from soils are extremely rare but most studies indicate that soils behave as a source to the atmosphere. For example, field experiments have demonstrated that forest litter can be a large source of acetaldehyde and acetone that significantly contribute to the overall canopy scale flux (Schade and Goldstein, 2001). Emissions of these VOCs from decaying litter are suggested to be due to abiological reactions involving Malliard type reactions because sterilization of litter by heating to 200^{o} C overnight did not stop the emissions (Warneke, 1999). In this scheme, thermochemical reactions between reduced sugars and amino acids derived from carbohydrates and proteins produce a variety of products including acetaldehyde and acetone. This process also occurs for example during the cooking of food and coffee roasting and is important in producing their characteristic odors and tastes. Unfortunately, the use of zero air in the soil enclosures not only eliminates the possibility of uptake but maximizes the concentration gradient between the soil-atmosphere and the atmosphere. These measurements can only give us an upper limit on acetaldehyde and acetone emissions and therefore the use of ambient air is required for an accurate exchange measurement. To date, there have been very few published studies on the exchange of VOCs from soils under ambient conditions. The few that have been performed also indicate that soils can be a significant source of VOCs to the atmosphere. For example, methanol and acetone were emitted from agricultural soils during the 2003 European heat wave (Schade and Custer, 2004). Another study found that seasonal canopy scale emissions of acetone and acetaldehyde

were highest during the fall supporting the idea that decaying litter is a major source of these compounds to the atmosphere (Karl et al., 2004).

In the case of isoprene, there have been a few excellent studies which demonstrate the ability of soils to behave as sinks for isoprene due to microbial consumption (Cleveland and Yavitt, 1997, 1998; Pegoraro et al., 2005). Unfortunately, none of these experiments were performed on natural soils under ambient concentrations of isoprene and therefore the ability of soils to consume isoprene under natural conditions is unclear (Fall and Copley, 2000). Although performed on potted soil, recent evidence also suggests that soil can be a sink for some VOCs (Asensio et al., 2007) which previous studies have missed due to the use of zero air. Therefore, in order to access the role of soil and soil/litter in the exchange of acetaldehyde, isoprene, and acetone under natural conditions, we made direct flux measurements from various soil and soil/litter plots using a GC-FID and a PTR-MS during the summers of 2005 and 2006.

6.3 Experimental Details

6.3.1 Raleigh Distillation during Acetaldehyde Uptake

This experiment was designed to verify the Raleigh distillation of headspace acetaldehyde during uptake by live leaves in a static enclosure. Mechanical wounding of the leaves was performed in order to greatly increase the initial gas phase acetaldehyde concentrations within the enclosure. Live white oak (*Quercus rubra*) and red maple (*Acer rubrum*) leaves were obtained from trees surrounding the Marine Science Research Center at Stony Brook University. ~5 leaves were placed in a static enclosure in ambient air and mechanically wounded by tearing them in half. The enclosure was immediately brought into the laboratory and connected to the GC-C-IRMS system for $\delta^{13}C$ measurements of acetaldehyde in the headspace. Measurements were made approximately every 30 minutes. Strong increases in the ^{13}C content of acetaldehyde with time were used to indicate the presence of biological sinks for acetaldehyde. Control measurements were performed by wounding the leaves by hand in the enclosure and then removing the leaves. A second control was performed on unwounded live red maple and white oak leaves by placing them in the static enclosure and replacing the air with helium. This greatly stimulates ethanolic fermentation resulting in the net production of acetaldehyde. Because the biological sink for acetaldehyde may still be active under these conditions, we hypothesize that the ^{13}C content will only slightly increase with time due to the dilution effect by the source. A simple box model simulation was created to demonstrate that the fractionation of the acetaldehyde during uptake can lead to enhancements in the ^{13}C content of the remaining acetaldehyde even with a KIE as low as 5.1 ‰.

In order to examine when the biological sink(s) is lost by senescent leaves, similar Raleigh distillation experiments were performed on senescent red maple

leaves. Senescent red maple (*Acer rubrum*) leaves were obtained from the forest floor beneath a group of trees isolated in court yard at the Marine Science Research Center at Stony Brook University. The Leaves were obtained from the forest floor immediately following the dropping of the leaves during the fall and continued until early winter. Approximately 20 leaves were placed in a static enclosure during early fall while more than 50 were required during December and incubated for ~ 1 hour in order to accumulate the necessary acetaldehyde in the headspace for carbon isotope analysis by GC-C-IRMS. The minimum concentration for a $\delta^{13}C$ measurement was found to be ~10 ppbv. Instead of wounding the leaves to increase the initial gas phase acetaldehyde concentrations, the leaves were simply incubated in a static enclosure for one hour. Unlike the live leaves which required wounding to generate enough headspace acetaldehyde for carbon isotope analysis, acetaldehyde concentrations increased with time inside the enclosures containing the senescent red maple leaves. The presence of the biological sink could be detected by an enhancement in ^{13}C of the gas phase acetaldehyde despite the increase in concentrations with time.

6.3.2 Soil Flux and Ambient Concentration Measurements

During the summers of 2005 and 2006, ambient concentration and soil flux measurements of acetone, acetaldehyde, and isoprene were performed at both the PROPHET tower and the 'DIRT' plots at the University of Michigan Biological station (Pellston, Michigan) using a GC-FID system. One full diurnal cycle of the ambient concentrations of these compounds were obtained outside of the PROPHET tower lab at approximately 1 m height to provide some information on the exchange rates of these compounds. However, because concentrations are dependent upon many other factors such as atmospheric sinks and meteorological conditions, direct enclosure based flux measurements from bare soil, soil plus litter, soil plus double litter, and just litter were performed.

PROPHET tower summer 2005

Because of the lack of a calibration standard for acetaldehyde during the summer of 2005, all acetaldehyde measurements were made with a PTR-MS instrument. Surrounding the PROPHET tower during the summer of 2005, four stainless steel soil collars were driven approximately 3 cm deep into undisturbed soil surrounding the tower lab where the GC-FID system was located. These plots were given at least one week to recover before measurements were started. A 21.7 liter dynamic soil enclosure was placed over the collar consisting of Teflon sheets bolted in an aluminum frame and a flow rate of 1.6 L min^{-1} was continuously drawn out of the enclosure (1.0 L min^{-1} to the GC-FID system and 0.6 to the dehydration membrane). For details on the operation of the membrane and the GC-FID system see the Chapter 2. The GC-FID was fully automated using Labview 6.1 and Chemstation 10.1 to collect and analyze a 2 L sample every 40

minutes. Because the residence time of air in the enclosure was approximately 13.6 minutes, the enclosure was placed on the soil collar for ~20 minutes before a sample was taken (10 minute sampling time) and afterwards the sampling inlet was hung on a tree near the ground (~1 m height) to measure the ambient concentration (On the soil collar for a total of ~30 min). The pressure inside the enclosure was maintained at ambient pressure by the entry of ambient air through leaks in the enclosure. The formation of dew inside the chamber was minimized through the dynamic air flow and by alternating between measurements on the soil collar and ambient air. Temperature and relative humidity were recorded every minute inside the chamber using a small battery powered USB device. An experimental membrane by MTR (see chapter 2) was used to continuously dehydrate the sample air leaving the enclosure which was shown to be necessary due to the extremely high water vapor concentrations during the daytime. The use of the membrane allowed for continuous monitoring of VOCs, even during the night when condensation inside tubing occurred for other instruments such as the PTR-MS. An intercomparison between acetone concentration measurements was done between the GC-FID system utilizing the MTR membrane and a PTR-MS system in order to access the accuracy of the VOC measurements. For this setup, an additional 1 L min^{-1} was drawn out of the enclosure to the PTR-MS. Unfortunately, condensation of water vapor occurred inside the Teflon transfer line between the soil enclosure and the PTR-MS at night and even during the day where the lines entered the air conditioned mobile lab. This is because the transfer line did not draw the air sample from the MTR membrane outlet but directly from the soil enclosure. Therefore, the intercomparison was limited to times when condensation was not present. In contrast, the Membrane/GC-FID system was able to operate continuously without condensation in the transfer lines because of the strong dehydration effect of the membrane. Measurements were even possible during times of very high humidity such following an intense rain storm. The results from the intercomparison demonstrate that the absolute concentration values and the temporal variability in acetone concentrations are very similar for both analytical systems (Figure 49).

Linear calibration plots were generated by introducing three different VOC concentrations into the soil enclosure resting on a Teflon ground sheet at a flow rate of 3 L (see Figure 36 for enclosure plumbing diagrams). VOC fluxes in nmoles hr^{-1} m^{-2} were calculated based on the flow rate through the enclosure F in L min^{-1}, the surface area of the enclosure in m^2, and the difference in measured concentrations between the enclosure and the ambient air in ppbv.

$$Flux = \frac{ppbv_{enclosure} - ppbv_{ambient}}{22.4(\frac{L}{mole}) * Area(m^2)} * Flow\left(\frac{L}{min}\right) * \frac{60\,min}{hour}$$

DIRT Plots summer 2006

During the summer of 2006, all measurements were made at the DIRT or Detritus Input and Removal Treatment plots at UMBS. These plots are set up to "Assess how rates and sources of plant litter inputs control the accumulation and dynamics of organic matter and nutrients in forest soils over decadal time scales". In order to access the importance of litter on the flux of acetone, isoprene, and acetaldehyde from soils, two distinct plots were analyzed including a plot with no litter input and one with double litter input. Measurements of soil respiration was also taken with a LICOR 6400 portable photosynthesis unit in order to assess the role of microbial decomposition processes on the exchange of these VOCs. At all plots, the ambient temperature and relative humidity was recorded. In order to measure soil fluxes of acetaldehyde under natural conditions, ambient air was allowed to enter a small Teflon chamber with a volume of 0.5 L through a hole in the side instead of zero air. Two VOCARB-3000 traps were taken directly into the field and sample air was directly trapped on one while ambient air was trapped onto the other in parallel using a small diaphragm pump (KNF) powered by a 12 VDC battery. The volume passed through the traps was calculated by measuring the flow rate (~70 ml min^{-1}) and the sampling time (20 min). They were then returned to the lab, mounted on the preconcentration system and VOC quantification was carried out by GC-FID. Because of the lack of water removal prior to VOC preconcentration on the traps, nearly half of the samples were lost due to excessive water interfering with the separation of VOCs by the analytical column and their detection by the FID. The low sample collection flow rate ensured pressure equilibration between the air inside and outside of the enclosure. With the hydrocarbon traps attached to the GC-FID system, linear calibrations were generated for isoprene, acetone, and acetaldehyde using a dynamic dilution system and gravimetrically prepared VOC standards. During calibration, a known volume (1.5 L) of calibration air was passed over the hydrocarbon traps prior to their installation on the GC-FID. For all samples collected at the DIRT plots, the flux F of VOCs in units of nmoles m^{-2} hr^{-1} was calculated as follows:

$F = \frac{nmoles_{soil} - nmoles_{ambient}}{A \cdot t}$, where A is the area of the chamber and t is the sampling time.

6.4 Results and Discussion

6.4.1 Carbon Isotope Fractionation of Acetaldehyde during Uptake by Leaves

GC-C-IRMS measurements demonstrate that the discrimination against the "heavier" acetaldehyde isotopologues during uptake by live vegetation also occurs from mechanically wounded red maple (*Acer ruber*) and white oak (*Quercus`rubra*) leaves placed in a static enclosure (Figure 37). However, unlike the dynamic enclosure, the static system is not in steady state as evidenced by the change in acetaldehyde concentration with time. The $\delta^{13}C$ of acetaldehyde in the headspace above the wounded leaves became strongly ^{13}C enriched over time, in parallel with the net consumption of acetaldehyde in the headspace. Simple box modeling simulations suggest that these results can be explained by an initial emission pulse of acetaldehyde from the wounding event in combination with a 5.1 ‰ carbon isotope effect during uptake (Figure 38). In contrast, when unwounded leaves from the same species were placed in a helium atmosphere to induce ethanolic fermentation, the $\delta^{13}C$ of acetaldehyde in the headspace remained relatively constant over time, in parallel with the net production of acetaldehyde in the headspace. However, even in this case, there is a detectable increase in the $\delta^{13}C$ of acetaldehyde with time. This indicates that the presence of the biological sink for acetaldehyde in leaves can be detected even in the presence of net production. Therefore, by placing leaves in a static enclosure and measuring the $\delta^{13}C$ values of headspace acetaldehyde after a short incubation time, the ability to consume acetaldehyde and therefore fractionate it can be assessed.

In order to demonstrate the loss of the biological sink for acetaldehyde from senescent leaves and to determine when this occurs, this technique is applied to senescent red maple (*Acer rubrum*) leaves. Sample collection began after early senescence during the fall immediately following leaf fall and continued through early winter. The results reveal that the $\delta^{13}C$ values of acetaldehyde in the headspace of the enclosure during the first week following leaf fall are strongly enhanced in ^{13}C (Figure 39). However, this enhancement is rapidly lost and after one week the $\delta^{13}C$ values of acetaldehyde become very similar to bulk biomass. This suggests that acetaldehyde is fractionated during uptake in plants and this ability is rapidly lost by leaves as they transition from senescence to decay. However, a similar analysis of the buds present during early spring indicates that the biological sink is present again (data not shown). We therefore conclude that leaf senescence and decay are a strong net source of acetaldehyde to the atmosphere not only because of increased production due to decomposition processes (Warneke, 1999), but also because of the rapid loss of biological sink(s) following senescence. Although the flux of acetaldehyde from the leaf litter was

not directly measured, the need for additional biomass in the enclosure to produce a peak height of 1.0 V increased with time during the fall and into early winter. This suggests that despite the continued presence of the biological sink during the first week following decay, the net emission rates are the largest during this period. This may be due to both biological (catabolic metabolism) and abilogical (thermochemical decomposition reactions) processes whose rates are the greatest during early senescence and decline thereafter. To verify this, future work should focus on accurately measuring the gross fluxes of acetaldehyde uptake and emission during this transition under ambient conditions.

6.4.2 Ambient Concentrations and Soil/Litter Flux Measurements of Acetaldehyde, Acetone, and Isoprene

When ambient concentrations of acetaldehyde, acetone, and isoprene were made at the ground (~1 m) at the PROPHET tower, a strong diurnal pattern was observed (Figure 40). However, there are very large differences in concentration magnitudes for the different compounds. Whereas maximum isoprene concentrations can reach well over 10 ppbv, acetone is around 6 ppbv while acetaldehyde barely makes it over 1 ppbv. However, the concentrations cannot be used as an indication of the flux of these compounds and so direct flux measurements are necessary.

UMBS soil plots lacking litter displayed no net exchange of acetaldehyde although strong uptake rates of acetone and isoprene occurred presumably mediated by microbial activity (Figure 41). To our knowledge, these are the first measurements under ambient conditions to report the role of soil as a sink for acetone and isoprene. The importance of litter on the exchange of acetaldehyde was demonstrated by comparing flux measurements from a plot with no litter and one with double litter (Figure 42). While the plot with no litter was neutral with respect to acetaldehyde exchange, the plot with double litter was a strong source. When litter alone was examined, it was shown to be a source for acetaldehyde and acetone but neutral towards isoprene (Figure 43). While soil plots containing litter remained as a sink for isoprene, a complex pattern for acetone exchange occurred with net uptake during the night and net emissions during the day (Figure 44). These results suggest that the soil sink for acetone dominates the litter source during the night but during the day the opposite is true. Therefore it appears that the production of acetone in litter is much more temperature sensitive than its consumption in soil. While acetone switches between a net source to a net sink at night, acetaldehyde remains a source even at temperatures down to 14 ^{o}C (Figure 50). This suggests that the microbial sink for acetone in the soils at UMBS is much greater than that for acetaldehyde, possibly because acetone concentrations are higher. However, it was recently reported that Mediterranean soils have a very small bus significant microbial sink for acetaldehyde (Asensio et al., 2007).

So, while isoprene is consumed by soils and acetaldehyde is produced from decaying litter, the exchange of acetone is influenced by both processes. The fluxes for all of the compounds are linearly correlated with temperature (Acetaldehyde: Figure 45, Isoprene: Figure 46, Acetone: Figure 47). For acetaldehyde, this is likely due to an increase in thermochemical production rates in the litter with increasing temperature. The increase in the temperature sensitivity of acetaldehyde emissions from the plot with double litter compared with the normal litter plot indicates that the quantity of litter is a very important control over acetaldehyde emission rates. However, because the temperature range is different for these two plots, additional data is needed to support this conclusion. The strong correlations between isoprene uptake rates and air temperature may be partially due to a stimulation of microbial activity at higher temperatures. However, it is likely that an indirect effect is responsible. The stimulation of isoprene emissions from the live vegetation with higher temperatures leads to higher ambient isoprene concentrations. This increases the driving force for isoprene uptake in the soil because of the increased atmosphere/soil-atmosphere concentration gradient. While all plots behave as a net sink for isoprene, there is considerable variability in the sensitivity of isoprene uptake to temperature. This may be because of the heterogeneous nature of microbial activity in soils responsible for isoprene consumption, the dependence on soil moisture and organic content, or the variable relationship between air temperature and ambient isoprene concentrations. For acetone fluxes at low temperatures during the night, all plots with litter behave as a net sink for whereas during the warmer temperatures of the day they turn into a net source. We suggest that the soil sink (microbial?) is only weakly temperature dependent whereas emissions from the litter are much more sensitive to temperature. While the flux response to temperature is similar for the different plots, there can be considerable differences in the magnitude of the flux between plots for a given temperature. All plots lacking litter were sinks for acetone at all temperatures during both the day and the night (Figure 48). However, no significant correlation with air temperature was detected. Although this may be due to a lack of data, the result supports other recent research that concluded that the uptake of VOCs by soil is much more dependent upon soil moisture than on temperature (Asensio et al., 2007).

Soil + litter flux measurements of acetaldehyde, acetone, and isoprene reported here during the summer of 2005 and 2006 are put into context of canopy scale flux measurements of the same compounds made during the summer of 2002 (Karl et al., 2004) (Figure 51). The maximum measured acetaldehyde fluxes from plots with soil + litter is approximately 9.6 % of the average maximum canopy scale acetaldehyde flux. Therefore, it appears that the litter can contribute a significant portion of the canopy scale acetaldehyde flux from this ecosystem.

Karl et al., (2004) reported that the maximum canopy scale fluxes of acetaldehyde occurred during the fall and it was suggested that this was caused by a large increase in decaying litter. It is possible that a large flux of acetaldehyde is emitted from decaying litter following senescence but is reduced with time due to the decomposing of proteins and carbohydrates, the proposed source during decay. In this way, the soil + litter may contribute a much more significant percentage of the total canopy scale flux of acetaldehyde during the fall. Therefore, there is a clear need for seasonal flux measurements of acetaldehyde from soil + litter to verify this hypothesis. An additional reason for the higher canopy scale acetaldehyde flux during the fall may be the loss of the biological sink in the leaves following senescence.

When compared with a similar study in California, Schade and Goldstein, (2001) found that the flux of acetaldehyde from the soil + litter makes up a much more significant portion of the total canopy scale flux (80%). While the magnitude of the canopy scale fluxes are similar, the emissions from the soil + litter were much higher in the California study compared with the Michigan Study presented here. However in California, the amount of litter on the forest floor was greatly increased by a previous Manzanita underbrush clearing. Another reason for the large acetaldehyde fluxes measured in Schade and Goldstein, (2001) is the use of zero air in the enclosures which maximizes the flux of all VOCs.

Acetone emissions measured here during the summer of 2005 and 2006 from the soil + litter plots represent up to 3.5 % of the canopy scale flux measurements during the summer of 2002 by (Karl et al., 2004). This represents a small but significant portion of the total canopy scale flux and may also make up a much higher percentage in the fall. Like acetaldehyde, this may because of higher emission rates from the litter during the fall but this remains to be verified. To our knowledge, this is the first report of the ability of the soil to behave as a sink for acetone under ambient conditions. A variety of diverse bacteria have been found to grow aerobically using acetone as a source of carbon and energy and we suggest that similar bacteria are present in the soils at UMBS. This process is thought to be mediated by an acetone carboxylase enzyme which activates acetone (Birks and Kelly, 1997) to acetoacetone. Although small when compared to the average maximum canopy scale flux during the day (-1.5%), it may be the only significant sink for acetone within the ecosystem. Therefore at night, when emissions from the live and decaying vegetation are greatly reduced, the soil act as a net sink. This creates a strong vertical concentration gradient throughout the canopy (data not shown).

Isoprene is the most abundant VOC emitted at UMBS and is the dominate VOC emitted by vegetation globally (Guenther et al., 1995). Therefore, a clear understanding of the processes involved in both production and consumption are needed. While the biochemistry and the factors controlling isoprene emissions

have been well described in live plants, the importance of soils is unknown. While previous studies have verified the presence of microbial sinks within soils, they have been conducted under unnatural conditions with isoprene concentrations many orders of magnitude higher than occurs in real ecosystems. Therefore, to our knowledge the results presented here are the first to demonstrate the significance of this sink under ambient conditions in the field. However, the maximum isoprene sink is -3.4% of the average maximum canopy scale flux measurements made by (Karl et al., 2004). Although small, this may be the only significant sink for isoprene at night and may partially be the reason for the continuous decay in isoprene concentrations within the canopy at night as measured here and by others. Previous authors have attributed the decay in isoprene concentrations at night to the presence of night-time OH (Faloona et al., 2001; Hurst et al., 2001). We suggest that in addition, the soil sink for isoprene may be responsible for this decay.

6.5 Conclusions

In conclusion, stable carbon isotope data presented here supports our hypothesis that the emission of acetaldehyde by senescent leaves is associated with both the loss of the biological sinks and the gain of abiotic thermochemical decomposition sources. We also demonstrate that under ambient conditions, acetaldehyde and acetone emissions occur from the forest floor at UMBS although the magnitude is small when compared to the emissions from the entire ecosystem. Further research should determine if the magnitude of the emissions from the forest floor dramatically increases during the fall. We also discovered for the first time that both acetone and isoprene are consumed by soils under ambient conditions although they also make up a small fraction of the total emissions. An interesting pattern emerged for acetone with net uptake by the forest floor during the night and net emissions during the day. We suggest that this is due to a much larger temperature sensitivity of the litter source than the assumed microbial sink in the soil. The exchange rates of all compounds was found to be dependent upon air temperature indicating that if future temperatures are warmer, large changes in flux rates may be possible. In the case of acetone for example, higher temperatures at night may eliminate the ability of the soil to act as a net sink since the overlying litter source may overwhelm it. Because the soil sink may be the only significant sink in the canopy, this may change the entire vertical structure of acetone concentrations at night. We suggest that the effect of temperature may be direct in some cases such as the production of acetone and acetaldehyde through thermochemical reactions in leaf litter and indirect as in the case of isoprene where higher temperatures leads to higher production rates by the live vegetation. This would lead to higher uptake rates to the soil due to larger atmosphere soil-atmosphere concentration gradients. Direct stimulation of microbial activity with

higher temperatures is also possible. In conclusion, while emission/deposition fluxes to and from the forest floor was found to be small relative to canopy scale fluxes, a wide variety of interactions and feedbacks may be possible within the ecosystem. Therefore the biological, physical, and chemical nature of these fluxes and their environmental controls deserves additional research.

6.6 Figures

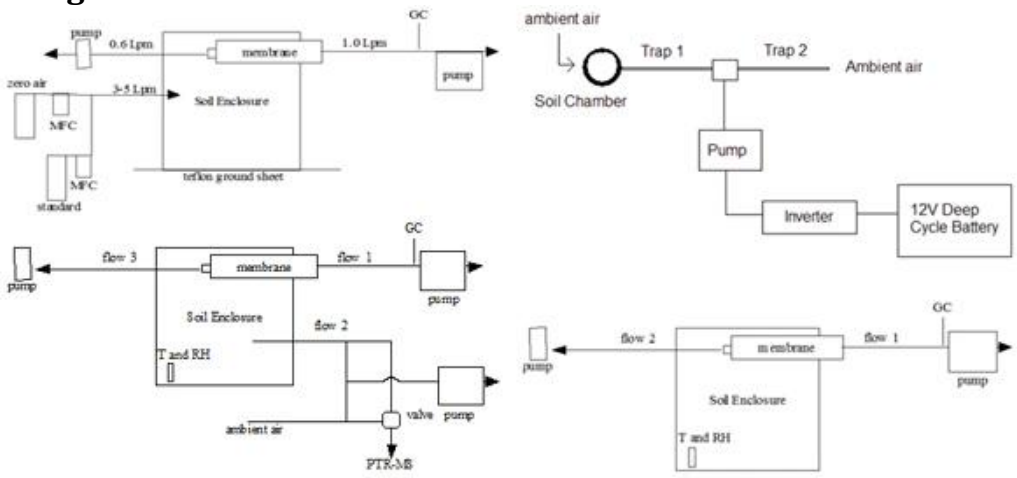

Figure 36: Schematic of soil enclosures for soil flux measurements during the summer of 2005 and 2006 at the University of Michigan Biological Station.
The top left figure shows the setup for calibrating the GC for enclosure based flux measurements of acetone, acetaldehyde, and acetone. The bottom left shows the setup for the acetone flux intercomparison measurements between the GC-FID and the PTR-MS. The bottom right figure shows the normal setup for soil flux measurements by the GC-FID. Because of the remote location of the DIRT plots, during the summer of 2006 the samples of ambient air and enclosure air were obtained in parallel using a small membrane pump powered by a 12 VDC battery (top right).

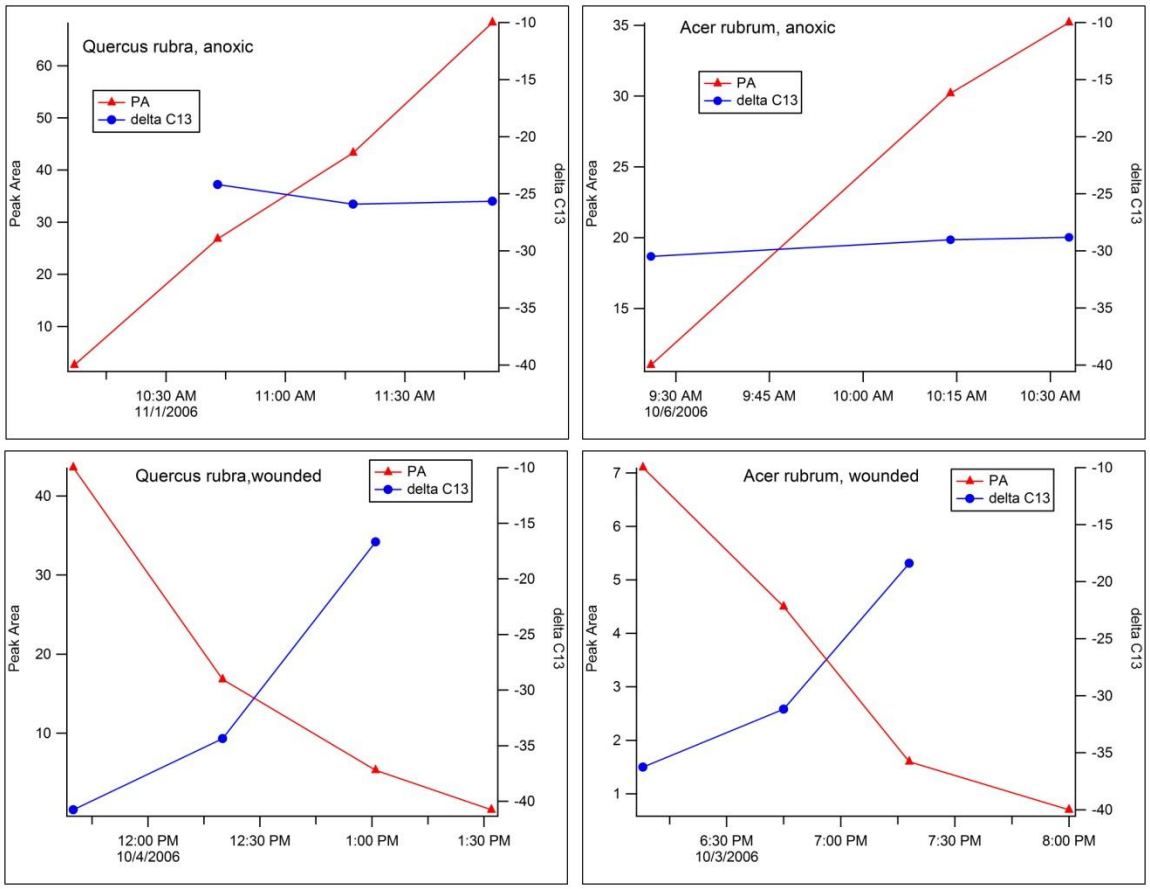

Figure 37: Time series of acetaldehyde peak areas and $\delta^{13}C$ values during wounding and anoxia in static enclosures.

Quercus`rubra (left column) and Acer rubrum (right column) leaves were detached and placed in a static enclosure with a helium atmosphere (top row) or mechanically wounded in air (bottom row). Under anoxic conditions, carbohydrate fermentation results in the accumulation of acetaldehyde in the enclosure headspace. Under these conditions, the measured $\delta^{13}C$ values acetaldehyde in the headspace is relatively constant over time and similar to bulk C3 biomass. In contrast, wounding in air induces the accumulation of ^{13}C depleted acetaldehyde which is subsequently consumed by leaves. Fractionation of the remaining acetaldehyde in the headspace during uptake may explain its strong enhancement in ^{13}C over time.

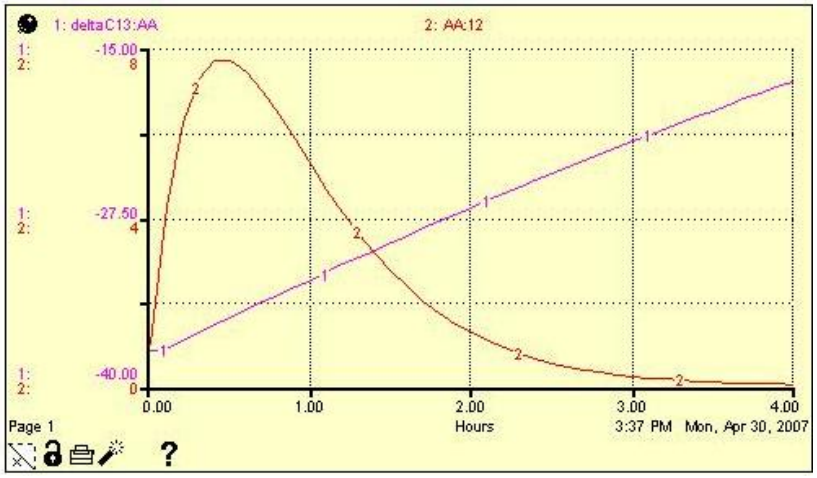

Figure 38 A Stella box model simulation of acetaldehyde carbon isotope fractionation during uptake by live leaves with a kinetic isotope effect of 5.1‰.

The initial burst of emissions stimulated by the wounding event leads to the rapid accumulation of acetaldehyde. This then stimulates the uptake of the acetaldehyde in the headspace which results in a strong draw down of the concentration (top figure) with the associated enhancement in ^{13}C of the remaining acetaldehyde.

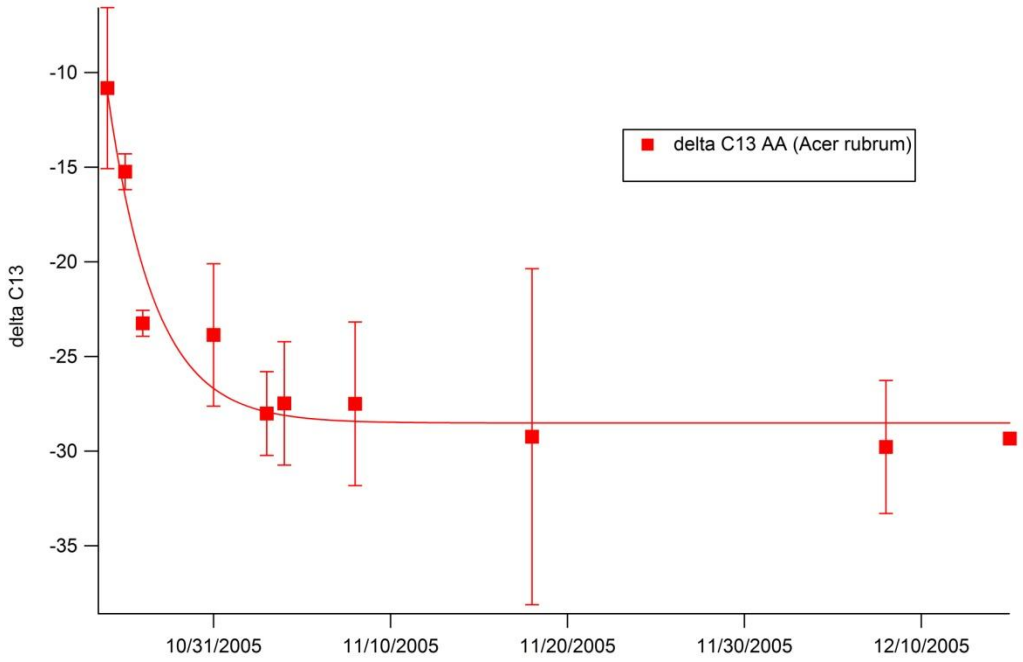

Figure 39: Measured $\delta^{13}C$ values of acetaldehyde from decaying Red Maple (Acer rubrum) leaves collected from the forest floor on the Stony Brook University campus and placed in static enclosures.

Sample collection began after early senescence during the fall and continued through early winter. The $\delta^{13}C$ values of acetaldehyde in the headspace of the enclosure during the first week following leaf fall are enhanced in ^{13}C. However, this enhancement is rapidly lost and within one week the $\delta^{13}C$ values become very similar to bulk biomass. This suggests that acetaldehyde is fractionated during uptake in plants and this ability is rapidly lost by leaves as they transition from senescence to decay.

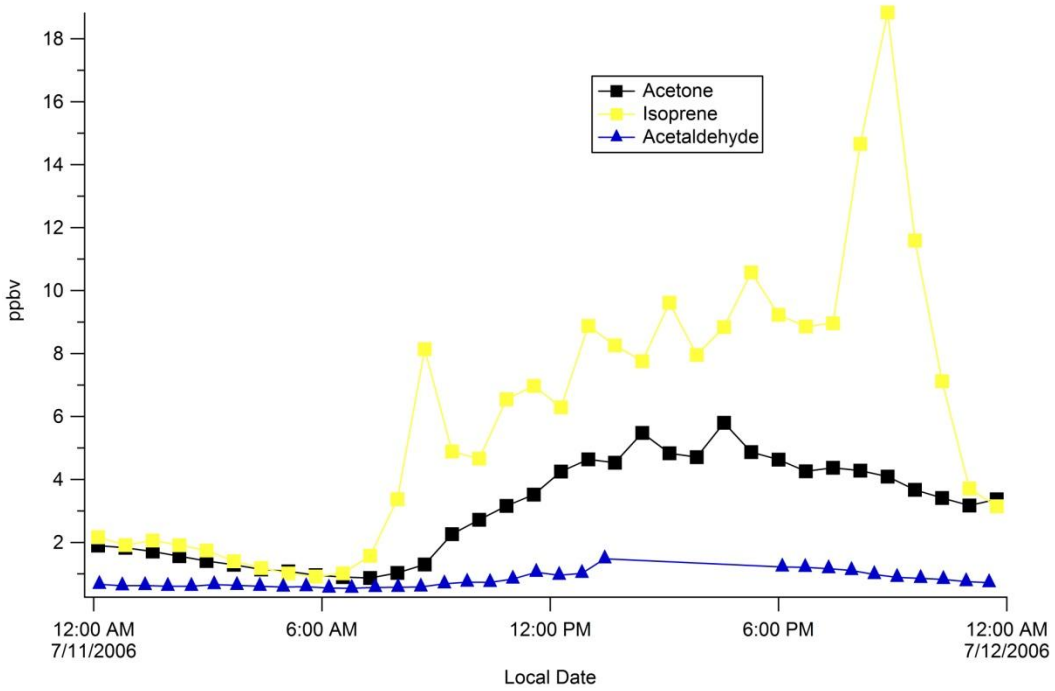

Figure 40: Diurnal pattern of ambient isoprene, acetone, and acetaldehyde concentrations at ~1 m height near the PROPHET tower.
Whereas maximum isoprene concentrations can reach well over 10 ppbv, acetaldehyde barely makes it over 1 ppbv.

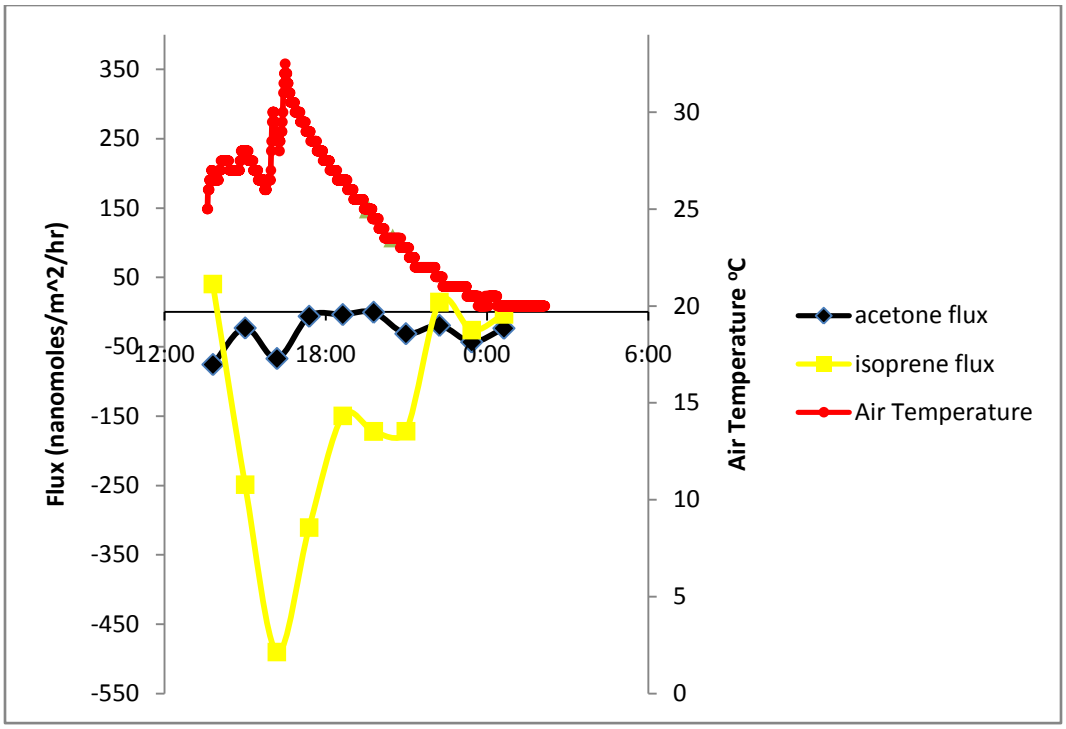

Figure 41: Flux measurements of acetone and isoprene from a soil plot lacking litter.
When the overlying litter is removed from the soil, both isoprene and acetone are taken up from the atmosphere presumably mediated by microbial activities within the soil. The increase in uptake rates with temperature is likely due to the fact that the highest ambient concentrations exist at those temperatures and not necessarily to a stimulation of microbial activities.

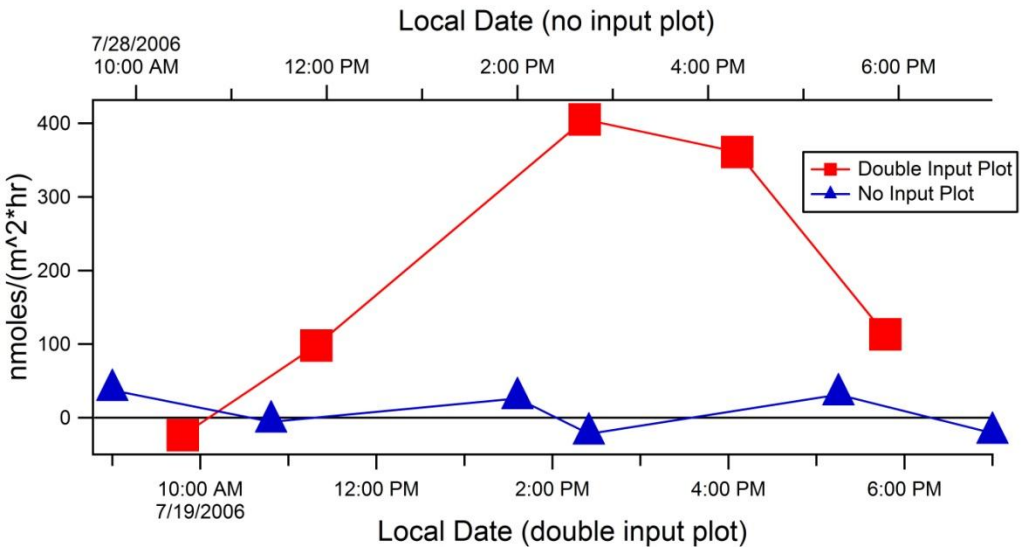

Figure 42: Acetaldehyde flux measurements of acetaldehyde from a soil plot lacking litter and one with double litter.

Emissions to the atmosphere are completely dependent upon the amount of litter present. In plots without litter, no net flux of acetaldehyde could be detected. However, in plots with double litter amounts, acetaldehyde emissions were large.

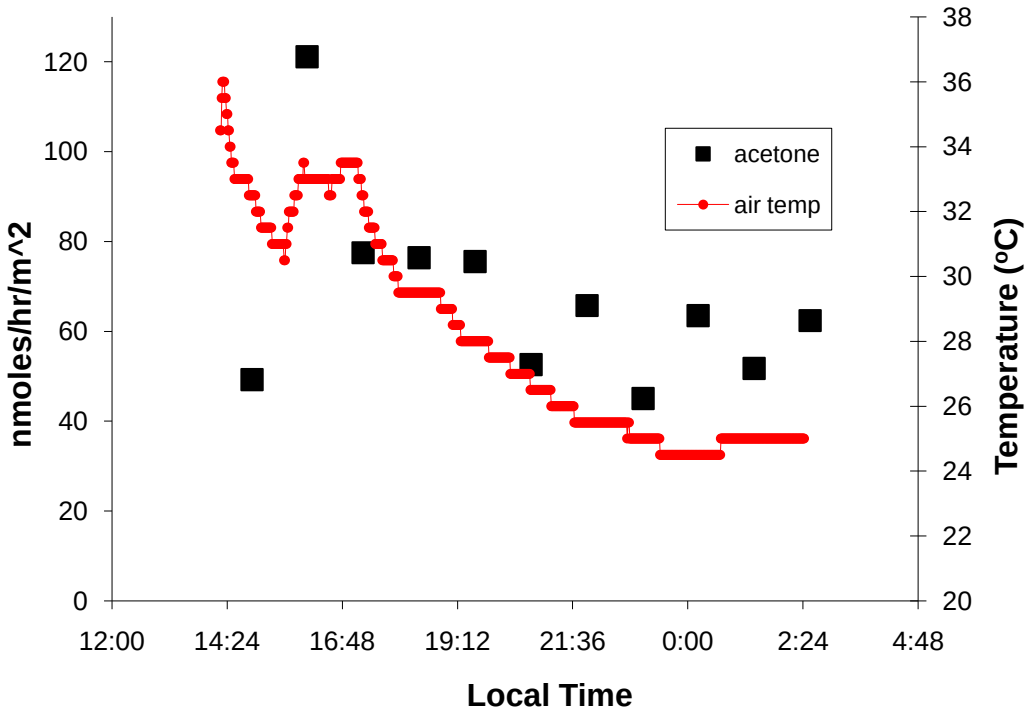

Figure 43: Fluxes of acetone and acetaldehyde from leaf litter.
Leaf litter (minus the soil) is a strong source of acetaldehyde and acetone to the atmosphere whereas it is neutral to isoprene (acetone and isoprene data not shown).

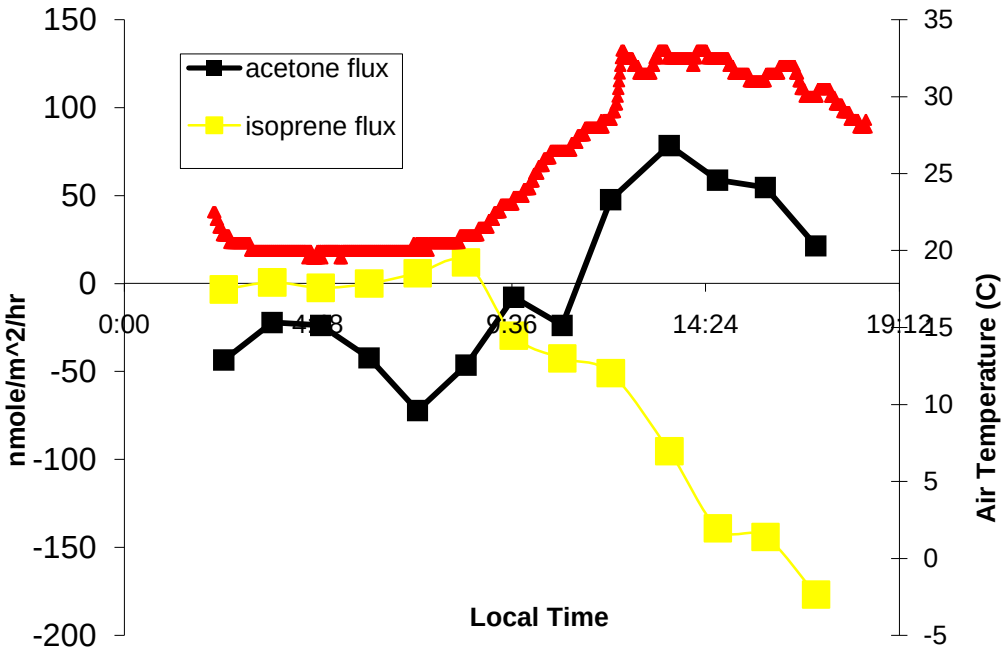

Figure 44: Exchange measurements of isoprene and acetone from a soil plot with normal litter. Plots with normal amounts of leaf litter are still sinks for isoprene. However, acetone exhibits a complex pattern of net uptake during the night and emissions during the day. We suggest that this is due to the interaction of the relatively constant microbial soil sink and the strongly temperature dependent decaying litter source. In contrast, acetaldehyde was continuously emitted (data not shown).

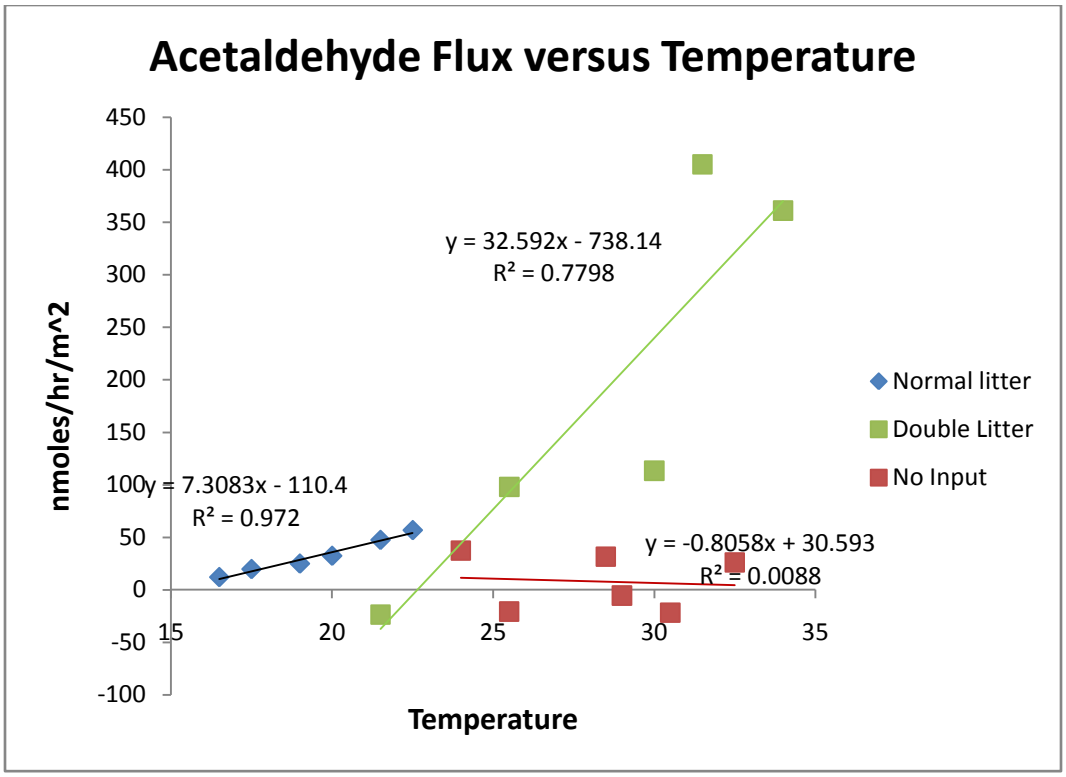

Figure 45: Emission rates of acetaldehyde from soil plots versus air temperature.
For plots without litter, there is no net exchange of acetaldehyde with the atmosphere. However, plots with double litter appear to have higher flux sensitivity to temperature. This is possibly due to the presence of more decaying biomass in the double input plots leading to higher emission rates.

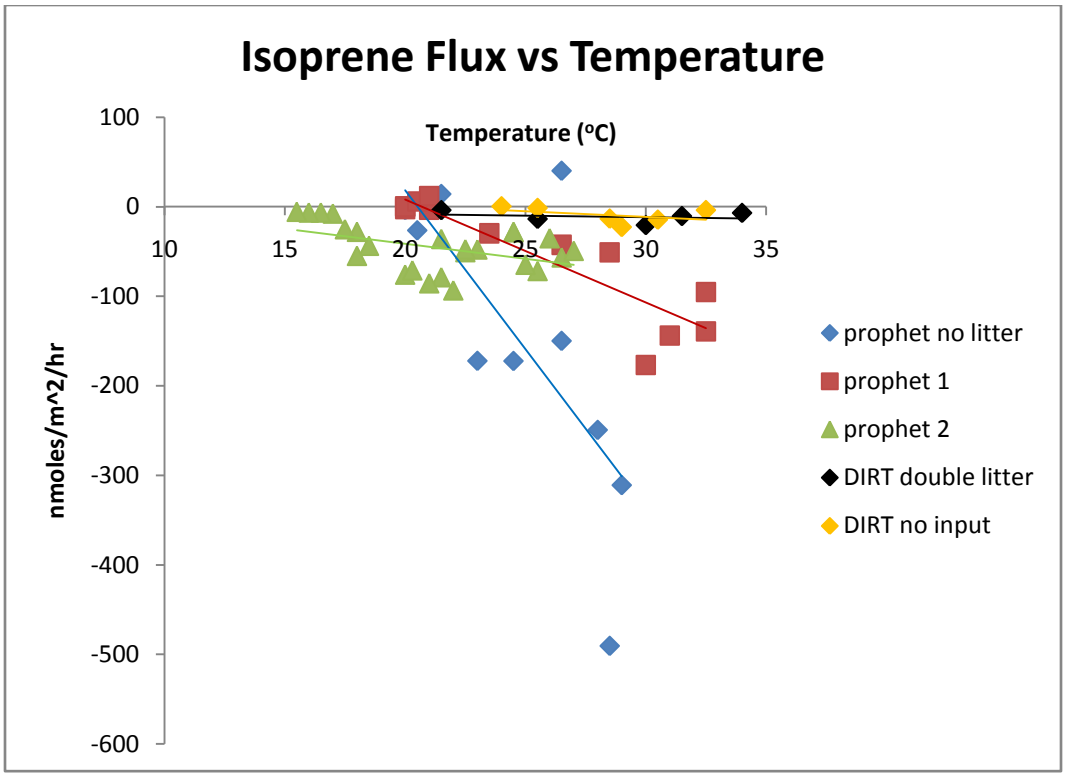

Figure 46: Uptake rates of isoprene from soil plots versus air temperature.
All plots studied (with and without litter) behaved as a net sink for isoprene under ambient conditions. There is a strong linear relationship between isoprene uptake rates and ambient temperature. While this may be partially due to a stimulation of microbial activity at higher temperatures, it is likely an indirect effect through the stimulation of isoprene emissions from the live vegetation. This increases the driving force for isoprene uptake because of the increased atmosphere/soil-atmosphere concentration gradient. While all plots behave as net sinks, there is considerable variability in the sensitivity to temperature. This may be because of the heterogeneous nature of microbial activity in soils responsible for isoprene consumption or the variable relationship between air temperature and ambient isoprene concentrations.

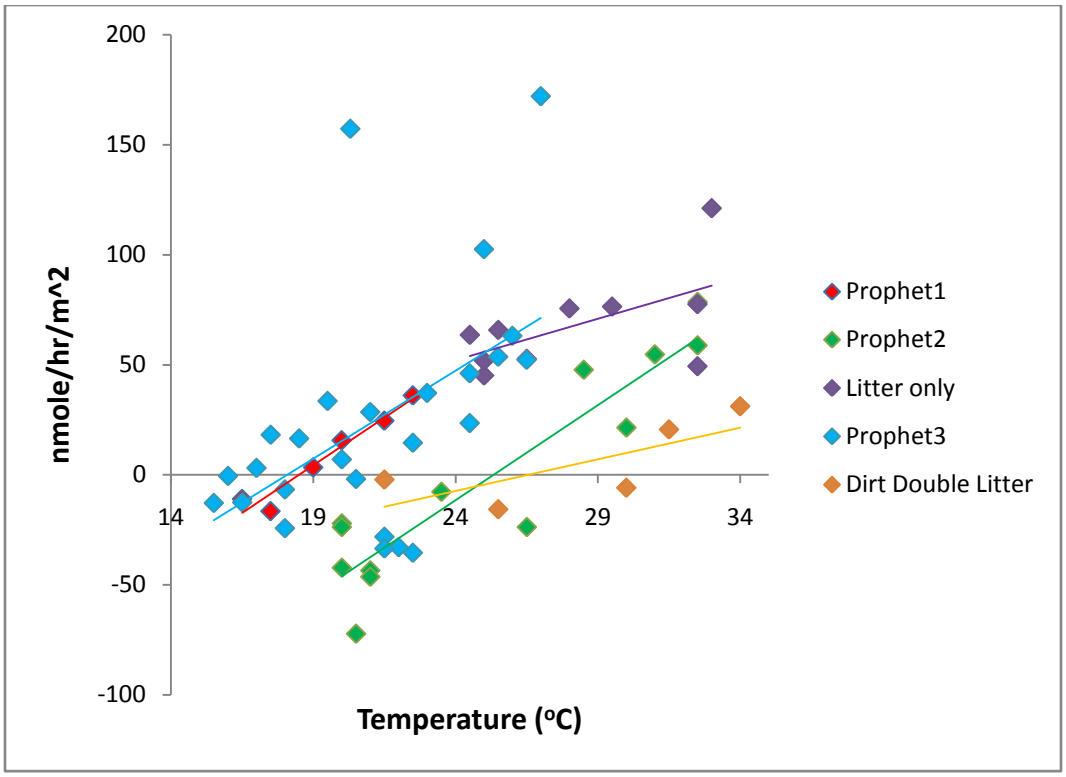

Figure 47: Exchange of acetone from soil plots with litter versus air temperature.
There is a linear relationship between acetone exchange rates and temperature for all plots with litter investigated. At low temperatures during the night, the plots behave as a net sink for acetaldehyde whereas during the warmer temperatures of the day they turn into a net source. We suggest that the soil sink (microbial?) is only weakly temperature dependent whereas emissions from the litter are much more sensitive to temperature. While the flux sensitivity to temperature (slope) is similar for the different plots, there can be considerable differences in the flux between plots for a given temperature.

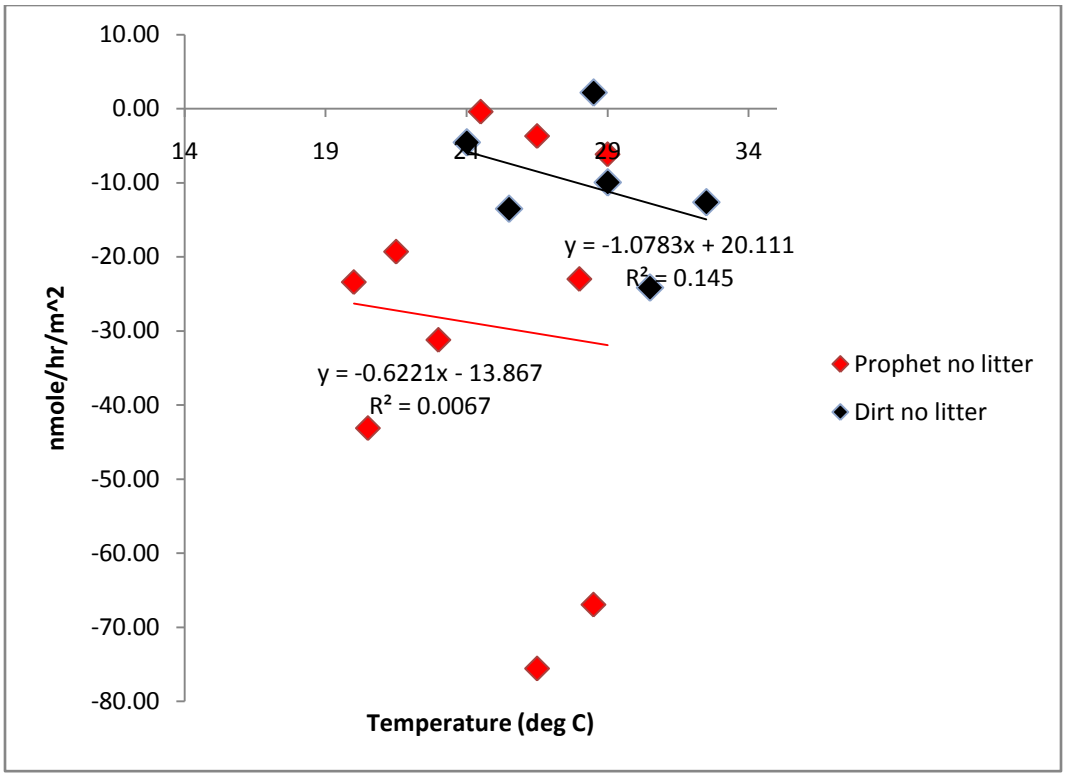

Figure 48: Emission of acetone from soil plots lacking litter versus air temperature.
When the overlying litter is removed, the soil is consistently a sink for acetaldehyde during both the day and the night. However, there does not appear to be a large dependence upon temperature although this could be due to an insufficient amount of data to observe a trend.

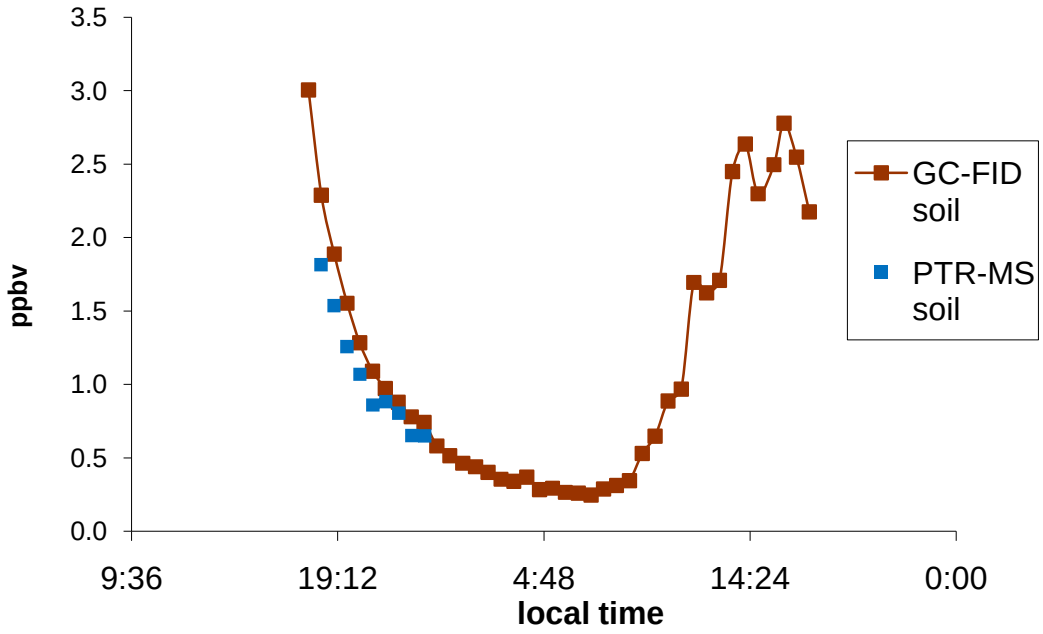

Figure 49: Intercomparison of acetone concentration measurements from a soil enclosure between a PTR-MS and a GC-FID utilizing a nanofiltration dehydration membrane module.
The results show good agreement although condensation in the transfer line to the PTR-MS prevented further comparison while the transfer line from the dehydration membrane to the GC-FID remained dry.

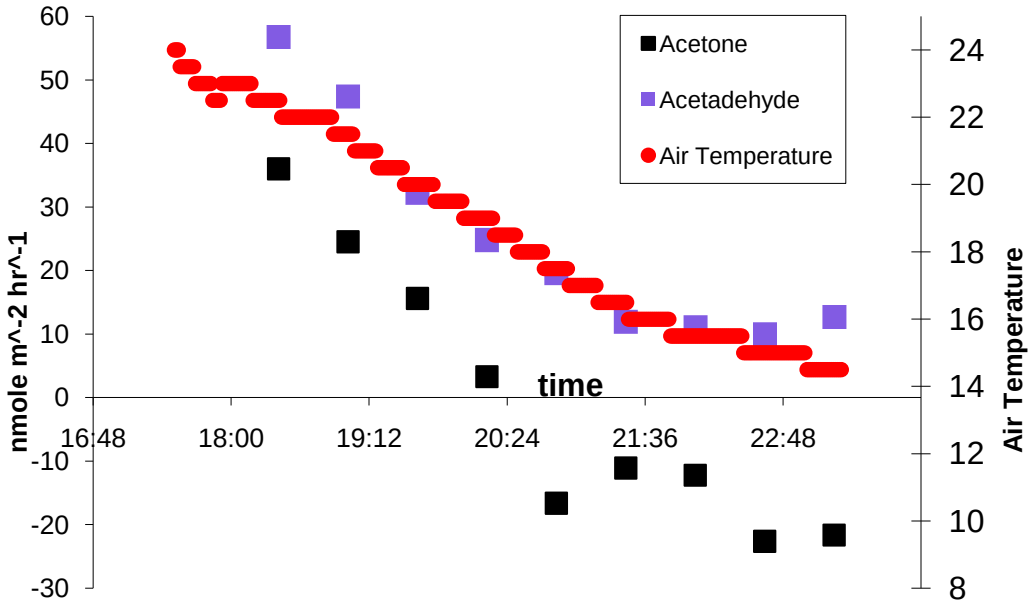

Figure 50: Exchange of acetaldehyde and acetone from a soil plot with litter during a very cool night. For plots with litter during the night, acetone switches between a net source to a net sink. However, acetaldehyde remains a source even at temperatures down to 14 ^{o}C. This suggests that the soil sink (microbial?) for acetone is much greater than that for acetaldehyde. Therefore, temperature strongly controls the production of both acetone and acetaldehyde, but only acetone has a significant soil sink.

Compound	min Flux	max Flux	What?	% of average soil max/canopy max	Reference
acetaldehyde	25	425	soil/litter	9.4	This study
acetaldehyde	-144	72	potted soil		Asensio 2007
acetaldehyde	417	1667	soil/litter	30.0	Shade and Goldstein 2001
acetone	-80	180	soil/litter	3.5	This study
acetone	1389	4444	soil/litter	80	Shade and Goldstein 2001
acetone	396.0	1440	potted soil		Asensio 2007
isoprene	~0	-500	soil/litter	-3.4	This study

Figure 51: Comparison of enclosure based soil flux measurements of acetaldehyde, acetone, and isoprene from several studies.
The significance of the measured fluxes are put into context of canopy scale measurements at the same site where available. All flux values are reported in nanomoles m^{-2} hr^{-1} and the maximum flux (either emission or uptake) is reported as a percentage of the average maximum canopy scale flux.

Chapter 7: Conclusions

The research reported within this dissertation has led to the following accomplishments, conclusions, and recommendations:

8.1 Instrumentation

1. Minimum gas phase acetaldehyde concentrations needed for $\delta^{13}C$ analysis in a 2.5 L sample is 10 ppbv. This limited isotope analysis to enclosure studies since ambient concentrations are rarely above 5 ppbv. However, the increased sensitivity of modern IRMS may allow for ambient measurements. Alternatively, larger sample volumes (e.g. 25 L) could lower the minimum concentration to less than 1 ppbv. Unfortunately, studies have shown that passing large sample volumes across Tenax-TA leads to fractionation due to sample breakthrough. To avoid this, a separate hydrocarbon trap is used to process the large sample volume (glass beads cooled to liquid nitrogen temperatures). Once transferred to the Tenax-TA trap, the analysis is the same as reported here (Rice and Quay, 2006).
2. The precision of $\delta^{13}C$ measurements of acetaldehyde was between 0.2‰ and 1.0‰. This was sufficient to measure relatively large changes in $\delta^{13}C$ values associated with both with both sources (ethanolic fermentation, fatty acid peroxidation, biomass decay) and sinks (oxidation to acetate).
3. Although this dissertation focused on acetaldehyde, $\delta^{13}C$ measurements were also preformed on methanol. The signatures from live vegetation were extremely depleted in ^{13}C, agreeing with published values from other plant species (Keppler et al., 2004). This can clearly be used as a signature of plant growth derived methanol. However, similar measurements from decaying leaf litter and from a commercial source did not show the anomalous depletion in ^{13}C but more closely resembled bulk biomass. This result may undermine the argument made by (Keppler et al., 2004) that methanogenic bacteria in soils feeding on methanol released from decomposing litter may contribute to the large depletion in ^{13}C of atmospheric methane.

8.2 Acetaldehyde Metabolism

1. While previously considered to be dormant under aerobic conditions, ethanolic fermentation coupled with the PDH bypass system was found to produce and consume acetaldehyde respectively under normal aerobic conditions. Therefore, these coupled pathways control the acetaldehyde compensation point, a major factor influencing its exchange with the atmosphere. Moreover, this result if verified, could be used to separate out the relative importance of live versus decaying biogenic methanol sources in forested ecosystems.

2. The acetaldehyde compensation point is much higher in the light than in the dark. This is best explained if acetaldehyde production (ethanolic fermentation) is more temperature/light dependent than its consumption (PDH bypass). Because pyruvate is known to accumulate during the light, this is consistent with the hypothesis that pyruvate concentrations strongly influence ethanolic fermentation rates within leaves. If found to be correct, the finding that ethanolic fermentation occurs under aerobic conditions in leaves requires a reevaluation of fundamental plant metabolism.
3. Emission measurements of acetaldehyde, ethanol, and acetic acid reveal the large stimulation of ethanolic fermentation and the PDH bypass system rates following a light to dark transition. Coinciding with the peak in acetaldehyde emission burst is a similar peak in carbon dioxide emissions. Similar to carbon dioxide during the light enhanced dark respiration (LEDR), we find that emissions of fermentation metabolites are dependent on prior photosynthesis. By analogy with LEDR, we term the process light enhanced dark fermentation (LEDF) and suggest that both LEDR and LEDF are stimulated by the rapid accumulation pyruvate upon darkening.
4. Estimation of the internal concentrations of any volatile metabolite from plants could be done to probe the relative strengths of sources and sinks using gas phase compensation point measurements. The total pool size would be the internal gas phase concentrations (the compensation point) plus the aqueous phase concentrations at equilibrium (Henry's Law).
4. A survey of the stable carbon isotope signatures of acetaldehyde emitted from plants under various conditions was carried out. A significant result from these studies is the elucidation of a new biochemical pathway leading to acetaldehyde production from plants under stress. We hypothesize that stress induces the rapid accumulation of reactive oxygen species (ROS) which lead to the peroxidation of membrane derived fatty acids. Acetaldehyde depleted in ^{13}C is a major product of these reactions due similar ^{13}C depletion in fatty acids. In contrast, acetaldehyde emitted from ethanolic fermentation, decaying litter, and leaf heating experiments all have a similar carbon isotope composition as bulk biomass.

8.3 Plant Physiological and Environmental controls

1. Stomata are found to be the dominant pathway for acetaldehyde exchange with plants due to the presence of both source(s) and sink(s) which strongly buffers the internal concentrations from large changes due to changes in stomatal conductance. Acetaldehyde is therefore a part of a potentially large group of plant volatile metabolites under long term stomatal control.

2. There is a significant carbon isotope effect during the uptake of acetaldehyde by plants. Because of their slower diffusion rates into and within the plant when compared to the lighter carbon isotope ^{12}C, the heavier ^{13}C isotopes in acetaldehyde are discriminated against during uptake.
3. Similar to what is done with carbon dioxide, the carbon isotope composition of gas phase acetaldehyde within and above an ecosystem could possibly be exploited for the partitioning of net ecosystem acetaldehyde exchange fluxes into gross emission and uptake fluxes. In addition to vertical acetaldehyde concentration measurements, $\delta^{13}C$ profiles should also be obtained. During the day, in the air near the top of the canopies where sun leaves are acting as a net emission source through ethanolic fermentation, the carbon isotope composition should resemble bulk biomass. On the other hand, the remaining acetaldehyde surrounding shade leaves and leaves at night will be enriched in ^{13}C due to fractionation during uptake. By plotting acetaldehyde concentration versus $\delta^{13}C$, a Keeling plot can be generated. At high acetaldehyde concentrations, the $\delta^{13}C$ may approach that of bulk biomass. At low concentrations, acetaldehyde may be enriched in ^{13}C due to fractionation during uptake. The intercept on the $\delta^{13}C$ axis will be the theoretical source value (ethanolic fermentation).
4. Decaying leaf litter is a strong source of acetaldehyde due to the loss of biological sink(s) and an increase in abiotic decomposition processes.

8.4 Canopy Scale Studies

1. Canopy tops behaved as a strong net source of acetaldehyde during the day while reduced net emissions and even net uptake was observed deeper within the canopies. Net uptake generally predominated at night. While the lower foliar density of California resulted in net emissions throughout the canopy during the day, the higher foliar densities in Michigan and North Carolina allowed for the emissions from the upper canopy to be partially recaptured by the lower shaded canopy. Therefore, ecosystem scale net emission rates are inversely dependent on foliar density due to an increase in the percentage of sun versus shade leaves.
2. Although not described in this dissertation, the contrasting canopy scale exchange patterns between California and North Carolina/Michigan were reproduced from a simple canopy scale compensation point model which included the effects of the canopy light and temperature environment on stomatal conductance and acetaldehyde compensation point.

8.5 Emission modeling

1. We suggest the development of a canopy scale acetaldehyde model including stomatal conductance (controlling flux magnitude), temperature/light (controlling compensation point), and ambient acetaldehyde concentrations (influencing the partial pressure gradient between the substomatal airspace and the atmosphere).
2. There is then a bidirectional feedback between acetaldehyde exchange rates and its ambient concentrations. Because of the fact that the exchange of acetaldehyde influences ambient concentrations which in turn influences the exchange rates, we suggest the use of an online coupled emission/chemistry model.
3. An empirical parameterization of the compensation point could be produced as a function of temperature and then of light. This should be done for both sun and shade leaves.

Research Pictures

Figure 52: Making soil flux measurements of volatile organic compounds near the PROPHET tower in Northern Michigan, summer 2005.

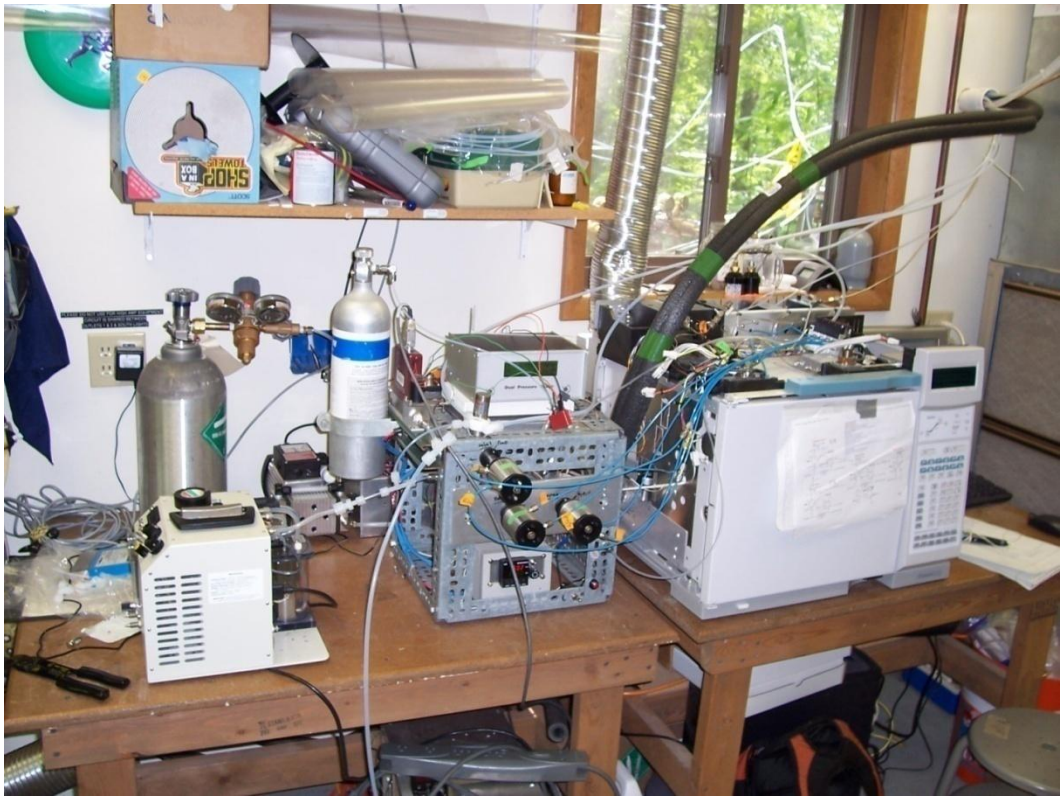

Figure 53: GC-FID with custom built cryogenic VOC preconcentration system in the PROPHET tower lab, summer 2005. System was fully automated with remote control abilities.

Figure 54: Setting up sampling tubing from a tower to the instrument trailer at a walnut orchard during CHATS 2007, near Dixon, CA.

Figure 55: VOC concentration measurements onboard the NCAR C-130 during INTEX-NA 2006.

Figure 56: Measuring the emissions of VOCs from a walnut branch during CHATS.

Figure 57: Setting up 3-D sonic anemometer on the top of the PROPHET tower, summer 2006.

References

Andreae MO, Crutzen PJ (1997) Atmospheric aerosols: Biogeochemical sources and role in atmospheric chemistry. Science 276: 1052-1058

Andreae MO, Merlet P (2001) Emission of trace gases and aerosols from biomass burning. Global Biogeochemical Cycles 15: 955-966

Arey J, Crowley DE, Crowley M, Resketo M, Lester J (1995) Hydrocarbon Emissions from Natural Vegetation in California South-Coast-Air-Basin. Atmospheric Environment 29: 2977-2988

Arey J, Winer AM, Atkinson R, Aschmann SM, Long WD, Morrison CL (1991) The Emission of (Z)-3-Hexen-1-Ol, (Z)-3-Hexenylacetate and Other Oxygenated Hydrocarbons from Agricultural Plant-Species. Atmospheric Environment Part a-General Topics 25: 1063-1075

Arnts RR, Petersen WB, Seila RL, Gay BW (1982) Estimates of Alpha-Pinene Emissions from a Loblolly-Pine Forest Using an Atmospheric Diffusion-Model. Atmospheric Environment 16: 2127-2137

Asensio D, Penuelas J, Filella I, Llusia J (2007) On-line screening of soil VOCs exchange responses to moisture, temperature and root presence. Plant and Soil 291: 249-261

Atkin OK, Evans JR, Siebke K (1998) Relationship between the inhibition of leaf respiration by light and enhancement of leaf dark respiration following light treatment. Australian Journal of Plant Physiology 25: 437-443

Atkinson R, Arey J (2003) Atmospheric Degradation of Volatile Organic Compounds. Chem. Rev. 103: 4605-4638

Atkinson R, Arey J (2003) Gas-phase tropospheric chemistry of biogenic volatile organic compounds: a review. Atmospheric Environment 37: S197-S219

Augusti A, Schleucher J (2007) The ins and outs of stable isotopes in plants. New Phytologist 174: 473-475

Baez AP, Belmont R, Padilla H (1995) Measurements of Formaldehyde and Acetaldehyde in the Atmosphere of Mexico-City. Environmental Pollution 89: 163-167

Ballentine DC, Macko SA, Turekian VC (1998) Variability of stable carbon isotopic compositions in individual fatty acids from combustion of C4 and C3 plants: implications for biomass burning. Chemical Geology 152: 151-161

Barbour MM, McDowell NG, Tcherkez G, Bickford CP, Hanson DT (2007) A new measurement technique reveals rapid post-illumination changes in the carbon isotope composition of leaf-respired CO2. Plant Cell and Environment 30: 469-482

Barclay KD, McKersie BD (1994) Peroxidation reactions in plant membranes: effects of free fatty acids. Lipids 29: 877-883

Becerra R, Cannady JP, Walsh R (2001) The gas-phase reaction of silylene with acetaldehyde - Part 1. Direct rate studies, isotope effects, RRKM modelling and ab initio studies of the potential energy surface. Physical Chemistry Chemical Physics 3: 2343-2351

Birks SJ, Kelly DJ (1997) Assay and properties of acetone carboxylase, a novel enzyme involved in acetone-dependent growth and CO2 fixation in Rhodobacter capsulatus and other photosynthetic and denitrifying bacteria. Microbiology-Uk 143: 755-766

Blubaugh DJ, Govindjee (1988) Sites of Inhibition by Disulfiram in Thylakoid Membranes. Plant Physiology 88: 1021-1025

Bode K, Helas G, Kesselmeier J (1997) Biogenic contribution to atmospheric organic acids. *In* G Helas, Slanina, Steinbrecher R, ed, Biogenic Volatile Organic Compounds in the Atmosphere. SPB Academic Publishing, Amsterdam

Bowling DR, Tans PP, Monson RK (2001) Partitioning net ecosystem carbon exchange with isotopic fluxes of CO2. Global Change Biology 7: 127-145

Bown AW, Pullen J, Shadeed NM (1984) Disulfiram Metabolism in Isolated Mesophyll-Cells and Inhibition of Photosynthesis and Cyanide-Resistant Respiration. Plant Physiology 76: 846-848

Brasseur G, Chatfield R (1991) The fate of biogenic trace gases in the atmosphere. *In* Trace Gas Emissions by Plants. Academic Press, New York, pp 1-28

Bucher M, Brander KA, Sbicego S, Mandel T, Kuhlemeier C (1995) Aerobic Fermentation in Tobacco Pollen. Plant Molecular Biology 28: 739-750

Cazale AC, Rouet-Mayer MA, Barbier-Brygoo H, Mathieu Y, Lauriere C (1998) Oxidative burst and hypoosmotic stress in tobacco cell suspensions. Plant Physiology 116: 659-669

Ceron RM, Ceron JG, Muriel M (2006) Diurnal and seasonal trends in carbonyl levels in a semi-urban coastal site in the Gulf of

Campeche, Mexico. Atmospheric Environment doi:10.1016/j.atmosenv.2006.08.008

Chameides WL, Lindsay RW, Richardson J, Kiang CS (1988) The Role of Biogenic Hydrocarbons in Urban Photochemical Smog - Atlanta as a Case-Study. Science 241: 1473-1475

Cleveland CC, Yavitt JB (1997) Consumption of atmospheric isoprene in soil. Geophysical Research Letters 24: 2379-2382

Cleveland CC, Yavitt JB (1998) Microbial consumption of atmospheric isoprene in a temperate forest soil. Applied and Environmental Microbiology 64: 172-177

Cojocariu C, Escher P, Haberle KH, Matyssek R, Rennenberg H, Kreuzwieser J (2005) The effect of ozone on the emission of carbonyls from leaves of adult Fagus sylvatica. Plant Cell and Environment 28: 603-611

Cojocariu C, Kreuzwieser J, Rennenberg H (2004) Correlation of short-chained carbonyls emitted from Picea abies with physiological and environmental parameters. New Phytologist 162: 717-727

Dawson TE, Burgess SS, Tu KP, Oliveira RS, Santiago LS, Fisher JB, Simonin KA, Ambrose AR (2007) Nighttime transpiration in woody plants from contrasting ecosystems. Tree Physiol 27: 561-575

Day DA, Millar AH, Wiskich JT, Whelan J (1994) Regulation of Alternative Oxidase Activity by Pyruvate in Soybean Mitochondria. Plant Physiology 106: 1421-1427

de Gouw JA, Howard CJ, Custer TG, Fall R (1999) Emissions of volatile organic compounds from cut grass and clover are enhanced during the drying process. Geophysical Research Letters 26: 811-814

Delwiche CF, Sharkey TD (1993) Rapid Appearance of C-13 in Biogenic Isoprene When (Co2)-C-13 Is Fed to Intact Leaves. Plant Cell and Environment 16: 587-591

Deniro MJ, Epstein S (1977) Mechanism of Carbon Isotope Fractionation Associated with Lipid-Synthesis. Science 197: 261-263

Dennis KJ, Shibamoto T (1990) Gas-Chromatographic Analysis of Reactive Carbonyl-Compounds Formed from Lipids Upon Uv-Irradiation. Lipids 25: 460-464

DeZwart LL, Venhorst J, Groot M, Commandeur JNM, Hermanns RCA, Meerman JHM, VanBaar BLM, Vermeulen PE (1997) Simultaneous determination of eight lipid peroxidation degradation products in urine of rats treated with carbon tetrachloride using gas chromatography with electron-capture detection. Journal of Chromatography B 694: 277-287

Dindorf T (2000) Untersuchungen zum Austausch von Carbonylen

zwischen Ba¨umen und der Atmospha¨re. Johannes Gutenberg University of Mainz, Mainz, Germany

Dolferus R, Debruxelles G, Dennis ES, Peacock WJ (1994) Regulation of the Arabidopsis Adh-Gene by Anaerobic and Other Environmental Stresses. Annals of Botany 74: 301-308

Dolferus R, Jacobs M, Peacock WJ, Dennis ES (1994) Differential Interactions of Promoter Elements in Stress Responses of the Arabidopsis Adh Gene. Plant Physiology 105: 1075-1087

Dong DX, Xu YQ (2006) Immediate oxidative burst onto the leaves after cutting the stem or flooding the roots of Nicotiana benthamiana. Plant Physiology and Biochemistry 44: 158-160

Dubtsov SN, Dultsev EN, Dultseva GG, Skubnevskaya GI (2000) Kinetics of aerosol formation during photolysis of acetaldehyde. Chemical Physics Reports 18: 1609-1619

Enoiu M, Wellman M, Leroy P, Ziegler JM, Mitrea N, Siest G (2000) Gas and liquid chromatography-mass spectrometry of aldehydic products from lipid peroxidation. Analusis 28: 285-290

Fall R (2003) Abundant oxygenates in the atmosphere: A biochemical perspective. Chemical Reviews 103: 4941-4951

Fall R, Copley SD (2000) Bacterial sources and sinks of isoprene, a reactive atmospheric hydrocarbon. Environmental Microbiology 2: 123-130

Fall R, Karl T, Hansel A, Jordan A, Lindinger W (1999) Volatile organic compounds emitted after leaf wounding: On-line analysis by proton-transfer-reaction mass spectrometry. Journal of Geophysical Research-Atmospheres 104: 15963-15974

Fall R, Monson RK (1992) Isoprene Emission Rate and Intercellular Isoprene Concentration as Influenced by Stomatal Distribution and Conductance. Plant Physiology 100: 987-992

Faloona I, Tan D, Brune W, Hurst J, Barket D, Couch TL, Shepson P, Apel E, Riemer D, Thornberry T, Carroll MA, Sillman S, Keeler GJ, Sagady J, Hooper D, Paterson K (2001) Nighttime observations of anomalously high levels of hydroxyl radicals above a deciduous forest canopy. Journal of Geophysical Research-Atmospheres 106: 24315-24333

Farmer EE, Ryan CA (1992) Octadecanoid-derived signals in plants. Trends Cell Biol 2: 236-241

Farquhar GD, Ehleringer JR, Hubick KT (1989) Carbon Isotope Discrimination and Photosynthesis. Annual Review of Plant Physiology and Plant Molecular Biology 40: 503-537

Funk JL, Mak JE, Lerdau MT (2004) Stress-induced changes in carbon sources for isoprene production in Populus deltoides. Plant Cell and Environment 27: 747-755

Graus M, Schnitzler JP, Hansel A, Cojocariu C, Rennenberg H, Wisthaler A, Kreuzwieser J (2004) Transient release of oxygenated volatile organic compounds during light-dark transitions in grey poplar leaves. Plant Physiology 135: 1967-1975

Greenberg JP, Guenther AB, Helmig D, Klinger L, Zimmerman P (1994) Field-Measurements of Biogenic Voc Fluxes from an Urban Forest by Gradient and Enclosure Techniques. Abstracts of Papers of the American Chemical Society 207: 243-ENVR

Greenberg JP, Zimmerman PR (1984) Nonmethane Hydrocarbons in Remote Tropical, Continental, and Marine Atmospheres. Journal of Geophysical Research-Atmospheres 89: 4767-4778

Grover SD, Laties GG (1981) Disulfiram Inhibition of the Alternative Respiratory Pathway in Plant-Mitochondria. Plant Physiology 68: 393-400

Guenther A (1997) Seasonal and spatial variations in natural volatile organic compound emissions. Ecological Applications 7: 34-45

Guenther A, Greenberg J, Harley P, Helmig D, Klinger L, Vierling L, Zimmerman P, Geron C (1996) Leaf, branch, stand and landscape scale measurements of volatile organic compound fluxes from U.S. woodlands. Tree Physiol 16: 17-24

Guenther A, Hewitt CN, Erickson D, Fall R, Geron C, Graedel T, Harley P, Klinger L, Lerdau M, Mckay WA, Pierce T, Scholes B, Steinbrecher R, Tallamraju R, Taylor J, Zimmerman P (1995) A Global-Model of Natural Volatile Organic-Compound Emissions. Journal of Geophysical Research-Atmospheres 100: 8873-8892

Guenther A, Karl T, Harley P, Wiedinmyer C, Palmer PI, Geron C (2006) Estimates of global terrestrial isoprene emissions using MEGAN (Model of Emissions of Gases and Aerosols from Nature). Atmospheric Chemistry and Physics 6: 3181-3210

Haagensmit AJ, Fox MM (1956) Ozone Formation in Photochemical Oxidation of Organic Substances. Industrial and Engineering Chemistry 48: 1484-1487

Halliwell B, Gutteridge JMC (1999) Free radicals in biology and medicine, Ed 3rd. Clarendon Press ;

Oxford University Press, Oxford

New York

Hao Q, Maret W (2006) Aldehydes release zinc from proteins. A pathway from oxidative stress/lipid peroxidation to cellular functions of zinc. Febs Journal 273: 4300-4310

Harley P, Greenberg J, Niinemets U, Guenther A (2007) Environmental controls over methanol emissions from leaves. Biogeosciences Discussions 4: 2593-2640

Harry DE, Kimmerer TW (1991) Molecular-Genetics and Physiology of Alcohol-Dehydrogenase in Woody-Plants. Forest Ecology and Management 43: 251-272

Hayward S, Tani A, Owen SM, Hewitt CN (2004) Online analysis of volatile organic compound emissions from Sitka spruce (Picea sitchensis). Tree Physiology 24: 721-728

Herrington JS, Fan ZH, Lioy PJ, Zhang JF (2007) Low acetaldehyde collection efficiencies for 24-hour sampling with 2,4-dinitrophenylhydrazine (DNPH)-coated solid sorbents. Environmental Science & Technology 41: 580-585

Hobbie EA, Werner RA (2004) Intramolecular, compound-specific, and bulk carbon isotope patterns in C-3 and C-4 plants: a review and synthesis (vol 161, pg 371, 2004). New Phytologist 162: 240-240

Holzinger R, Sandoval-Soto L, Rottenberger S, Crutzen PJ, Kesselmeier J (2000) Emissions of volatile organic compounds from Quercus ilex L. measured by Proton Transfer Reaction Mass Spectrometry under different environmental conditions. Journal of Geophysical Research-Atmospheres 105: 20573-20579

Holzinger R, Warneke C, Hansel A, Jordan A, Lindinger W, Scharffe DH, Schade G, Crutzen PJ (1999) Biomass burning as a source of formaldehyde, acetaldehyde, methanol, acetone, acetonitrile, and hydrogen cyanide. Geophysical Research Letters 26: 1161-1164

Hurst JM, Barket DJ, Herrera-Gomez O, Couch TL, Shepson PB, Faloona I, Tan D, Brune W, Westberg H, Lamb B, Biesenthal T, Young V, Goldstein A, Munger JW, Thornberry T, Carroll MA (2001) Investigation of the nighttime decay of isoprene. Journal of Geophysical Research-Atmospheres 106: 24335-24346

Isebrands JG, Guenther AB, Harley P, Helmig D, Klinger L, Vierling L, Zimmerman P, Geron C (1999) Volatile organic compound emission rates from mixed deciduous and coniferous forests in Northern Wisconsin, USA. Atmospheric Environment 33: 2527-2536

Ishida-Fujii K, Goto S, Uemura R, Yamada K, Sato M, Yoshida N (2005) Botanical and geographical origin identification of industrial ethanol by stable isotope analyses of C, H, and O. Bioscience Biotechnology and Biochemistry 69: 2193-2199

Jacob DJ, Field BD, Li QB, Blake DR, de Gouw J, Warneke C, Hansel A, Wisthaler A, Singh HB, Guenther A (2005) Global budget of methanol: Constraints from atmospheric observations. Journal of Geophysical Research-Atmospheres 110: -

Jacobson BS, Smith BN, Epstein S, Laties GG (1970) The prevalence of carbon-13 in respiratory carbon dioxide as an indicator of the types of endogenous substrate. The change from lipid to carbohydrate during the respiratory rise in potato slices. J Gen Physiol 55: 1-17

Janson R, De Serves C, Romero R (1999) Emission of isoprene and carbonyl compounds from a boreal forest and wetland in Sweden. Agricultural and Forest Meteorology 98-9: 671-681

Jardine K, Karl T, Harley P, Lerdau M, Mak J, Guenther A (2007) Acetaldehyde production in plants: Stress induced peroxidation of fatty acids? Plant Cell and Environment (submitted)

Jardine K, Karl T, Harley P, Lerdau M, Mak J, Guenther A (2007) Plant physiological and environmental controls over the exchange of acetaldehyde between plants and the atmosphere. Atmospheric Environment (submitted)

Jardine K, Karl T, Harley P, Lerdau M, Mak J, Guenther A (2008) Ethanolic fermentation and the pyruvate dehydrogenase bypass system in poplar leaves under aerobic conditions

Plant Cell and Environment (submitted)

Jardine K, Karl T, Harley P, Lerdau M, Mak J, Guenther A (2008) Plant physiological and environmental controls over the exchange of acetaldehyde between plants and the atmosphere. Biogeosciences (submitted)

Johnson BJ, Dawson GA (1993) A Preliminary-Study of the Carbon-Isotopic Content of Ambient Formic-Acid and 2 Selected Sources - Automobile Exhaust and Formicine Ants. Journal of Atmospheric Chemistry 17: 123-140

Joseph G, Kelsey RG (2004) Ethanol synthesis and aerobic respiration in the laboratory by leader segments of Douglas-fir seedlings from winter and spring. Journal of Experimental Botany 55: 1095-1103

Karl T, Curtis AJ, Rosenstiel TN, Monson RK, Fall R (2002) Transient releases of acetaldehyde from tree leaves - products of a pyruvate overflow mechanism? Plant Cell and Environment 25: 1121-1131

Karl T, Fall R, Jordan A, Lindinger W (2001) On-line analysis of reactive VOCs from urban lawn mowing. Environmental Science & Technology 35: 2926-2931

Karl T, Fall R, Rosenstiel TN, Prazeller P, Larsen B, Seufert G, Lindinger W (2002) On-line analysis of the (CO2)-C-13 labeling of leaf isoprene suggests multiple subcellular origins of isoprene precursors. Planta 215: 894-905

Karl T, Guenther A, Jordan A, Fall R, Lindinger W (2001) Eddy covariance measurement of biogenic oxygenated VOC emissions from hay harvesting. Atmospheric Environment 35: 491-495

Karl T, Guenther A, Spirig C, Hansel A, Fall R (2004) Seasonal variation of biogenic VOC emissions above a mixed hardwood forest in northern Michigan (vol 30, pg 2186, 2003). Geophysical Research Letters 31: -

Karl T, Harley P, Guenther A, Rasmussen R, Baker B, Jardine K, Nemitz E (2005) The bi-directional exchange of oxygenated VOCs between a loblolly pine (Pinus taeda) plantation and the atmosphere. Atmospheric Chemistry and Physics 5: 3015-3031

Karl T, Harley P, Baker B, Jardine K, Nemitz E, Guenther A (2005) The bi-directional exchange of oxygenated VOCs between a loblolly pine (Pinus taeda) plantation and the atmosphere. Atmos. Chem. Phys. Discuss. 5: 5875-5907

Karl T, Harren F, Warneke C, de Gouw J, Grayless C, Fall R (2005) Senescing grass crops as regional sources of reactive volatile organic compounds. Journal of Geophysical Research-Atmospheres 110: -

Karl T, Potosnak M, Guenther A, Clark D, Walker J, Herrick JD, Geron C (2004) Exchange processes of volatile organic compounds above a tropical rain forest: Implications for modeling tropospheric chemistry above dense vegetation. Journal of Geophysical Research-Atmospheres 109: -

Karl TG, Spirig C, Rinne J, Stroud C, Prevost P, Greenberg J, Fall R, Guenther A (2002) Virtual disjunct eddy covariance measurements of organic compound fluxes from a subalpine forest using proton transfer reaction mass spectrometry. Atmospheric Chemistry and Physics 2: 279-291

Karlik JF, McKay AH, Welch JM, Winer AM (2002) A survey of California plant species with a portable VOC analyzer for biogenic emission inventory development. Atmospheric Environment 36: 5221-5233

Keppler F, Kalin RM, Harper DB, McRoberts WC, Hamilton JTG (2004) Carbon isotope anomaly in the major plant C-1 pool and its global biogeochemical implications. Biogeosciences 1: 123-131

Kesselmeier J (2001) Exchange of short-chain oxygenated volatile organic compounds (VOCs) between plants and the atmosphere: A compilation of field and laboratory studies. Journal of Atmospheric Chemistry 39: 219-233

Kesselmeier J, Bode K, Hofmann U, Muller H, Schafer L, Wolf A, Ciccioli P, Brancaleoni E, Cecinato A, Frattoni M, Foster P, Ferrari C, Jacob V, Fugit JL, Dutaur L, Simon V, Torres L (1997) Emission of short chained organic acids, aldehydes and monoterpenes from Quercus ilex L. and Pinus pinea L. in relation to physiological activities, carbon budget and emission algorithms. Atmospheric Environment 31: 119-133

Kesselmeier J, Kuhn U, Rottenberger S, Biesenthal T, Wolf A, Schebeske G, Andreae MO, Ciccioli P, Brancaleoni E, Frattoni M, Oliva ST, Botelho ML, Silva CMA, Tavares TM (2002) Concentrations and

species composition of atmospheric volatile organic compounds (VOCs) as observed during the wet and dry season in Rondonia (Amazonia). Journal of Geophysical Research-Atmospheres 107

Kesselmeier J, Staudt M (1999) Biogenic volatile organic compounds (VOC): An overview on emission, physiology and ecology. Journal of Atmospheric Chemistry 33: 23-88

Kim BH, von Arnim AG (2006) The early dark-response in Arabidopsis thaliana revealed by cDNA microarray analysis. Plant Mol Biol 60: 321-342

Kimmerer TW, Kozlowski TT (1982) Ethylene, Ethane, Acetaldehyde, and Ethanol-Production by Plants under Stress. Plant Physiology 69: 840-847

Kimmerer TW, Macdonald RC (1987) Acetaldehyde and Ethanol Biosynthesis in Leaves of Plants. Plant Physiology 84: 1204-1209

Kinnee E, Geron C, Pierce T (1997) United States land use inventory for estimating biogenic ozone precursor emissions. Ecological Applications 7: 46-58

Kirch HH, Bartels D, Wei YL, Schnable PS, Wood AJ (2004) The ALDH gene superfamily of Arabidopsis. Trends in Plant Science 9: 371-377

Kondo T, Hasegawa K, Uchida R, Onishi M (1998) Absorption of atmospheric C-2-C-5 aldehydes by various tree species and their tolerance to C-2-C-5 aldehydes. Science of the Total Environment 224: 121-132

Kotchoni SO, Gachomo EW (2006) The reactive oxygen species network pathways: an essential prerequisite for perception of pathogen attack and the acquired disease resistance in plants. Journal of Biosciences 31: 389-404

Kotchoni SO, Kuhns C, Ditzer A, Kirch HH, Bartels D (2006) Over-expression of different aldehyde dehydrogenase genes in Arabidopsis thaliana confers tolerance to abiotic stress and protects plants against lipid peroxidation and oxidative stress. Plant Cell and Environment 29: 1033-1048

Kreuzwieser J, Harren FJM, Laarhoven LJJ, Boamfa I, te Lintel-Hekkert S, Scheerer U, Huglin C, Rennenberg H (2001) Acetaldehyde emission by the leaves of trees - correlation with physiological and environmental parameters. Physiologia Plantarum 113: 41-49

Kreuzwieser J, Kuhnemann F, Martis A, Rennenberg H, Urban W (2000) Diurnal pattern of acetaldehyde emission by flooded poplar trees. Physiologia Plantarum 108: 79-86

Kreuzwieser J, Papadopoulou E, Rennenberg H (2004) Interaction of flooding with carbon metabolism of forest trees. Plant Biology 6: 299-306

Kreuzwieser J, Scheerer U, Rennenberg H (1999) Metabolic origin of acetaldehyde emitted by poplar (Populus tremula x P-alba) trees. Journal of Experimental Botany 50: 757-765

Kurosaki Y (2006) Photodissociation of acetaldehyde, CH3CHO -> CH4+CO: II. Direct ab initio molecular dynamics study. Chemical Physics Letters 421: 549-553

Langebartels C, Wohlgemuth H, Kschieschan S, Grun S, Sandermann H (2002) Oxidative burst and cell death in ozone-exposed plants. Plant Physiology and Biochemistry 40: 567-575

Le Deunff E, Davoine C, Le Dantec C, Billard JP, Huault C (2004) Oxidative burst and expression of germin/oxo genes during wounding of ryegrass leaf blades: comparison with senescence of leaf sheaths. Plant J 38: 421-431

Lerdau M (2002) Plants talk - But can they listen? Science 298: 361-361

Lerdau M, Gray D (2003) Ecology and evolution of light-dependent and light-independent phytogenic volatile organic carbon. New Phytologist 157: 199-211

Lerdau M, Guenther A, Monson R (1997) Plant production and emission of volatile organic compounds. Bioscience 47: 373-383

Lewis A, Hopkins J, Carpenter L, Stanton J, Read K, Pilling M (2005) Sources and sinks of acetone, methanol, and acetaldehyde in North Atlantic marine air. Atmos. Chem. Phys. 5: 1963-1974

Li M, Zhang JS, Shen W, Meng QX (2004) Quantum chemical study on reaction of acetaldehyde with hydroxyl radical. Chinese Journal of Chemistry 22: 792-797

Li P, Perreau KA, Covington E, Song CH, Carmichael GR, Grassian VH (2001) Heterogeneous reactions of volatile organic compounds on oxide particles of the most abundant crustal elements: Surface reactions of acetaldehyde, acetone, and propionaldehyde on SiO2, Al2O3, Fe2O3, TiO2, and CaO. Journal of Geophysical Research-Atmospheres 106: 5517-5529

Li SY, Li Q, Shen JJ, Dong F, Sigmon VK, Li YZ, Ren J (2006) Attenuation of acetaldehyde-induced cell injury by overexpression of aldehyde dehydrogenase-2 (ALDH2) transgene in human cardiac myocytes: role of MAP kinase signaling. Journal of Molecular and Cellular Cardiology 40: 283-294

Lindinger W, Hansel A (1997) Analysis of trace gases at ppb levels by proton transfer reaction mass spectrometry (PTR-MS). Plasma Sources Science & Technology 6: 111-117

Liu F, Schnable PS (2002) Functional specialization of maize mitochondrial aldehyde dehydrogenases. Plant Physiology 130: 1657-1674

Loreto F, Barta C, Brilli F, Nogues I (2006) On the induction of volatile organic compound emissions by plants as consequence of wounding or fluctuations of light and temperature. Plant Cell and Environment 29: 1820-1828

Luecken DJ, Hutzell WT, Gipson GL (2006) Development and analysis of air quality modeling simulations for hazardous air pollutants. Atmospheric Environment 40: 5087-5096

Macdonald RC, Kimmerer TW (1993) Metabolism of Transpired Ethanol by Eastern Cottonwood (Populus-Deltoides-Bartr). Plant Physiology 102: 173-179

Mak CH, Brand JL, Koehler BG, George SM (1987) Isotope Effect in the Surface-Diffusion of Hydrogen and Deuterium on Ru(001). Surface Science 188: 312-320

Mak JE, Brenninkmeijer CAM (1994) Compressed-Air Sample Technology for Isotopic Analysis of Atmospheric Carbon-Monoxide. Journal of Atmospheric and Oceanic Technology 11: 425-431

Mak JE, Yang WB (1998) Technique for analysis of air samples for C-13 and O-18 in carbon monoxide via continuous-flow isotope ratio mass spectrometry. Analytical Chemistry 70: 5159-5161

Marandino CA, De Bruyn WJ, Miller SD, Prather MJ, Saltzman ES (2005) Oceanic uptake and the global atmospheric acetone budget. Geophysical Research Letters 32: -

Martin RS, Villanueva I, Zhang JY, Popp CJ (1999) Nonmethane hydrocarbon, monocarboxylic acid, and low molecular weight aldehyde and ketone emissions from vegetation in central New Mexico. Environmental Science & Technology 33: 2186-2192

Mathur R, Shankar U, Hanna AF, Odman MT, McHenry JN, Coats CJ, Alapaty K, Xiu AJ, Arunachalam S, Olerud DT, Byun DW, Schere KL, Binkowski FS, Ching JKS, Dennis RL, Pierce TE, Pleim JE, Roselle SJ, Young JO (2005) Multiscale air quality simulation platform (MAQSIP): Initial applications and performance for tropospheric ozone and particulate matter. Journal of Geophysical Research-Atmospheres 110: -

Mcfarlan.M, Albritto.Dl, Fehsenfe.Fc, Ferguson EE, Schmelte.Al (1973) Ion-Molecule Reaction and Mobility Measurements in a Flowing

Afterglow Drift Tube. Bulletin of the American Physical Society 18: 1525-1525

Mellema S, Eichenberger W, Rawyler A, Suter M, Tadege M, Kuhlemeier C (2002) The ethanolic fermentation pathway supports respiration and lipid biosynthesis in tobacco pollen. Plant Journal 30: 329-336

Miller LG, Kalin RM, McCauley SE, Hamilton JTG, Harper DB, Millet DB, Oremland RS, Goldstein AH (2001) Large carbon isotope fractionation associated with oxidation of methyl halides by methylotrophic bacteria. Proceedings of the National Academy of Sciences of the United States of America 98: 5833-5837

Moyano E, Encinas-Villarejo S, Lopez-Raez JA, Redondo-Nevado J, Blanco-Portales R, Bellido ML, Sanz C, Caballero JL, Munoz-Blanco J (2004) Comparative study between two strawberry pyruvate decarboxylase genes along fruit development and ripening, post-harvest and stress conditions. Plant Science 166: 835-845

Muller K, Haferkorn S, Grabmer W, Wisthaler A, Hansel A, Kreuzwieser J, Cojocariu C, Rennenberg H, Herrmann H (2006) Biogenic carbonyl compounds within and above a coniferous forest in Germany. Atmospheric Environment 40: S81-S91

Niemela O, Parkkila S, Ylaherttuala S, Villanueva J, Ruebner B, Halsted CH (1995) Sequential Acetaldehyde Production, Lipid-Peroxidation, and Fibrogenesis in Micropig Model of Alcohol-Induced Liver-Disease. Hepatology 22: 1208-1214

Niinemets U, Reichstein M (2003) Controls on the emission of plant volatiles through stomata: Differential sensitivity of emission rates to stomatal closure explained. Journal of Geophysical Research-Atmospheres 108: -

Novitskiy G, Traore K, Wang L, Trush MA, Mezey E (2006) Effects of ethanol and acetaldehyde on reactive oxygen species production in rat hepatic stellate cells. Alcoholism-Clinical and Experimental Research 30: 1429-1435

Noziere B, Riemer DD (2003) The chemical processing of gas-phase carbonyl compounds by sulfuric acid aerosols-2,4-pentanedione. Atmospheric Environment 37: 841-851

opdenCamp RGL, Kuhlemeier C (1997) Aldehyde dehydrogenase in tobacco pollen. Plant Molecular Biology 35: 355-365

Orhan H, Gurer-Orhan H, Vriese E, Vermeulen NPE, Meerman JHN (2006) Application of lipid peroxidation and protein oxidation biomarkers for oxidative damage in mammalian cells. A comparison with two fluorescent probes. Toxicology in Vitro 20: 1005-1013

Pang XB, Shi XY, Mu YJ, He H, Shuai SJ, Chen H, Li RL (2006) Characteristics of carbonyl compounds emission from a diesel-engine using biodiesel-ethanol-diesel as fuel. Atmospheric Environment 40: 7057-7065

Park R, Epstein S (1961) Metabolic fractionation of C & C in plants. Plant Physiol 36: 133-138

Parys E, Jastrzebski H (2006) Light-enhanced dark respiration in leaves, isolated cells and protoplasts of various types of C-4 plants. Journal of Plant Physiology 163: 638-647

Parys E, Romanowska E, Siedlecka M (2004) Light-enhanced dark respiration in leaves and mesophyll protoplasts of pea in relation to photorespiration, respiration and some metabolites content. Acta Physiologiae Plantarum 26: 37-46

Parys E, Staszewski L (1992) Effect of Oxygen on Photosynthesis and Respiration in Maize at Low Irradiances. Plant Physiology and Biochemistry 30: 207-212

Pegoraro E, Abrell L, Van Haren J, Barron-Gafford G, Grieve KA, Malhi Y, Murthy R, Lin GH (2005) The effect of elevated atmospheric CO2 and drought on sources and sinks of isoprene in a temperate and tropical rainforest mesocosm. Global Change Biology 11: 1234-1246

Raghavendra AS, Padmasree K, Saradadevi K (1994) Interdependence of Photosynthesis and Respiration in Plant-Cells - Interactions between Chloroplasts and Mitochondria. Plant Science 97: 1-14

Rasmusse.Ra (1972) Survey of Plant Species That Release Isoprene to Atmosphere. Abstracts of Papers of the American Chemical Society: 13-&

Raupach MR (1989) Applying Lagrangian Fluid-Mechanics to Infer Scalar Source Distributions from Concentration Profiles in Plant Canopies. Agricultural and Forest Meteorology 47: 85-108

Raymond P, Alani A, Pradet A (1985) Atp Production by Respiration and Fermentation, and Energy-Charge during Aerobiosis and Anaerobiosis in 12 Fatty and Starchy Germinating-Seeds. Plant Physiology 79: 879-884

Rhee TS, Mak J, Rockmann T, Brenninkmeijer CAM (2004) Continuous-flow isotope analysis of the deuterium/hydrogen ratio in atmospheric hydrogen. Rapid Communications in Mass Spectrometry 18: 299-306

Rice AL, Quay PD (2006) Isotopic analysis of atmospheric formaldehyde by gas chromatography isotope ratio mass spectrometry. Analytical Chemistry 78: 6320-6326

Rottenberger S, Kuhn U, Wolf A, Schebeske G, Oliva ST, Tavares TM, Kesselmeier J (2004) Exchange of short-chain aldehydes between

Amazonian vegetation and the atmosphere. Ecological Applications 14: S247-S262

Rottenberger S, Kuhn U, Wolf A, Schebeske G, Oliva ST, Tavares TM, Kesselmeier J (2005) Formaldehyde and acetaldehyde exchange during leaf development of the Amazonian deciduous tree species Hymenaea courbaril. Atmospheric Environment 39: 2275-2279

Roughan PG (1997) Stromal concentrations of coenzyme A and its esters are insufficient to account for rates of chloroplast fatty acid synthesis: evidence for substrate channelling within the chloroplast fatty acid synthase. Biochemical Journal 327: 267-273

Rudolph J, Lowe DC, Martin RJ, Clarkson TS (1997) A novel method for compound specific determination of delta C-13 in volatile organic compounds at ppt levels in ambient air. Geophysical Research Letters 24: 659-662

Sanchez LB (1998) Aldehyde dehydrogenase (CoA-acetylating) and the mechanism of ethanol formation in the amitochondriate protist, Giardia lamblia. Archives of Biochemistry and Biophysics 354: 57-64

Schade GW, Custer TG (2004) OVOC emissions from agricultural soil in northern Germany during the 2003 European heat wave. Atmospheric Environment 38: 6105-6114

Schade GW, Goldstein AH (2001) Fluxes of oxygenated volatile organic compounds from a ponderosa pine plantation. Journal of Geophysical Research-Atmospheres 106: 3111-3123

Schade GW, Goldstein AH (2002) Plant physiological influences on the fluxes of oxygenated volatile organic compounds from ponderosa pine trees. Journal of Geophysical Research-Atmospheres 107: -

Seco R, Penuelas J, Filella I (2007) Short-chain oxygenated VOCs: Emission and uptake by plants and atmospheric sources, sinks, and concentrations. Atmospheric Environment 41: 2477-2499

Shi XY, Pang XB, Mu YJ, He H, Shuai SJ, Wang JX, Chen H, Li RL (2006) Emission reduction potential of using ethanol-biodiesel-diesel fuel blend on a heavy-duty diesel engine. Atmospheric Environment 40: 2567-2574

Shibamoto T (2006) Analytical methods for trace levels of reactive carbonyl compounds formed in lipid peroxidation systems. Journal of Pharmaceutical and Biomedical Analysis 41: 12-25

Singh HB, Salas LJ, Chatfield RB, Czech E, Fried A, Walega J, Evans MJ, Field BD, Jacob DJ, Blake D, Heikes B, Talbot R, Sachse G, Crawford JH, Avery MA, Sandholm S, Fuelberg H (2004) Analysis of the atmospheric distribution, sources, and sinks of oxygenated volatile

organic chemicals based on measurements over the Pacific during TRACE-P. Journal of Geophysical Research-Atmospheres 109: -

Singh HB, Tabazadeh A, Evans MJ, Field BD, Jacob DJ, Sachse G, Crawford JH, Shetter R, Brune WH (2003) Oxygenated volatile organic chemicals in the oceans: Inferences and implications based on atmospheric observations and air-sea exchange models. Geophysical Research Letters 30: -

Skubnevskaya GI, Dubtsov SN, Dultsev EN, Dultseva GG, Tsang W (2004) New nanoparticle formation under UV impact on acetaldehyde vapor in nitrogen and air flow. Journal of Physical Chemistry B 108: 11393-11398

Sommariva R, Bloss WJ, Brough N, Carslaw N, Flynn M, Haggerstone AL, Heard DE, Hopkins JR, Lee JD, Lewis AC, McFiggans G, Monks PS, Penkett SA, Pilling MJ, Plane JMC, Read KA, Saiz-Lopez A, Rickard AR, Williams PI (2006) OH and HO2 chemistry during NAMBLEX: roles of oxygenates, halogen oxides and heterogeneous uptake. Atmospheric Chemistry and Physics 6: 1135-1153

Stelzig DA, Allen RD, Bhatia SK (1983) Inhibition of Phytoalexin Synthesis in Arachidonic Acid-Stressed Potato Tissue by Inhibitors of Lipoxygenase and Cyanide-Resistant Respiration. Plant Physiology 72: 746-749

Tadege M, Bucher M, Stahli W, Suter M, Dupuis I, Kuhlemeier C (1998) Activation of plant defense responses and sugar efflux by expression of pyruvate decarboxylase in potato leaves. Plant Journal 16: 661-671

Tadege M, Dupuis I, Kuhlemeier C (1999) Ethanolic fermentation: new functions for an old pathway. Trends in Plant Science 4: 320-325

Taylor PH, Yamada T, Marshall P (2006) The reaction of OH with acetaldehyde and deuterated acetaldehyde: Further insight into the reaction mechanism at both low and elevated temperatures. International Journal of Chemical Kinetics 38: 489-495

Tcherkez G, Cornic G, Bligny R, Gout E, Ghashghaie J (2005) In vivo respiratory metabolism of illuminated leaves. Plant Physiol 138: 1596-1606

Tovar-Mendez A, Miernyk JA, Randall DD (2003) Regulation of pyruvate dehydrogenase complex activity in plant cells. European Journal of Biochemistry 270: 1043-1049

Trainer M, Hsie EY, Mckeen SA, Tallamraju R, Parrish DD, Fehsenfeld FC, Liu SC (1987) Impact of Natural Hydrocarbons on Hydroxyl and Peroxy-Radicals at a Remote Site. Journal of Geophysical Research-Atmospheres 92: 11879-11894

Tsuji H, Meguro N, Suzuki Y, Tsutsumi N, Hirai A, Nakazono M (2003) Induction of mitochondrial aldehyde dehydrogenase by submergence facilitates oxidation of acetaldehyde during re-aeration in rice. Febs Letters 546: 369-373

Utama I, Wills R, Ben-Yehoshua S, Kuek C (2002) In Vitro efficiancy of Plant Volatiles for Inhibiting the Growth of Fruit and Vegetable Decay Microorganisms. Journal of Agricultural and Food Chemistry 2002: 6371-6377

Vanlerberghe GC (1997) Course and fine control of the partitioning of electrons to the non-energy conserving alternative oxidase. Plant Physiology 114: 61001-61001

Vanlerberghe GC, Day DA, Wiskich JT, Vanlerberghe AE, Mcintosh L (1995) Alternative Oxidase Activity in Tobacco Leaf Mitochondria - Dependence on Tricarboxylic-Acid Cycle-Mediated Redox Regulation and Pyruvate Activation. Plant Physiology 109: 353-361

Vanlerberghe GC, McIntosh L (1997) Alternative oxidase: From gene to function. Annual Review of Plant Physiology and Plant Molecular Biology 48: 703-734

Vartapetian BB, Jackson MB (1997) Plant adaptations to anaerobic stress. Annals of Botany 79: 3-20

Vartapetian BB, Pulli S, Fagerstedt K (1997) Plant response and adaptation to anaerobiosis. Annals of Botany 79: R1-R1

Villanueva-Fierro I, Popp CJ, Martin RS (2004) Biogenic emissions and ambient concentrations of hydrocarbons, carbonyl compounds and organic acids from ponderosa pine and cottonwood trees at rural and forested sites in Central New Mexico. Atmospheric Environment 38: 249-260

Viskari EL, Vartiainen M, Pasanen P (2000) Seasonal and diurnal variation in formaldehyde and acetaldehyde concentrations along a highway in Eastern Finland. Atmospheric Environment 34: 917-923

Wagner BA, Buettner GR, Burns CP (1994) Free Radical-Mediated Lipid-Peroxidation in Cells - Oxidizability Is a Function of Cell Lipid Bis-Allylic Hydrogen Content. Biochemistry 33: 4449-4453

Warneke C, Karl T, Judmaier H, Hansel A, Jordan A, Lindinger W, Crutzen PJ (1999) Acetone, methanol, and other partially oxidized volatile organic emissions from dead plant matter by abiological processes: Significance for atmospheric HOx chemistry. Global Biogeochemical Cycles 13: 9-17

Warneke C, Karl T., Judmaier A, Hansel A, Jordan A, Lindinger W, Crutzen P (1999) Acetone, methanol, and other partially oidized volatile organic emissions from dead plant matter by abiological

processes; Significance for atmospheric HOx chemistry. Global Biogeochem. Cycles 13: 9-17

Warneke C, Luxembourg SL, de Gouw JA, Rinne HJI, Guenther AB, Fall R (2002) Disjunct eddy covariance measurements of oxygenated volatile organic compounds fluxes from an alfalfa field before and after cutting. Journal of Geophysical Research-Atmospheres 107: -

Wedding RT (1989) Malic Enzymes of Higher-Plants - Characteristics, Regulation, and Physiological-Function. Plant Physiology 90: 367-371

Wen S, Feng YL, Yu YX, Bi XH, Wang XM, Sheng GY, Fu JM, Peng PA (2005) Development of a compound-specific isotope analysis method for atmospheric formaldehyde and acetaldehyde. Environmental Science & Technology 39: 6202-6207

Went FW (1960) Blue Hazes in the Atmosphere. Nature 187: 641-643

Zhang SL, Lax D, Li Y, Noren GR, Staley NA, Einzig S (1996) Acetaldehyde induces myocardial iron delocalization and lipid peroxidation: Possible mechanism in alcoholic cardiomyopathy - Acetaldehyde induces iron delocalization. Acp-Applied Cardiopulmonary Pathophysiology 6: 151-159

Zuckermann H, Harren FJM, Reuss J, Parker DH (1997) Dynamics of acetaldehyde production during anoxia and post-anoxia in red bell pepper studied by photoacoustic techniques. Plant Physiology 113: 925-932